Friedrich-Schiller-Universität Jena

Protein analysis and tissue culture of the sex pheromone gland of Lepidoptera

Diploma Thesis

submitted by

Andrea Barthel

to obtain the academic degree in biology

First examiner: Dr. Astrid T. Groot

Second examiner: Prof. Dr. David G. Heckel

Department of Entomology

Max Planck Institute for Chemical Ecology

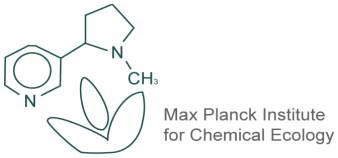

Biologisch-Pharmazeutische Fakultät

Friedrich-Schiller-Universtität Jena

February 2010

Contents

List of Figures

List of Tables

Abbreviations

APS	Ammonium Persulfate
ALD	Aldehyde
cAMP	Cyclic adenosine monophosphate
CC	Corpora cardiaca
cDNA	complementary Deoxyribonucleic acid
CHAPS	3-[(3-Cholamidopropyl)dimethylammonio]-1-propanesulfonate
CoA	Coenzyme A
DNAse	Deoxyribonuclease
dNTP	Deoxyribonucleotide
dsRNA	Double-stranded Ribonucleic acid
DTT	1,4-Dithiothreit
EDTA	Ethylenediaminetetraacetic Acid
FAR	fatty acid reductase
FID	ßame-ionization detector
FBS	fetal bovine serum
GC	gas chromatography
GC-MS	gas chromatography-mass spectrometer
H.a.	*Helicoverpa amigera*
H.v.	*Heliothis virescens*
HACD	3-hydroxyacyl-CoA dehydrogenase
HezPBAN	*Heliothis zea* Pheromone Biosynthesis Activating Neuropeptide
IAA	Indole-3-acetic acid
IPG	immobilized pH gradient
JH	juvenile hormone
LB-medium	Lysogeny broth medium
NC	North Carolina
OH	Alcohol
PBAN	Pheromone Biosynthesis Activating Neuropeptide
PBS	Sodium perborate
PCR	Polymerase chain reaction
qRT-PCR	quantitative real time polymerase chain reaction
RH	Room temperature
RISC	Ribonucleic acid-induced silencing complex
RNA	Ribonucleic acid
RNAi	Ribonucleic acid interference
RNAse	Ribonuclease
SDS	Sodium Dodecyl Sulfate
SOG	Sub-oesophageal ganglion

siRNA	small Ribonucleic acid interference
TCA	Trichloroacetic Acid
TEMED	Tetramethylethylenediamine
Tris	Tris(hydroxymethyl)aminomethane
Z7-16:ALD	(Z)-7-hexadecenal
Z9-14:ALD	(Z)-9-tetradecenal
Z9-16:ALD	(Z)-9-hexadecenal
Z11-16:ALD	(Z)-11-hexadecanal
Z11-16:OH	(Z)-11-hexadecen-1-ol
14:ALD	tetradecanal
16:ALD	hexadecanal
20-E	20-hydroxyecdysone

Zusammenfassung

Obwohl die Pheromon-Biosynthese in den letzten Jahren Gegenstand vieler Studien war, ist der molekulare Mechanismus der diesem Ablauf zugrunde liegt immer noch nicht im Detail verstanden. Die Kontrolle der Pheromon-Biosynthese wir durch PBAN (Pheromone-Biosynthesis-Activating Neuropeptide) reguliert und ein wichtiges Enzym in der Produktion von diesen Pheromon-Komponenten ist die Fettacyl-Reduktase (FAR), welche benötigt wird, um oxygenierte funktionelle Gruppen in ungesättigten Fettsäuren zu produzieren. Diese Diplomarbeit beschäftigte sich mit zwei Themengebieten. Der erste Teil dieser Arbeit ist auf die Funktion von FAR in der Pheromon-Biosynthese von *H. virescens* (*H.v.*) Weibchen fokussiert. Der zweite Teil dieser Diplomarbeit ist auf die Identifizierung von Proteinen fokussiert, welche in der PBAN-aktivierten Pheromon-Drüse von *H.v.* vorkommen. Insbesondere fokussiert diese Studie die folgende Fragen: 1) Besteht die Möglichkeit die Pheromonproduktion der Sex-Pheromon-Drüse von *H. v.* in einem *in vitro* Assay zu bestimmen?, 2) Ist doppelsträngige RNA-vermittelte RNA-Interferenz (RNAi) von FAR wirkungsvoll um einen Knockout Phänotyp im Pheromonprofil und im Expressionlevel von FAR in *H. v.* zu erzeugen? und 3) Gibt es einen Unterschied im Proteom von PBAN-aktivierten und PBAN-nicht-aktivierten Pheromon-Drüsen in *H.v.*?

1) Die Zugabe von 0.5 pmol PBAN für 120 Minuten zu Pheromon-Drüsen, welche in Grace's Insect Medium mit 5% Antibiotika und Juvenilhormon (50 μg/ml) inkubiert wurden, führte zu einer maximalen Pheromonproduktion von *H. v.* Drüsen *in vitro*. Unter diesen Bedingungen konnte die Pheromonhauptkomponente Z11-16:ALD im Pheromon-Extrakt detektiert werden. Wenn die Pheromon-Drüsen für 3 Stunden in Gewebekultur inkubiert wurden, konnte eine durchschnittliche Menge von 9 ng Z11-16:ALD gemessen werden.

2) Die Fettacyl-Reduktase (FAR) wurde für RNAi-Experimente ausgewählt, da sie eine wichtige Rolle in der Pheromon-Biosynthese spielt. Zunächst wurde untersucht, welches der vier FARs, die in der Pheromon-Drüse gefunden wurden (Vogel *et al.* [107]), das Pheromon-Drüsen spezifische FAR ist. Basierend auf den Ergebnissen der quantitativen real-time PCR konnte ich zeigen, dass FAR1 (gene accession number EZ407233; Vogel *et al.* [107]) hauptsächlich in der Pheromon-Drüse exprimiert wird. Aus diesem Grund wurde FAR1 für die RNAi Experimente verwendet. Erstaunlicherweise konnte ich nach der Inkubation der Pheromon-Drüse in Medium welches 0.1-0.5 μg dsRNA von FAR1 enthielt, nach 3 Stunden die doppelte Menge von Z11-16:ALD (15 ng Z11-16:ALD), im Vergleich zur Kontrolle, nachweisen. Des Weiteren führte die Zugabe von Lipofectamin (Transfektions-Reagent) in Kombination mit dsRNA, für mehr als 3 Stunden, zu einer Reduktion der Pheromonproduktion (1 ng Z11-16:ALD), im Vergleich zu unbehandelten Drüsen und Drüsen, welche nur mit dsRNA inkubiert wurden (2

ng Z11-16:ALD). Somit konnte gezeigt werden, dass Lipofectamin die Aufnahme von dsRNA in die Zellen der Pheromon-Drüse von *H. v.* unterstützt.

RNAi Experimente wurden ebenfalls *in vivo* durchgeführt, um den Effekt von dsRNA von FAR1 auf Drüsen lebender Weibchen zu untersuchen. Wenn dsRNA von FAR1 in frisch verpuppte Larven injiziert wurde, konnte jedoch im Vergleich zu unbehandelten Puppen kein signifikanter Unterschied im Pheromon-Profil von *H. v.* und im Expressionlevel von FAR1 festgestellt werden. Daraus folgt, dass weitere Experimente mit RNAi in *H. v.* durchgeführt werden müssen, um die *in vitro* und *in vivo* Assays zu optimieren.

3) Weiterhin wurden Proteomanalysen durchgeführt, um Unterschiede im Proteom von *in vivo* PBAN-aktivierten und PBAN-nicht-aktivierten Drüsen zu untersuchen. Ich konnte Chaperonin, MItochondriale-Prozessierung-Peptidase, Glutathion-S-Transferase und 3-Hydroxy-CoA Dehydrogenase als diejenigen Proteine identifizieren, welche nur in PBAN-aktivierten Pheromon-Drüsen gefunden wurden. Aufgrund vergleichender Studien mit der cDNA Bibliothek von *H. v.* konnten vier bis dahin noch nicht identifizierte Proteine (Chaperonin, 3-Hydroxy-CoA-Dehydrogenase, Aktin-Depolymerisierungs-Faktor 1 und ein spannungsabhängiger Anionenkanal) in den Pheromon-Drüsen von *H. v.* gefunden werden. Um zu zeigen, dass 3-Hydroxy-CoA-Dehydrogenase (HACD), ein Enzym der ß-Oxidation der Fettsäure Synthese, auch auf Genom-Ebene in PBAN-aktivierten Drüsen hochreguliert ist, wurden qRT-PCR Experimente durchgeführt. Die erste Untersuchung zeigte eine höhere Expression der HACD in PBAN-aktivierten Pheromon-Drüsen, als in PBAN-nicht-aktivierten Drüsen von *H. v.* Weibchen. Dieses Ergebnis konnte jedoch nicht reproduziert werden.

Die Zusammenfassung meiner Ergebnisse:

1) Etablierung eines *in vitro* Assays um die Pheromonproduktion von Sex-Pheromon-Drüsen von *H. virescens* zu analysieren.

2) Es konnte gezeigt werden, dass eines der vier FARs (FAR1) hauptsächlich in der Pheromon-Drüse exprimiert wird und somit wahrscheinlich in die Pheromon-Biosynthese involviert ist. Auf Grund verschiedener Faktoren, war es jedoch nicht möglich, die Pheromonproduktion der Sex-Pheromon-Drüse *in vitro* und *in vivo* zu inhibieren.

3) MIt Hilfe von Proteom-Analysen konnten vier Proteine in der Sex-Pheromon-Drüse identifiziert werden, die zu vor noch nicht in diesem Gewebe beschrieben wurden. Des Weiteren, könnte die erstellte Proteom-Karte der Sex-Pheromon-Drüse von *H. virescens* eine wichtige Grundlage für weiterführende Analysen darstellen, da bis zum jetzigen Zeitpunkt keine Proteomstudien an Sex-Pheromon-Drüsen von *H. virescens* und anderen Lepidoptera Arten durchgeführt wurden.

Abstract

In recent years, the pheromone biosynthesis has been the topic of intensive investigations, but the molecular mechanisms underlying the pheromone production are not completely understood. The control of the pheromone biosynthesis is regulated by PBAN (Pheromone Biosynthesis-Activating Neuropeptide) and in the production of these pheromone components fatty-acyl reductase (FAR) is a key enzyme, which is required to produce the oxygenated functional groups of unsaturated fatty acids. This thesis consists of two parts. The first part is focused on assessing the action of FAR in female *H. virescens* (*H. v.*) in the pheromone biosynthesis. The second part of my thesis is focused on the identification of proteins present in the sex pheromone gland of *H. v.* when activated by PBAN. Specifically, this study sought to answer the following questions: 1) Is it possible to determine the pheromone production of *H. v.* sex pheromone gland in a defined *in vitro* assay?, 2) Is double-stranded RNA-mediated interference RNA (RNAi) of FAR effective to generate a knock-out phenotype in the pheromone profile and the expression level of FAR in *H. v.*? and 3) Is there a difference between the proteome of PBAN-activated and PBAN-non-activated pheromone glands of *H. v.*?

1) *In vitro* sex pheromone production was maximally stimulated in *H. v.* when 0.5 pmol PBAN was added for 120 minutes to glands incubated in tissue medium containing 50 μl Grace's insect medium with 5% antibiotics and Juvenile hormone (50 μg/ml). Under these conditions I could detect the major pheromone component Z11-16:ALD when I extracted the gland afterwards. A mean amount of 9 ng Z11-16:ALD was obtained when pheromone glands were incubated for 3 hours in tissue culture.

2) For RNAi experiments, I assessed whether one of four FARs, that were found in the sex pheromone gland of *H. v.* (Vogel *et al.* [107]), was mainly expressed in the pheromone glands. Based on my quantitative real-time PCR (qRT-PCR) finding that FAR1 (gene accession number EZ407233; Vogel *et al.* [107]) was mostly expressed in the gland and not in the rest of the body, this FAR was used for RNAi. Surprisingly, after incubation of sex pheromone glands in medium containing 0.1-0.5 μg dsRNA of FAR1 for 3 hours, I found around 15 ng Z11-16:ALD and thus almost the double amount of Z11-16:ALD in glands incubated with dsRNA, compared to control glands. When I added lipofectamine, a potent transfection reagent, the pheromone production decreased in combination with dsRNA to 1 ng Z11-16:ALD in comparison to 2 ng Z11-16:ALD in control glands and glands incubated only with dsRNA for more than 3 hours. Thus, lipofectamine is an efficient transfection reagent for delivering dsRNA into sex pheromone gland cells of *H. v.*.

In vivo RNAi studies were also conducted to assess the effect of dsRNA of FAR1 on glands in live females. Injection of dsRNA of FAR1 in zero-day old female pupae of *H. v.* did not result in a significant difference in the pheromone profile and the expres-

sion level of FAR1 in comparison to control females that were not injected with dsRNA of FAR1. Thus, the *in vitro* and *in vivo* RNAi experiments in *H. v.* have to be improved.

3) Proteome analysis was conducted to determine the effect of PBAN on the proteome of sex pheromone glands of *H. v. in vivo*. In this analysis, I identified chaperonin, mitochondrial processing peptidase, glutathione s-transferase and 3-hydroxy-CoA dehydrogenase as the proteins that were only present in PBAN-activated pheromone glands, compared to non-activated glands. Furthermore, compared to the cDNA library of *H. v.*, I found four proteins that had not been identified so far in the sex pheromone gland of *H. v.*, namely chaperonin, 3-hydroxy-CoA dehydrogenase, actin depolymerizing factor 1 and a voltage depending anion channel. With one of the identified proteins, 3-hydroxy-CoA dehydrogenase (HCAD), an enzyme in the ß-oxidation step in fatty acid synthesis, I conducted qRT-PCR to verify whether this enzyme was indeed up-regulated in glands that had been stimulated with PBAN. The first qRT-PCR results showed that HCAD is mostly expressed in pheromone glands from females that were injected with PBAN compared to control glands. However, this result was not reproducible.

In conclusion, my main results are:
First, I have been able to established an *in vitro* assay for the sex pheromone gland of *H.v.* to determine the pheromone production *in vitro*.
Second, I have been able to show that one of the four FARs is mostly expressed in the sex pheromone gland of *H.v.*, and thus the candidate that is most likely involved in the biosynthesis of sex pheromone production in *H.v.*. However, I was not successful in inhibiting sex pheromone production *in vivo* or *in vitro*, but this may be due to a number of factors.
Third, with proteome analysis I identified four proteins in the sex pheromone gland that had not been identified before. Furthermore, the established proteome map of the sex pheromone gland of *H.v.* may serve as an important basis for further analysis, because to my knowledge no studies were conducted so far on the proteome of sex pheromone gland of *H.v.* or any other lepidopteran.

1 Introduction

1.1 The biochemistry and biosynthesis of the sex pheromone of *Heliothis virescens*

The tobacco budworm (*Heliothis virescens* (*H.v.*), Lepidoptera: Noctuidae) is a generalist moth of the Noctuidae family (Lepidoptera) that occurs throughout North and South America [102, 22]. The larvae of *H.v.* attack a wide variety of crops (e.g., tobacco, cotton, alfalfa, clover, flax, soybean, cabbage, pea and tomato) and is extremely resistant to most common insecticides[102, 22].
Female moths of *H.v.* attract conspecific males by the release of a sex pheromone. Pheromones are blends of active substances that are released to the outside by an organism to cause a definite behavioral process in a conspecific organism [44]. Pheromones are important mediators of chemical communication for a variety of individuals [99]. Most lepidopteran females produce and release sex pheromone from glands located between the eighth and ninth abdominal segments [6, 79]. The sex pheromone gland of *Heliothis* species is a complete ring of glandular epithelium between the 8th and the 9th abdominal segments [36, 79]. Most sex pheromone gland cells are secretory cells which are hypertrophied and modified epidermal cells containing an endoplasmic reticulum which is involved in the fatty acid metabolism [8].

The sex pheromone communication system is based on the release of specific pheromone blends from the sex pheromone gland [96]. Sex pheromones of female Lepidoptera are fatty acid-derived compounds with 12 to 18 carbons in chain length and an oxygenated functional group consisting of alcohols, aldehydes and acetate esters with zero to three double bounds [95]. Species specificity in the sexual communication system is achieved by differences in the presence and the amount of specific pheromone components. For instance, most heliothine females share a common major pheromone component and differ from each other only through a different combination in the amount and the presence of minor pheromone components [86, 102]. The main sex pheromone component for *H.v.* is (Z)-11-hexadecenal (Z11-16:ALD) [86, 102, 48, 67, 83]. Minor components found in *H.v.* are hexadecanal (16:ALD), (Z)-7-hexadecenal (Z7-16:ALD), (Z)-9-hexadecenal (Z9-16:ALD), tetradecanal (14:ALD), (Z)-9-tetradecenal (Z9-14:ALD), and (Z)-11-hexadecenol (Z11-16:OH) [86, 102, 48, 67, 83]. In addition, acetates are absent in the sex pheromone blend of *H.v.*, whereas *Heliothis subflexa*, a closely related species, produce acetates [33].

Biosynthesis of these sex pheromones starts with *de novo* synthesis of saturated fatty acids from acetyl-CoA. These saturated fatty acids are modified by defined enzymatic steps in the pheromone gland [37, 99, 12, 41, 85, 96]. The detailed biosynthesis of sex pheromones in *H. v.* is shown in Figure 1.1. Initially, PBAN interacts with a PBAN receptor on pheromone gland cells to induce an influx of extracellular calcium [39, 38, 71, 85] which causes the production of cAMP [73, 71, 85]. Then, cAMP acts through kinases and phosphatases to activate acetyl-CoA carboxylase which initiate the biosynthetic pathway [38, 99, 85]. Acetyl-CoA carboxylase and fatty acid synthetase (FAS) produce 14-, 16- and 18-carbon fatty acid precursors [41, 38, 99, 85]. These precursors are modified by defined enzymes in specific biosynthetic steps to produce a defined pheromone blend [41, 38, 99]. Specific desatures (delta-D11-desatures plays an important role in many species) acts on fatty acids of various chain lengths to form unsaturated fatty acids [41, 38, 99]. Then fatty-acyl reductase (FAR) converts fatty-acyl pheromone precursors to their corresponding alcohols or aldehyde [38, 99, 85, 41]. Additionally, aldehydes could be formed by an oxidation of alcohols and alcohols could be produced by reduction of aldehydes [38, 99]. Production of acetate esters occurs through acetyl transferase which function on alcohols to form acetate esters [38, 99]. This biosynthetic pathway gives rise to the production of a defined blend of chemical components that makes up the sex pheromone of *H. v.*.

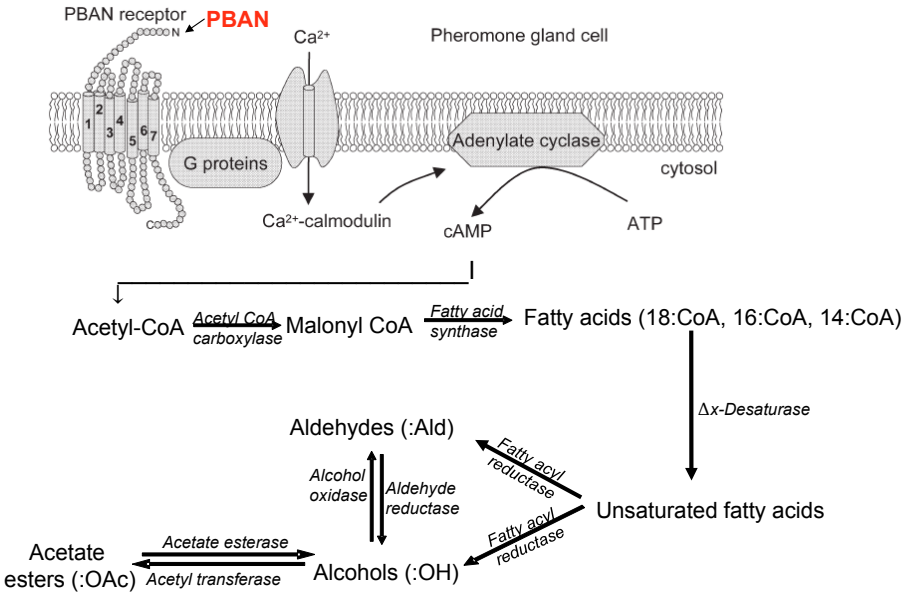

Figure 1.1: Proposed pheromone biosynthesis pathway in *Heliothis virescens* (adapted from Jurenka [38] and Vogel *et al.* [107])

1.1.1 Endocrine regulation of pheromone production in *Heliothis virescens*

Production of the sex pheromone of *H.v.* is under circadian control which is regulated by Pheromone-Biosynthesis-Activating Neuropeptide (PBAN) [76]. PBAN was first identified in the suboesophageal ganglion as a 33-amino acid C-terminal amidated peptide [76]. PBAN belongs to the pyrokinin/myotropin family of peptides with a common C-terminal FXPRLamide [71]. It is produced in the suboesophageal ganglion (SOG) and released from the corpora cardiaca (CC) to stimulate pheromone biosynthesis in the pheromone gland [76, 78, 98]. Studies have demonstrate that PBAN functions directly on cells of the sex pheromone gland [40, 24, 53]. Recently, a PBAN-receptor from pheromone glands of *H.v.* was identified [46]. PBAN binding to this receptor initiates a signal transduction to stimulate pheromone production (Figure 1.1). This induces an extracellular calcium influx and thereby an activation of cAMP as a second messenger [71]. Then, calcium and cAMP induce the signal cascade which results in the production of a defined pheromone blend [73]. Studies have shown that stimulation of *de novo* pheromone biosynthesis by PBAN also occurs in *in vitro* sex pheromone glands of various moth species [74].

The production of sex pheromone can be regulated by the action of other hormones in addition to PBAN. In many insect species, juvenile hormone (JH) is an important endocrine regulator of metamorphosis, reproduction and aging [109]. Production and release of JH is induced by the corpora allata (CA) and several neuropeptides produced by the central nervous system (CNS) [90]. For instance, JH acts on the regulation of pheromone biosynthesis in cockroaches [88] and bark beetles [89]. In Lepidoptera, the role of JH in the regulation of pheromone production has been demonstrated in *Pseudaletia unipuncta* [17] and in *Agrotis ipsilon* [66]. In *Pseudaletia unipuncta*, the corpora allata (CA) were demonstrated as initiators for the release of PBAN and thus JH, which is produced in the CA, may act directly on the release of PBAN. JH may also be involved in the initiation of sex pheromone production in *H. armigera* [19], which is a closely related species of *H.v.*. However, no studies were performed on the involvement of JH in the sex pheromone production of *H.v. in vitro*. Since female receptivity and neuropeptides control JH production, this enzyme is likely a key endocrine regulator of female reproduction [109].

20-hydroxyecdysone (20-E) is an important regulator of egg maturation, as is JH [81, 87, 19] and is produced by the ovaries in adult female moths [10]. In *B. fumigata* and in *Musca domestica*, 20-E is in addition to JH an important factor in the pheromone production [2]. However, the involvement of 20-E in the pheromone production of lepidopteran species has not been clearly defined. For instance, sex pheromone gland potential of *Trichoplusia ni* is regulated by 20-E during the pupal stage [97]. Since it was demonstrated that 20-E regulates the pheromone production in some species, the

question became if 20-E function also in *Heliothine* moths. Preliminary studies in *H.v.*, suggest that 20-E acts directly or indirect in the suppression of pheromone production in female moths [82].

In summary it can be stated that three different types of hormones are important for the regulation of sex pheromones in insects including PBAN for lepidopteran species, JH for beetles and cockroaches and 20-E for Diptera. Since no studies were conducted so far to describe the effect of PBAN on the proteome of the sex pheromone gland of *H.v.* females *in vitro* and *in vivo*, my aim was to identify proteins in *H.v* pheromone glands upon PBAN activation by comparing the proteome of these glands to the proteome of glands were not activated with PBAN. In addition, since an indirect role of JH in influencing the circadian release of PBAN has been demonstrated [66], I will determine the effect of JH on the sex pheromone gland of *H. v. in vitro*. In contrast to JH, there are only few references about an interaction of 20-E and PBAN in lepidopteran species. Therefore, this study will also determine the role of 20-E in the *in vitro* sex pheromone production of *H. v.*.

1.2 RNAi experiments in *Heliothis virescens*

The term RNA interference (RNAi) was first introduced by Fire and coworkers [21] to characterize the observation that double-stranded RNA (dsRNA) can block gene expression when it is applied into *C.elegans*[20]. Double-stranded RNA (dsRNA) can specifically lower the level of the transcript of a target gene, when injected into or absorbed by an organism or induced into a cell or tissue culture. This specificity is based on the complementary sequence of dsRNA and target mRNA. RNAi is an important post-transcriptional control machinery which is capable to degrade a target mRNA [68]. This mechanism is implemented by a specific dsRNA endonuclease (Dicer) which functions on dsRNA to form small interfering RNAs (siRNAs) [68]. These approximately 21 bp dsRNA fragments assembled into a RNA-induced silencing complex (RISC) [68]. This complex find the target mRNAs and cleave them or inhibit their translation. Thus, RNAi has become a powerful and important tool to knock down and examine the function of specific genes, particularly in individuals where the benefit of mutants is impossible [100].

Among the insects, RNAi has been used successfully in the moths *Hyalophora cecropia*[5], *Spodoptera litura*[80], *Bombyx mori*[105], *Manduca sexta*[52], in the dipteran *Drosophila melanogaster*[31] and various other organism [20, 59, 108, 111]. The first report about RNAi in Lepidoptera was a study of Bettencourt and coworkers in 2002 about the effects of hemolin RNAi in *Hyalophora cecropia* [5]. Following this report,

RNAi in Lepidoptera became an important subject in entomology. Among some lepidopteran species, RNAi has been used successfully *in vivo* by injection of dsRNA into pupae [63, 80, 105, 52] and by feeding RNAi to larvae [64, 103].

However, in some cases, efficiency of dsRNA represents a problem. For instance, injection of dsRNA into eggs (e.g., *Bombyx mori* [69]) is efficient to induce a possible RNAi effect, but many embryos do not survive the procedure and thus the quantity of treated embryos is minimal and all of these organism have been damaged by injection of dsRNA [100]. One study showed that midgut aminopeptidase-N gene in larvae of *Spodoptera litura* was down-regulated by injection of dsRNA but declared that attempts to feed dsRNA were unsuccessful [80]. Variation in the midgut environment between individuals could regulate the possible effect of RNAi in feeding experiments [100].

In vitro RNAi studies could avoid these potential problems (e.g., survival rate, tissue damage or the influence of the midgut environment) that are associated with *in vivo* studies. To date, the majority of studies using dsRNA-mediated gene silencing *in vitro* have introduced the dsRNA into cell cultures [15, 11, 104]. Only few RNAi studies demonstrate that dsRNA is an effective method for reducing gene expression in tissue culture [43, 3]. This application is technically simple and affects only the gene target for disruption in the specific tissue. Even though the technique of RNAi has been studied extensively, there is no information available on RNAi in *H. v.*. For an understanding of the genes involved in pheromone production mechanism it would be really helpful if sex pheromone glands could be maintained in tissue culture. RNAi could be then used in a very targeted way. Also, with the aid of an *in vitro* assay, isolated pheromone glands could be studied under defined conditions, so that the impact of chemicals, hormones and enzymes on the pheromone gland could be investigated.

Earlier studies by Rafaeli and coworkers [75, 93, 70, 73, 74] have demonstrated that the application of *in vitro* bioassays of pheromone glands of *Heliothis* spp. are competent to determine the synthesis of sex pheromone components influenced by hormones. These *in vitro* studies were conducted using a successful short-term *in vitro* assay of pheromone glands of *H. armigera* or *H. zea* in which incorporation of radioactive compounds is stimulated by a pheromotropic factor [75, 93]. Studies of Rafaeli and coworkers have demonstrated that cyclic-AMP, as a second messenger system, is involved in the *in vitro* pheromone stimulation [70, 73]. Their finding suggest that the *in vitro* pheromone production is a direct consequence of hormonal stimulation. However, these successful studies used only short-time assays (at most 4 hours of incubation) to determine the pheromone production *in vitro*. In my study I attempt to develop a long-term *in vitro* assay to investigate the RNAi efficiency on pheromone glands *in vitro* to detect the initially gene silencing. Studies of Rafaeli *et al.* used Grace's insect medium and TC-199 as culture medium and therefore I selected Grace's insect medium in my *in vitro* assays.

Summarized, an *in vitro* assay could establish a method that would facilitate the identification of genes and pathway(s) of the pheromone biosynthesis in much more detail. Accordingly, I determined the *in vitro* conditions for culturing the sex pheromone gland of *H. v.*. This lepidopteran species was chosen because the fundamentals of the biosynthesis pathway of pheromone production in this insect have been studied and a cDNA library of *H. virescens* is available in our department. In this study RNAi may be used to investigate the pheromone production mechanism at tissue level of *H.v.*.

In the biosynthesis of sex pheromones, fatty-acyl reductase (FAR) is a key enzyme which is necessary for the production of oxygenated functional groups [56, 38, 99]. This enzyme converts fatty-acyl pheromone precursors to corresponding alcohols [56, 38, 99]. Recently, a substrate specific fatty-acyl reductase was identified from pheromone glands of *Bombyx mori* [56]. A previous study has shown that injection of dsRNA corresponding to the identified FAR results in a successful reduction of the precursor of bombykol in *Bombyx mori* [63]. Because of the key role of FAR in the pheromone biosynthetic pathway, I also focused my attention to this enzyme in *H. v.* for my first RNAi trails. The sequence of four different FARs of *H. v.* is available in our department (Vogel *et. al* [107]). In the present study, I first conducted qRT-PCR experiments to find whether one is a sex pheromone specific FAR of *H. v.*. Once I identified the pheromone gland specific FAR, I used RNAi *in vivo* and *in vitro* to attempt to silence sex pheromone production in the sex pheromone gland of *H. v.*. This study is the first attempt to determine the effect of dsRNA of FAR in the sex pheromone gland of *H. v.*. A successful result in silencing FAR genes could help to analyze the function of specific enzymes in the pheromone biosynthesis in more detail.

1.3 Proteome analysis of the sex pheromone gland of *Heliothis virescens*

Sex pheromone glands are assumed to express proteins for pheromone biosynthesis, energy metabolism and protein synthesis. The analysis of the sex pheromone gland proteome was performed for the following reasons. First, a cDNA library of *H.v.* is available in our department and thus this genome data can be used to identify proteins of the sex pheromone proteome. Second, the sex pheromone gland is a specialized organ specifically for sex pheromone biosynthesis. It might be possible to use the identified proteins of the sex pheromone gland for further analyses of the pheromone biosynthesis on the proteome level. Third, to our knowledge no studies so far has been conducted on the proteome of the sex pheromone gland of *H. v.* and only few proteome studies on other tissues of *H. v.* (e.g., midgut) have been published [50]. With the cDNA library of the *H. virescens* in our department, the next step is to determine the expression and functional analysis of the genes. Microarrays are frequently used for studies

of genes and their function to analyze the gene expression profile. Nevertheless, proteome analysis is necessary, because the amount of mRNA does not have to correspond to the amount of protein, and thus signals in microarray analyses do not indicate the amount of protein because of post-translational modifications, like phosphorylation, or protein-protein interactions [42]. Consequently, proteome analysis remains essential in the field of post-genome analyses and the results can be used to analyze the function of specific genes.

This study was initiated to determine the proteome of the sex pheromone gland in *H. virescens* with regard to differences in the proteome between PBAN-activated and PBAN-non-activated glands. I analyzed the proteome of the sex pheromone gland by 2D gel electrophoresis to establish a proteome profile and a database of all identified proteins as a basis for further analysis. This pheromone gland proteomic analysis should be considered as first approach for a detailed proteome analysis of *H. virescens*.

2 Materials and Methods

2.1 Insects

Heliothis virescens (JEN2, YHD3 and colonies obtained from NC) was reared in environmental chambers at 26 ± 1 °C RH, with a 16:8 h light:dark cycle. The larvae of *H.v.* were fed on an artificial pinto bean diet (composition is attached; see Supporting Information A) . Pupae were sexed and permitted to emerge separately in cups and placed in the climate chamber until further experiments. A 10 % honey-water solution was provided to adults. One to seven day old virgin female adults were used consistently in this study.

2.2 *In vitro* growth of sex pheromone glands

The aim of this study was to develop an *in vitro* assay, which might be an advantageous tool to silence genes in the specific sex pheromone gland tissue.
Females were surface-sterilized by submersing the tip in 0.1% NaOCl for 10 s and washed twice in the incubation medium. The excised sex pheromone glands were cultured singly in a micro well of a 96-microwell plate (MICROTEST™ Tissue Culture Plate 96 well Flat Bottom with Low Evaporation Lid), each well with 50 μl culture medium (see Figure 2.1). All tissue cultures were kept in an incubator at 27°C.

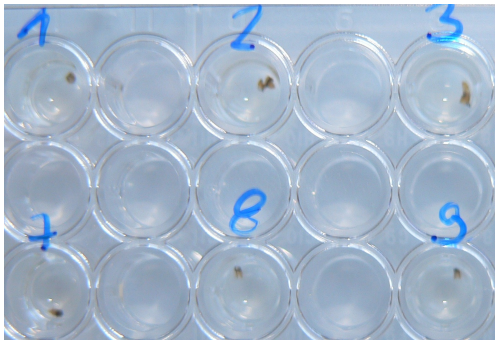

Figure 2.1: Sex pheromone glands of *H.v.* in a Tissue Culture Plate containing Grace's insect medium. Each sex pheromone gland was incubated in a separate well.

To develop an *in vitro* assay, various components have to be checked for their ability to maintain a pheromone gland alive *in vitro*. The first step was to establish a tissue

culture medium for the pheromone gland to determine whether the gland remained alive in the medium. Initially, Grace's insect medium supplemented with 10% FBS (fetal bovine serum), JH (50 μg/ml), 20-E (50 μg/ml) and 10% microbial inhibitors were selected as tissue culture medium because this defined medium has been used in some *in vitro* tissue cultures [49, 70, 23, 53, 94, 62]. As an indicator of viability of the sex pheromone gland *in vitro*, trypan blue was used [18]. The trypan blue exclusion method is based on the fact that alive and functioning cultured glands exclud the trypan blue dye, whereas dead cells turn into blue. Each day, about four glands were removed from the medium and 100 μl of 0.4% trypan blue was added to the pheromone gland. After an incubation for 3-5 minutes at room temperature, penetration or exclusion of the dye was determined by microscopic examinations.

Secondly, to determine the pheromone production, sex pheromone glands of *H.v.* were extracted after being in the medium and analyzed by GC (gas chromatography). PBAN (synthetic HezPBAN from *Heliothis zea*, Peninsula Laboratories, San Carlos, CA) was used to stimulate pheromone production *in vitro*. A concentration of 0.5 pmol was used to induce pheromone production [72, 23]. The PBAN stock solution (200 pmol/μl in 50% methanol and 1N HCl) was diluted with Grace's insect medium or PBS (phosphate buffered saline) to obtain the optimal solvent of PBAN for *in vitro* applications. Because studies have shown that PBAN stimulates a maximum of pheromone production after 120 min of incubation [23, 53], I used this incubation time in my experiments.

Initially, when analyzing the pheromone profile of *H.v.* by GC, I was not able to detected the main pheromone component Z11-16:ALD in pheromone glands incubated in Grace's insect medium supplemented with 10% FBS, JH (50 μg/ml), 20-E (50 μg/ml) and 10% microbial inhibitors, because there were too many other (contamination) peaks. Therefore, various culture mediums were tested for their ability to not interfere with the GC analysis as follows:
a) Grace's insect medium supplemented with 5% antibiotics
b) Grace's insect medium supplemented with 5% antibiotics and 10% FBS
c) Grace's insect medium supplemented with 5% antibiotics and 20-E (50 μg/ml)
d) Grace's insect medium supplemented with 5% antibiotics and JH (50 μg/ml)
e) Excell 401 supplemented with 5% antibiotics and JH
Grace's insect medium supplemented with 5% antibiotics and JH (composition d) was selected as tissue medium in all following assays. Contamination of the tissue culture medium was determined on an agar plate with LB-medium (lysogeny broth medium).

2.3 *In vitro* RNAi experiments

I first characterized four different FARs of *H.v.* (Vogel *et al.* [107]) by qRT-PCR to find which FAR is mostly expressed in the sex pheromone gland and not in the rest of the whole body. Four different pools of sex pheromone glands and one pool of the whole body were homogenized in TRIzol® using a Retsch® bead beater system (Retsch, Haan, Germany, Qiagen). Approximately 500 μl TRIzol® was added to the samples and incubated for 5 minutes at room temperature. Then 200 μl chloroform (or 1-Bromo-3-chloropropanol) was added and the solution was mixed and incubated at room temperature for 2 minutes. The emulsion was mixed again and incubated on ice for 5 minutes. After centrifuging at 10000 rpm for 15 minutes at 4 °C the upper phase was transferred to a new collection tube with 550 μl pre-cooled 2-propanol (Roth®), precipitated on ice for 60 minutes and centrifuged at 13000 rpm for 30 minutes at 4°C. The pellet obtained was dissolved in 1 ml 80 % EtOH and centrifuged at 16000 rpm for 10 minutes at 4°C. The resulting supernatant was removed, a second wash with 80 % EtOH was implemented and the accruing pellet dried for 10 minutes. The dried pellet was dissolved in 50 μl pre-heated (60°C) RNA Storage Solution (Ambion) and incubated at 60°C on a thermocycler for 15 minutes. One μl DNAse (Ambion), 10 μl Buffer (Ambion) and 39 μl RNAse-free Water (Ambion) was added to the emulsion to a final concentration of 100 μl and incubated at 37°C for 30 minutes. The resulting product was purified with the RNA clean-up Kit (Qiagen) according to the manufacturer's instructions. To check the concentration of the total RNA, 1 μl of the isolated RNA was measured by ultraviolet (UV) detection using NanoDrop ND-1000 (Thermo Scientific).

First-strand cDNA was synthesized using Verso™ SYBR® Green 2-Step QRT-PCR Kit Plus ROX Vial (Thermo Scientific, ABgene® UK) according to the manufacturer's instructions, starting with 800 ng of total RNA. Quantitative real-time PCR was performed in a total volume of 25 μl using a 96-well micro well plates (ABgene®, UK). One μl of cDNA (20 ng), 12 μl 2-Step QPCR SYBR green (ABgene®, UK), 0.5 μl ROX Reference Dye (ABgene®, UK), 10 pmol of forward and reverse primer and 9.5 μl RNAse free water (Ambion) were added to each micro well. The reaction for comparative quantification was run at 95°C for 15 min and 40 cycles at 95°C for 15 s, 56°C for 30 s and 72°C for 30 s and for SYBR green analysis the reaction was run with an additional melting-curve. All PCR reactions were performed in duplicates. To evaluate the amplification, two housekeeping genes, Rps 18 and EiFa4, were used as a reference. The reactions were run on Stratagene Mx3000P QPCR System. For the comparative quantification analysis of qRT-PCR, I used the computer program qBASE.

Table 2.1: qRT-PCR primers for RNAi experiments used in this study

Primer name	**Sequence (5′ → 3′)**
HvFAR 1q 139F	ATG AGC ATG TTT GCT GAC GA
HvFAR 1q 267R	CGC CGG TAT AAC TTG GAA GA
HvFAR 2q 122F	CTG TGC TGG CAA GCT GAA TA
HvFAR 2q 216R	GCC AAA GCA TAT CGT TGA GG
HvFAR 3q 137F	AAG GCG TGA AAT CTG AAG ACA
HvFAR 3q 266R	CCG ATT TCC ATG ACA TTT CC
HvFAR 4q 4F	TCA TGA GAA GGT GCA TGA GG
HvFAR 4q 151R	CTC AGC CAA ATG CTT CGT AA
EiF4A 499F	GTG CTG GAT GAA GCT GAT GA
EiF4A 610R	GCA TGG TAG CAG ACA GCA GA
RPS18 245F	GGT TCC TCA ACA GGC AGA AG
RPS18 328R	CCT CAC GAA GCT TTG AGT CC

For the RNAi test *in vitro*, tissue cultures were admitted with dsRNA corresponding to the sex pheromone specific FAR. For the experiments, cDNA of pheromone glands injected with PBAN or PBS and cDNA of the whole body of *H.v.* were used.
Various forward PCR primers and reverse primers (see table 2.2) were used to synthesize a region of the fatty acid reductase gene that contained a T7 promoter region (TAA TAC GAC TCA CTA TAG GG) on both the sense and antisense strands followed by sequences specific for the targeted genes.

Table 2.2: RNAi primers used in this study

Primer	**Sequence (5′ → 3′)**
HvFAR 1 1282R	TAA TAC GAC TCA CTA TAG GGT ACC GTG GAC TCT TCC CAA C
HvFAR 1 886F	TAA TAC GAC TCA CTA TAG GGT TAG GCA ACT GGT TTG GA
HvFAR 1 1667R	TAA TAC GAC TCA CTA TAG GGT ACG GCA AAA CAT GGA AAC A
HvFAR 1 1235R	TAA TAC GAC TCA CTA TAG GGC GCC GGT ATA ACT TGG AAG A

The PCR reaction was done under the following cycling conditions: 94°C for 2 min followed by 5 cycles of 94°C for 30 s, 65°C for 30 s, 72°C for 1 min, 35 cycles of 94°C for 30 s, 77°C for 30 s, 72°C for 1 min a final extension of 72°C for 3 min.
The PCR products were purified with the MiniElute® PCR Purification Kit (QIAGEN) and were then used as templates to synthesize dsRNA. The dsRNA was produced using the MEGAscript® RNAi kit (Ambion Inc., Austin, TX) according to the manufactures recommendations to obtain the corresponding long dsRNA without an additional annealing step. The *in vitro* transcription products were assessed for integrity on a 1% agarose gel, diluted in 6xOrange Loading Dye Solution (Fermentas) and the concentration was calculated by measuring its absorbance at 260nm.

For *in vitro* experiments, dsRNA of FAR was added directly into the tissue culture medium (1-5μl/well). To amplify the possible effect of RNAi *in vitro*, I tested lipofectamine in combination with dsRNA in tissue culture of the pheromone glands. This reagent is used to introduce a transfection of dsRNA into cells of tissue culture. The *in vitro* effect and the functionality of dsRNA on pheromone production was examined by comparing the production of the major component (Z11-16:ALD) and a minor component (16:ALD) to obtain a kind of pheromone profile. This pheromone profile could be used as a comparison to the pheromone production in *in vitro* glands without dsRNA.

2.4 *In vivo* RNAi experiments

RNAi experiments were also conducted *in vivo*. To determine the effect of RNAi *in vivo*, the same dsRNA of the sex pheromone specific FAR of experiments *in vitro* were used. In order to investigate the time point when FAR may be switched off by dsRNA, the pheromone production and the transcript level of FAR was observed at different time points. Pheromone glands and RNA were extracted after 0 to 6 hours (day 0) and after 24 to 36 hours (day 1) of females emerging from their pupal stage. For the injection of dsRNA into pupae of *H.v.*, the dsRNA of FAR was injected (5μg) in the abdominal tip of one-day old pupae using a 10 μl microsyringe (Hamilton). As a control, pupae were injected with 5 μl buffer (EDTA,Tris). Extracted sex pheromone glands were used for GC analysis to analyze the pheromone profile and for RNA extraction to determine differential transcription levels of FAR. For GC analysis, emerged female moths were injected with PBAN to stimulate pheromone production (see section below).

2.5 Gland extraction and GC analysis

To analyse the pheromone production of glands cultured *in vitro*, one μl PBAN stock solution was diluted in 399 μl Grace Insect medium to obtain a dilution of 5 pmol PBAN/ul, which is similar to the amount of PBAN that is generally injected in live females (e.g. [33]). Five μl of this solution was added to 45 μl tissue culture (i.e. 0.5 pmol) as defined above. After 120 minutes, the sex pheromone gland was removed from the medium and placed in a glass vial containing 50 μl hexane with 40 ng of pentadecane as internal standard, to determine the samples by GC. After 30 minutes, the sex pheromone glands were removed from the vial and the hexane extracts were stored at -20°C until GC analysis.

In the *in vivo* experiments, females of *H.v.* were injected with synthetic HezPBAN or with saline before the glands were extracted. For this 3 μl PBAN stock solution (200 pmol/μl in 50% methanol and 1N HCl) was diluted in 157 μl saline to obtain a dilution of 3.75 pmol PBAN/ul. Two μl of this solution (i.e. 7.5 pmol) was injected between the 8th and 9th abdominal segment of a female with a 10 μl syringe (31 gauge needle, Hamilton, Reno, NV). One and half hour after injection, the sex-pheromone gland of *Heliothis virescens* were extracted in hexane as described above.

For the GC analysis, the glands were reduced to 2 μl under a gentle stream of N_2. The 2 μl hexane extract and 2 μl octane was injected in a glass insert within a crimp-capped vial. The total extraction was injected into a HP7890 gas chromatograph (GC) linked with a high resolution polar capillary column (DB-WAXetr [extended temperature range]; 30m x 0.25mm x 0.5 μm) and a flame-ionization detector (FID). The column temperature was defined to 60°C for 2 minutes, after gone up to 180°C by 30°C/min and finally risen to 230°C by 5°C/min to elute all components of the pheromone gland. Then the column temperature was heated up to 245°C at 20°C/min and kept for 15 min to clean the column before the next injection.

To ensure the correct analysis of the compounds five samples with different medium and different concentrations of PBAN were checked by GC-MS. More precisely, three samples with Grace's insect medium containing a) 0.05 pmol, b) 0.5 pmol and c) 5 pmol PBAN and two samples with Excell 401 containing a) 0.5 pmol and b) 5 pmol PBAN were analyzed to obtain the optimal culture medium. The samples were injected into a HP6890 GC coupled to Massspec MS002 (Micromass, Manchester, UK) with electron (EI) at 70 eV, using a 30m x 0.25mm x 0.25μm DB-Wax column. The resulting data was analyzed with a spectral database (Wiley MS library v7) and was compared to the compounds of the samples.
For all experiments, the total amount of Z11-16:ALD and 16:ALD produced in the gland was determined by comparing the integrated pheromone peak area to the area of the internal standard and calculated as ng Z11-16:ALD and 16:ALD.

To compare possible difference in the pheromone profile *in vivo*, we conducted the following statistical analysis using SAS (SAS, 2009). Statistical analyses of data were done for *in vivo* experiments with FAR1. The pheromone profile of females injected with dsRNA of FAR1 was compared to the pheromone profile of females injected with buffer. First the the total amounts of pheromone were log-transformed to stabilize the variance. We used a MANOVA test to compare the overall pheromone composition between these two groups of females. To compare the differences in the relative amounts of each component, we conducted a 1-factor analysis of variance (ANOVA) using the GLM procedure of SAS (SAS, 2009) in which the treatment was viewed as fixed.

2.6 Protein analysis

To determine which proteins are found in the sex pheromone glands after PBAN-activation compared to the non-activated pheromone glands of *H.v.*, I used the Two-Dimensional Gel Electrophoresis, which is a powerful tool to identify differentially expressed proteins. For proteome research, I started by analyzing and identifying the proteins from *in vivo* glands, but at the end of my research period I also extracted proteins from *in vitro* glands.

For the *in vivo* analysis, 30 females of *H.v.* were injected with synthetic HezPBAN as described above and another pool of 30 females were injected with saline. One and half hour after injection, the sex pheromone glands of *H.v.* were dissected for protein analysis.

For the *in vitro* analysis, 30 pheromone glands of *H.v.* were incubated in tissue culture containing 0.5 pmol PBAN for 120 minutes as described above while 30 pheromone glands were incubated in medium without PBAN (see description above). After 120 minutes, the sex pheromone glands were removed from the medium for protein analysis.

The *in vivo* protein analysis was first determined by the Coomassie blue method. After this method, the *in vivo* and *in vitro* effect of PBAN were compared by Refraction 2D (NH DyeAGNOSTICS). Both methods of protein analysis differ from each other only by the staining technique, the initiating steps are common and as follows. At the outset of the protein analysis, pheromone glands were placed in the homogenization buffer (30 glands per 600 μl homogenization buffer) and then homogenized with a potter (Heidolph Instruments RZR 2020) on ice. After homogenizing thoroughly for at least 5 minutes, the tubes were centrifuged at 1500 x g for 10 min (4°C). The resulting supernatant was collected in a fresh tube. The pellet was resuspended completely in 100 μl homogenization buffer by vortexing and rehomogenized as above. At last the two supernatants were pooled and stored until further use at - 80°C.

A Bio-Rad Protein Assay were conducted, which is based on the method of Bradford, to obtain the concentration of the protein samples. The assay was implemented according to the manufacturer's instructions. Contamination, such as small ionic molecules, nucleic acid and lipids, were removed by precipitating the proteins with trichloroacetic acid (TCA, Sigma®) [91]. 50 μl TCA was added to 500 μl of protein sample. The solution was vortexed and incubated for 1 h on ice. After incubation, the samples were centrifuged at maximum speed for 10 min (4°C). The resulting supernatant was carefully removed. The pellet was washed with 1 ml of 100 % acetone (Roth®) and incubated for 15 min on ice. The samples were centrifuged at maximum speed for 10 min (4°C). The acetone wash was repeated. The resulting pellet was air dried and 300 μl of lysis buffer was added.

The 2-D Quant Kit (GE Healthcare) was used for the quantitative analysis and to remove any remaining contaminations of the samples. Before using the Kit, the samples were equilibrate for 2 h at 25 °C in a thermo mixer (eppendorf, 1000 rpm) and centrifuged for 30 min. The resulting supernatant of the protein samples were analyzed according to the manufactures recommendations to obtain the concentration of the solution. The desired amount of the protein sample, bromophenol blue and lyses buffer were mixed and loaded on an IPG strip (GE Healthcare, pH 3-11).

In the *in vivo* experiment, a concentration of 3.29 μg/μl for glands injected with PBAN and 2.36 μg/μl for glands injected with saline were obtained with the 2-D Quant Kit. For the pool of glands injected with PBAN, 91.24 μl sample (300 μg), 10 μl bromophenol blue and 348.76 μl lysis buffer were mixed and for the pool of glands injected with saline, 127.12 μl sample (300 μg), 10 μl bromophenol blue and 312.88 μl lysis buffer were mixed and loaded on an IPG strip. Thus, for each pool of glands, injected with saline or PBAN, a single 2D gel was produced.

For protein analysis with Refraction 2D, the effect of PBAN was compared between *in vivo* and *in vitro* experiments. For *in vivo* analysis, I yielded a concentration of 10.21μg/μl for glands injected with PBAN and 7.19 μg/μl for glands injected with saline. For the *in vitro* studies I obtained a concentration of 5.78 μg/μl for glands incubated with PBAN and 5.66 μg/μl for control glands. The Refraction 2D Labeling Kit was performed using the protocol and dyes (G-Dye 100, G-Dye 200 and G-Dye 300 of DyeAGNOSTICS which conform to Cy2, Cy3 and Cy5 of the Ettan™ DIGE system of GE-Healthcare). This technique allows that samples of both treatments can be analyzed on one single 2D gel. For Refraction 2D, each protein sample was diluted with lysis buffer to obtain a concentration of 50μg/10 μl. Of the *in vivo* produced samples, 10 μl (50μg) of proteins extracted from glands injected with PBAN was dyed with G-Dye 300, 10 μl (50μg) of proteins extracted from glands injected with saline was dyed with G-Dye 200, 10 μl (50μg) of the internal standard (pool of both samples) was dyed with G-Dye 100, 10 μl bromophenol and 404 μl lysis buffer were blended and this combina-

tion was loaded on one IPG strip. The same batch was done as a replicate but G-Dye 300 and G-Dye 200 were interchanged to avoid any possible effect of the dye on the intensity of the protein spot.

For examination of *in vitro* produced samples, 10 μl (50μg) of proteins extracted from glands incubated with PBAN dyed with G-Dye 300, 10 μl (50μg) of proteins extracted from glands incubated without PBAN dyed with G-Dye 200, 10 μl (50μg) of the internal standard dyed with G-Dye 100, 10 μl bromophenol and 404 μl lysis buffer were mixed and loaded on one IPG strip. Also a technical replicate was produced by interchanging G-Dye 300 and G-Dye 200.

The appropriate amount of the samples was pipetted into a chamber of the strip holder and overlaid with an IPG-strip. To prevent precipitation of the urea, approximately 2 ml mineral oil (BIO-RAD®) was pipetted over each IPG strip. The passive rehydration ensued overnight at 20°C in a Protean IEF Cell System (BIO-RAD®). For 24 cm IPG-strips the isoelectric focusing program runs for 8 hour at 50μA per strip, at 500V for 1h; 500V to 1000V in 1h; 1000V to 8000V in 3 h and additional at 8000V for 3h. After the isoelectric focusing I equilibrated the samples to saturate the IPG strip with the SDS equilibration buffer. First, the strip was incubated in 1 % DTT (1,4-Dithiothreit from Roth®, in SDS equilibration buffer) for 30 min on a shaking platform. DTT dissociates the disulfide bond of the proteins [29]. After the incubation the strip was transferred in 2,5 % IAA (Indole-3-acetic acid Amersham, in SDS equilibration buffer) and incubated for 30 min on a shaking platform. IAA carboxymethylated the free cysteine residues of the disulfide bond [29]. Following the equilibration of the IPG gel strips, the protein samples were separated in the second dimension on an SDS-PAGE gel on the basis of their molecular mass using Ettan Daltsix system (GE Healthcare). The SDS PAGE contains 12% acryl amide, 0.375M Tris HCl (pH 8.8), 0.1% SDS, 0,1% APS and 0.04% TEMED. The strips were placed on the acryl amide gel and run for 1 hour at 6 W and for 4 h at 20 W/gel (Ettan Dalt). Electrophoresis was done in a vertical slab gel apparatus (GE Healthcare) for Ettan DALT 6 gels. Protein ladders (Precision Plus Protein™ Standard Plugs) were run in parallel.

For the Coomassie blue method, the proteins were fixed overnight in 40 % ethanol and 10 % acetic acid and then stained with colloidal Coomassie blue over night. The resulting 2D protein patterns were scanned using the program PDQuest (BioRad Laboratories, Hercules, CA).

For Refraction 2D, the gels were scanned directly after running the SDS PAGE, using a FUJI-FILM 9000 scanner.

I analyzed the obtained protein patterns using the computer program Delta 2D (Decodon). With Delta 2D, the two different Coomassie-stained gels were overlaid, using spots which are common in both 2D gels. The protein spots were matched

automatically by SmartVectors™. The resulting gel image is a matched map of both gel images. After the automatic wrapping, I manually selected spots that seemed to be the same in both gels for matching. Thus, by wrapping these gel images, differences in spot position were eliminated. Afterwards, I qualitatively and quantitatively analyzed differences in spot pattern and in expression profiles of all spots. Additionally, Delta 2D used algorithms to detect protein spots, the result of which is displayed in a statistics table, including the maximum, minimum, or the mean intensity of a protein spot. The protein spots I picked by hand from the 2D gels that had been stained with Coomassie. After picking, the spots were destained, trypsinized and extracted following the protocol of Pauchet *et al.* [65]. The resulting peptide mixtures were analyzed by MALDI-TOF/MS. The MALDI-TOF spectra searches were conducted in the Protein Lynx Global Server software (PLGS2.2). The resulting peptide sequences were queried against the MS Ento database (http://nougat.ice.mpg.de/msEnto/) to obtain the protein sequence for a single spot. Protein sequences that were not identified directly in the cDNA library of *H. virescens* sex pheromone gland and *H. virescens* Heliobase were queried in further libraries such as, *H. armigera* Genomic DNA and butterflybase in the MS Ento database. All identified protein sequences were queried against NCBI_insecta (http://blast.ncbi.nlm.nih.gov/Blast.cgi) to identify the corresponding proteins.

One of the identified protein spots, spot 27, which was identified as 3-hydroxyacyl-CoA dehydrogenase, was further analyzed using qRT-PCR. The primers used for this experiment are listed in table 2.3 (called Pspot27).

Table 2.3: qRT-PCR primers for spot 27 (3-hydroxyacyl-CoA dehydrogenase) used in this study

Primer	**Sequence (5′ → 3′)**
Pspot27 qF1	CAG TGA ACC CAC CGT ACT ACG
Pspot27 qF2	TGG ACC AAG AAG GAG GTC TG
Pspot27 qR3	ATA CGG TTG AGC ACG AAT CC
Pspot27 qR4	TCG ACC AAC CTC CAA ACT TC

In order to determine the *in vivo* expression level of 3-hydroxyacyl-CoA dehydrogenase, total RNA was harvested from a pool of 10 pheromone glands of *H.v.* injected with PBAN, from a pool of 10 pheromone glands of *H.v.* that were injected with saline and from ten *H.v.* bodies , as well as from a pool of 10 glands of *H. armigera* injected

with PBAN and from a pool of 10 pheromone glands of *H. armigera* injected with saline. To investigate the *in vitro* expression level of 3-hydroxyacyl-CoA dehydrogenase, total RNA was harvested from 10 glands of *H. v.* (+PBAN1) that were incubated in tissue culture containing PBAN and from 10 glands of *H. v.* (-PBAN1) that were incubated in tissue culture without PBAN.
Additionally, one pool of glands of *H. v.* injected with PBAN (+PBAN2) was incubated in hexane for GC analysis and then processed with Trizol® for RNA extraction. This treatment was conducted to assess whether the same pool of glands could be used for analyzing the pheromone production as well as for the expression level. The qRT-PCR with all these pools was conducted as described above (section 2.3).

3 Results

3.1 *In vitro* analysis of the pheromone production

When pheromone glands of *H.v.* were cultured in Grace's insect medium supplemented with 10% FBS, JH (50 μg/ml), 20-E (50 μg/ml) and 10% microbial inhibitors, glands were able to survive for 5 days which was verified by the trypan blue coloring. Some blue cells were obtained after 6 days of incubation in the medium. This means that sex pheromone glands of *H.v.* were able to stay alive for even more than 5 days *in vitro*. After finding this defined medium in which sex pheromone glands were alive for 5 days, the pheromone production of those glands was determined by GC analysis. When 0.5 pmol PBAN was added to the tissue culture to stimulate sex pheromone production *in vitro*, I was not able to detect the main pheromone component Z11-16:ALD of glands incubated in the defined tissue culture medium, because of many additional peaks that were probably contamination peaks from the medium. Therefore, the addition of various culture medium components were tested separately (composition a-e, see in Materials and Methods) for their ability to not interfere with the GC analysis.

First, the GC analyses of hexane extract of glands incubated Grace's insect medium supplemented with 10% antibiotics (composition a) showed a flood of peaks, so that the pheromone peak was not distinguishable. When using 5% antibiotics, the GC analysis resulted an identifiable Z11-16:ALD pheromone peak (greater than 3 ng).

When FBS (composition b) was added to the Grace's insect medium supplemented with 5% antibiotics, the GC analysis of this samples showed a flood of peaks that were not corresponding to the pheromone peaks. Therefore, FBS was not used in the tissue culture medium in all following assays.

Extremely low results were obtained when 20-E (composition c) was added to the Grace's insect medium supplemented with with 5% antibiotics. Accordingly, 20-E was not used in the incubation medium in all following assays either.

The production of the major pheromone component was increased in pheromone glands incubated in Grace's insect medium containing 5% antibiotics, when 50 μg/ml of JH (composition d) was added to the medium.

When Excell 401 (composition e), with 5% antibiotics and 50 μg/ml of JH, was used as incubation medium, extraordinary variable results were obtained, with a pheromone production from most often non-detectable ranges to very high pheromone levels. In

contrast, a more consistent, although also variable, production of pheromone in isolated glands from *H.v.* was obtained in Grace's insect medium with the supplements of composition d. Therefore, Grace's insect medium (composition d) was selected as tissue culture medium in all following assays.

In all cases 0.5 pmol PBAN was added to the tissue medium around 120 min before the gland was extracted for further analysis. In addition to Grace's insect medium as solvent for PBAN, PBS was also tested, because PBS is used in *in vivo* application of PBAN [33]. In Figure 3.1, the amount and the percentage of Z11-16:ALD (major component) and 16:ALD (minor component), were compared in sex pheromone glands incubated in Grace's insect medium supplemented with 5% antibiotics and JH (50 μg/ml) and added with PBAN diluted in Grace's insect medium or in PBS. The amount of pheromone was higher in sex pheromone glands where PBAN was dissolved in Grace's insect medium, than where PBAN was dissolved in PBS (see Figure 3.1).

In conclusion, these experiments show that the sex pheromone gland cells of *H.v.* did not need any serum, 20-E or a high concentration of antibiotics in the tissue culture medium for survival and pheromone production. Since an obvious production of Z11-16:ALD was observed in tissue culture medium containing Grace's insect medium, 5% antibiotics and JH (50 μg/ml), this composition was chosen for the RNAi experiments.

After defining the best medium for the pheromone glands, I determined the sex pheromone production in the pheromone glands for different incubation times: 3 h, 6 h, 24 h, 72 h and 96 h. I obtained variable results, with Z11-16:ALD ranging from 1 ng/gland to 20 ng/gland (see Figure 3.2 and Figure 3.3). The Figures show an individual bar for each individual measurement of Z11-16:ALD in one sex pheromone gland. When sex pheromone glands were incubated for around 3 h in tissue culture medium, I found a mean of 9 $\pm$ 6,46 ng Z11-16:ALD in extracted glands (see Figure 3.2).

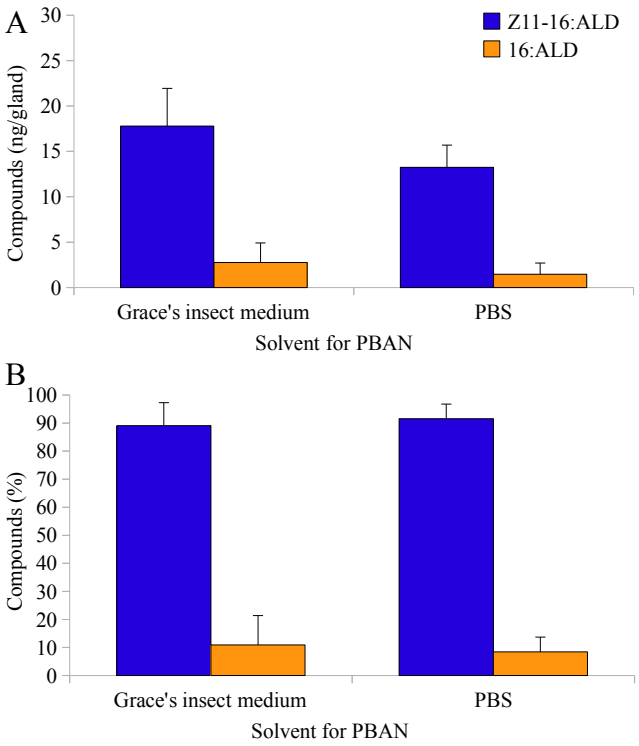

Figure 3.1: Comparison of the sex pheromone compounds, Z11-16:ALD and 16:ALD, in ng/gland (A) and in relative percent (B). Pheromone glands were incubated in Grace's insect medium containing 0.5 pmol PBAN diluted with Grace's insect medium or PBS. Bars represent averages of the standard derivations (n = 10 for both treatments).

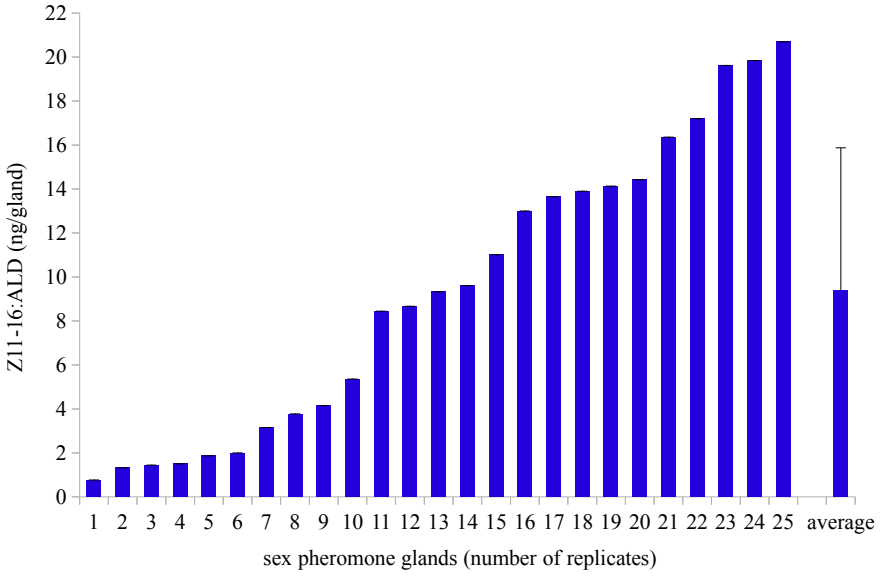

Figure 3.2: *In vitro* production of Z11-16:ALD in *H. v.* sex pheromone glands after 3 hours of incubation with 0.5 pmol PBAN. The x-axis represent the number of replicates on the left and the average (± SD) of all replicates on the right

Small amounts of pheromone was found when the sex pheromone glands were incubated for more than 3 hours. As shown in Figure 3.3 the amount of Z11-16:ALD decreased with prolonged times of incubation. When pheromone glands were cultured for 6 hours, their pheromone production dropped to 1,86 $\pm$ 1,72 ng/gland compared to 9 ng/gland after an incubation of 3 hours (Figure 3.3 A). This means that the production decreased about more than half after an incubation for 6 hours. At an incubation time of 24 hours (see Figure 3.3 B) and 96 hours (see Figure 3.3 D) a massive reduction in the pheromone production was found compared to 3 hours of incubation, as the Z11-16:ALD concentration 0.8 $\pm$ 0.7 ng/gland. Extremely variable results extending from 1 ng/gland to 6 ng/gland (1,02 $\pm$ 1,24 ng), were observed when pheromone glands were incubated for 72 hours (see Figure 3.3 C). These results show that there was a large variation in the amount of pheromone present in the glands at all incubation times (see Figure 3.3).

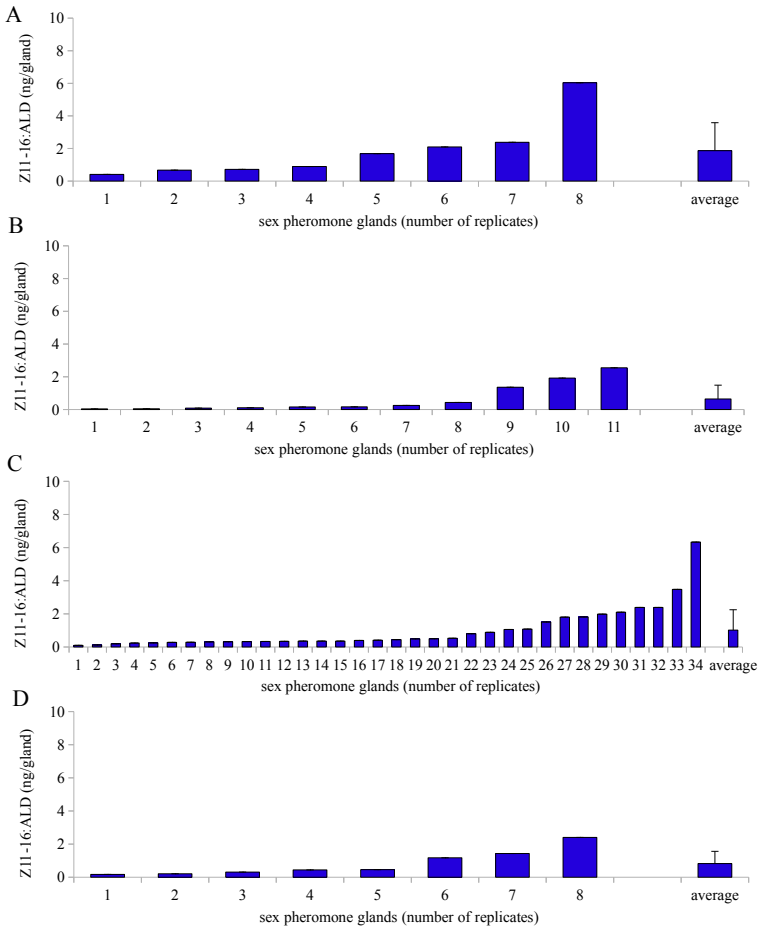

Figure 3.3: Z11-16:ALD present in *in vitro* PBAN-stimulated *H.v.* sex pheromone glands at different time points. Pheromone glands were incubated for 6 h (A), 24 h (B), 72 h (C) and 96 h (D) in medium containing 0.5 pmol PBAN. The x-axis represent the number of replicates and shows the pheromone production of each individual gland on the left and the average ($\pm$ SD) of all replicates on the right.

As an overview, Figure 3.4 shows the *in vitro* stimulation of Z11-16:ALD production in pheromone glands of *H.v.* at different times.

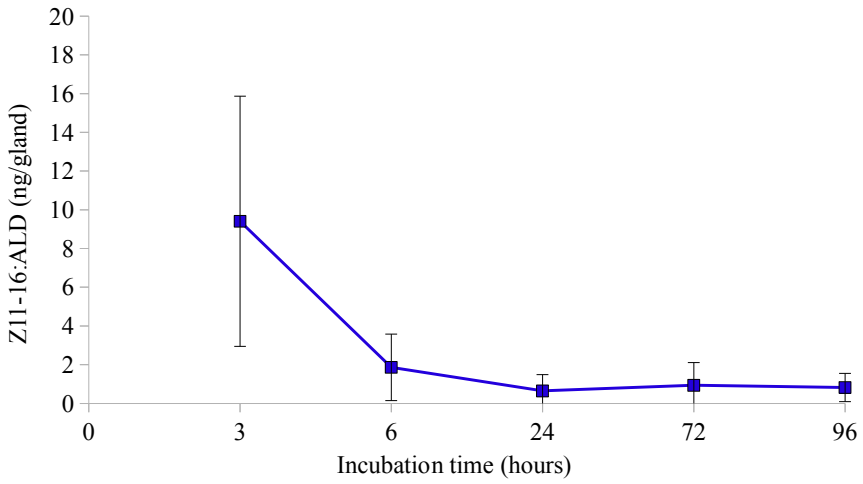

Figure 3.4: Time-course of Z11-16:ALD production in PBAN-stimulated pheromone glands of *H.v.*. Each point represents the mean of 8-40 sex pheromone glands of *H.v.* at different time points. Thin bars represent the standard derivations.

As described above, the major pheromone component, Z11-16:ALD, was chosen because of the fact that minor pheromone components were difficult to distinguish from contaminations in GC analysis. This was generally true for incubation times longer than 24 hours. When glands were incubated for up to 24 hours, it was possible to identify the minor component 16:ALD in the GC analysis as well (see Figure 3.5). To determine if the ratio of the two pheromone components were the same *in vitro* as *in vivo*, the ratio of the major component Z11-16:ALD and the minor component 16:ALD were compared. Figure 3.5 shows that *in vitro* Z11-16:ALD is the major component and 16:ALD is one of the minor components in pheromone glands incubated in medium, similar to what is found in the pheromone glands extracted *in vivo* [33]. Normally, the *in vivo* pheromone composition is referred relative to the amount of the major component (Z11-16:ALD), or as a relative percentage of all components relative to the total amount of pheromone components [33]. However, I calculated the *in vitro* amount of Z11-16:ALD and 16:ALD by comparing the integrated pheromone peak area to the area of the internal standard and, calculated the ng Z11-16:ALD and 16:ALD and analyzed the relative percentage of Z11-16:ALD and 16:ALD relative to the total amount of both pheromone components.

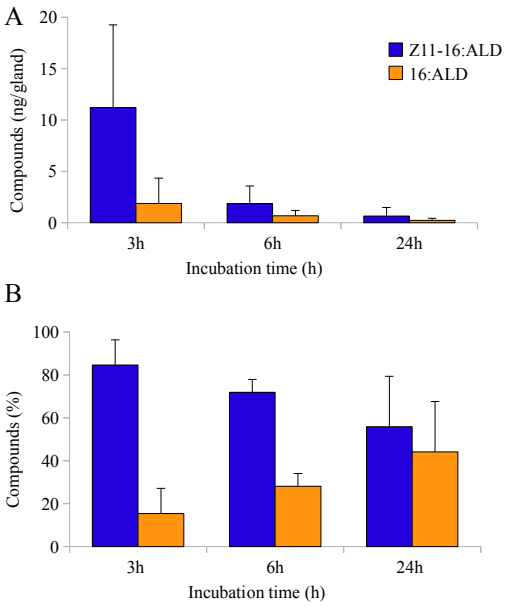

Figure 3.5: Comparison of Z11-16:ALD and 16:ALD pheromone production at different time points in *H.v.*. Pheromone glands were incubated in medium containing 0.5 pmol PBAN for 3 h, 6 h and 24 h to compare the relative amount (A) and the relative percent (B) of Z11-16:ALD and 16:ALD. Thin bars represent the standard derivations (3h: n = 25; 6h: n = 8; 24h: n = 11).

3.2 *In vitro* RNAi assay

3.2.1 Characterization of FAR by qRT-PCR.

qRT-PCR experiments were designed to determine which FAR was mostly expressed in the sex pheromone glands of *H.v.* compared to the rest of the body. I assayed four FARs and examined the expression level in cDNA derived from a) four different pools of 10 glands each injected with PBAN, b) three pools of 10 glands injected with PBS and c) a pool of 10 bodies from *H.v.*, comprising all tissue from males and females. As shown in Figure 3.6, FAR1 (3.6A) was only expressed in the pheromone gland, FAR2 (3.6B) was expressed in all tissues , FAR3 (3.6C) was mostly expressed in the gland and slightly in the body and FAR4 (3.6D) was only expressed in the body. The qRT-PCR for FAR1 was repeated, because of the high standard deviation, which was due to pipetting the cDNA template separately (see Figure 3.6). In the repeated experiment, I used a master mix including the cDNA template. As shown in Figure 3.7, the result that FAR1(gene accession number EZ407233 (Vogel *et al.* [107]) is only expressed in the pheromone gland was reproducible. These findings indicate that FAR1 is involved in the sex pheromone production of *H.v.*, because this FAR is the one which is only expressed in the pheromone gland. Based on these findings, I chose FAR1 for RNAi experiments.

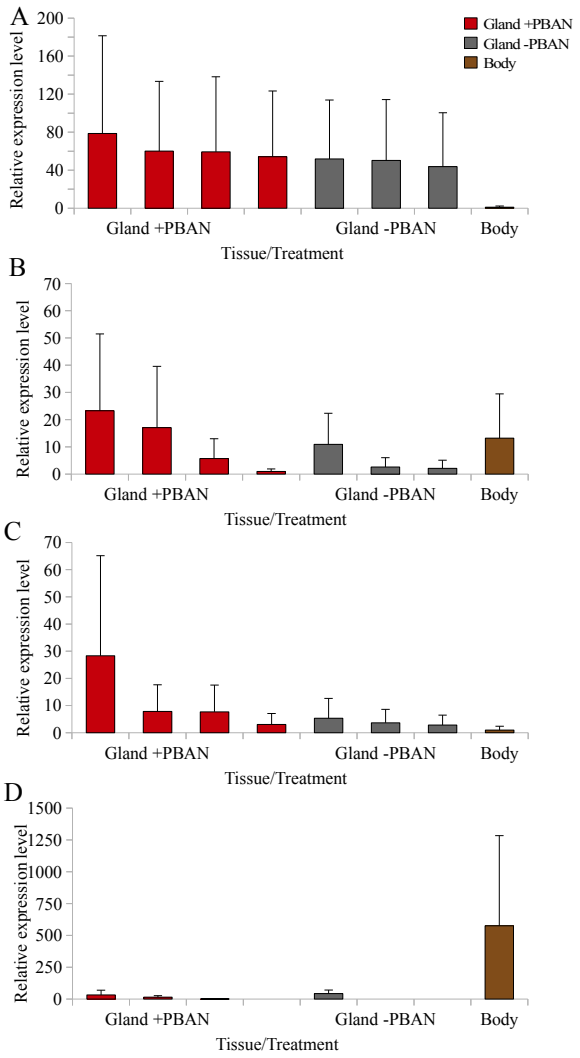

Figure 3.6: Expression levels (± SEM) of FAR1 (A), FAR2 (B), FAR3 (C) and FAR4 (D) in 4 pools of sex pheromone glands injected with PBAN (red bars), 3 pools of glands injected with saline (grey bars) and one pool of the body of *H.v.* (brown bars).

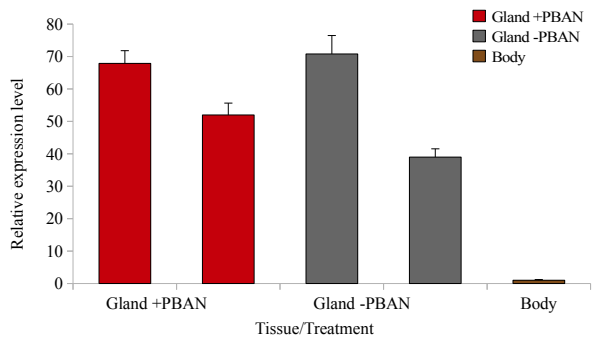

Figure 3.7: Expression level (± SEM) of FAR1 in 4 pools of sex pheromone glands injected with PBAN (red bars), 3 pools without PBAN (grey bars) and in one pool of the body of *H.v.* (brown bars).

3.2.2 *In vitro* RNAi assay with FAR1

To test RNAi in *H. v.*, I used the *in vitro* assay that I established previously (described in section 3.1), added 0.1-0.5 μg dsRNA of FAR1 to each individual sex pheromone gland in tissue culture and measured the pheromone production by GC analysis to compare the amount of Z11-16:ALD with control glands (i.e. where FAR1 was not added to the medium). When sex pheromone glands were incubated for 3 hours in medium containing dsRNA of FAR1, variable amounts of Z11-16:ALD were obtained, ranging from 5 ng to 32 ng Z11-16:ALD (see Figure 3.8). Much lower amounts of pheromone was detected when pheromone glands were incubated for 6 hours (see Figure 3.9A) in medium containing dsRNA of FAR1. In this case, the amount of Z11-16:ALD ranged from nearly non-detectable levels to 3 ng Z11-16:ALD. When pheromone glands of *H.v.* were incubated for 3 days in tissue culture including dsRNA of FAR1, an amount of 0.5 ng to 4 ng Z11-16:ALD was found (see Figure 3.9B, which was similar to the amounts found after 6 hours.

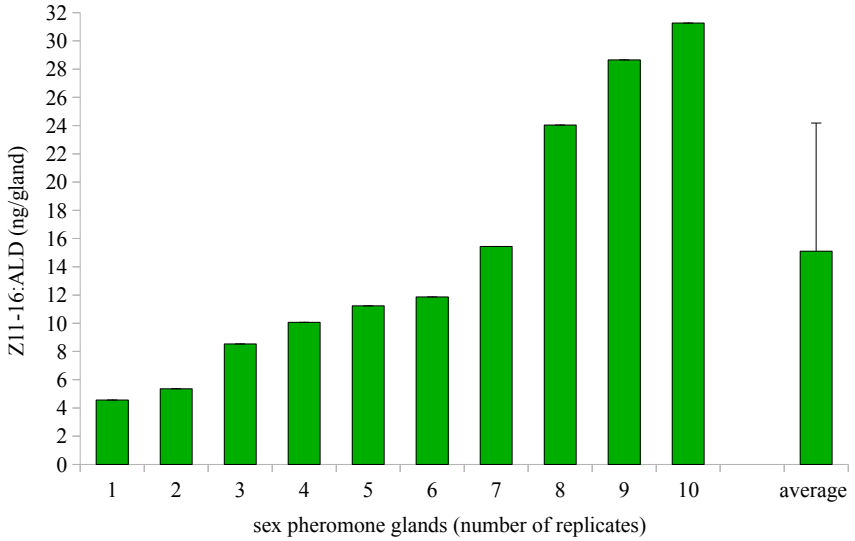

Figure 3.8: *In vitro* PBAN-stimulated Z11-16:ALD production after 3h in *H.v.* sex pheromone glands treated with 0.1-0.5 μg dsRNA of FAR1. The x-axis represent the number of replicates and shows the pheromone production of each individual gland on the left and the average ($\pm$ SD) of all replicates on the right.

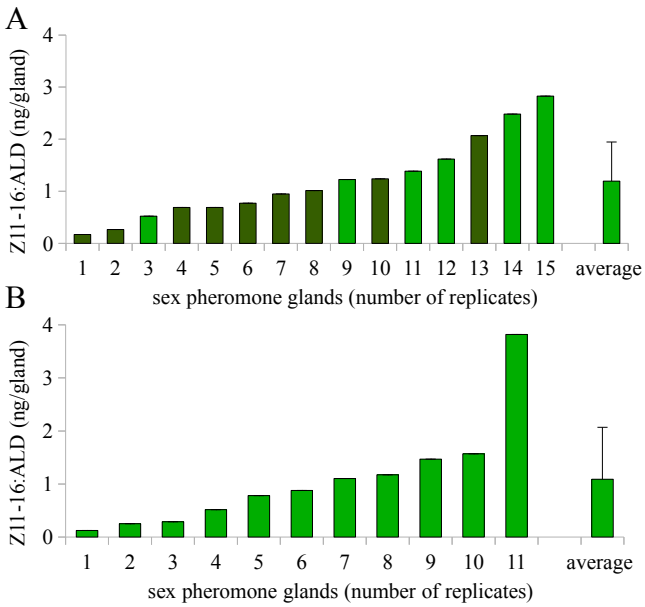

Figure 3.9: *In vitro* PBAN-stimulated Z11-16:ALD production at different time points in *H.v.* sex pheromone glands treated with 0.1-0.5 μg dsRNA of FAR1. Pheromone glands were incubated for 6 h (A; light green = dsRNA alone, dark green = dsRNA + lipofectamine) and 3 d (B) in medium containing 0.5 pmol PBAN. The x-axis represent the number of replicates and shows the pheromone production of each individual gland on the left and the average ($\pm$ SD) of all replicates on the right.

To amplify the possible effect of RNAi, I added lipofectamine in combination with dsRNA of FAR1 to individual sex pheromones in tissue culture. When pheromone glands were incubated for 6 hours in medium containing lipofectamine and dsRNA, the pheromone amount decreased to 1 ng/gland in comparison to 2 ng/gland of glands incubated only with dsRNA or without dsRNA (see Figure 3.10). Thus, lipofectamine may help to silence FAR1.

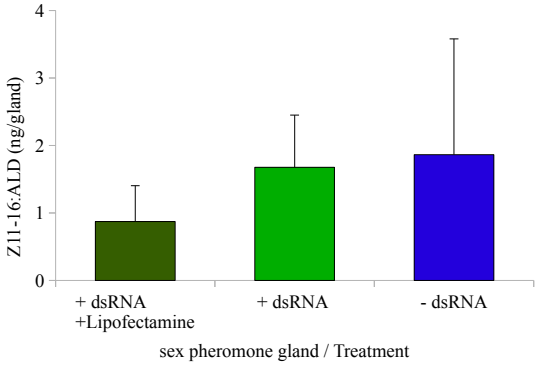

Figure 3.10: Effect of lipofectamine in combination with dsRNA on pheromone glands *in vitro*. Sex pheromone glands were incubated for 6 hours in medium containing 0.5 pmol PBAN treated with 0.1-0.5 μg dsRNA of FAR1 and lipofectamine, dsRNA and without dsRNA. Thin bars represent the standard derivations (dsRNA + lipofectamine: n = 9; +dsRNA: n = 6; -dsRNA: n = 8).

As an overview, Figure 3.11 shows the amount of Z11-16:ALD at different times of glands treated with dsRNA of FAR1 compared to control glands. Stimulated pheromone glands treated with dsRNA (green line) showed a slightly higher amount of Z11-16:ALD at 3 hours of incubation, compared to control glands (blue line). A low amount of Z11.16:ALD occured in pheromone glands of both treatments at 6 to 96 hours of incubation. I indicated the standard error, instead of the standard deviation in Figure 3.11. As shown, the standard error of both treatments overlap and thus the amount of Z11-16:ALD in both treatment is similar at all incubation times.

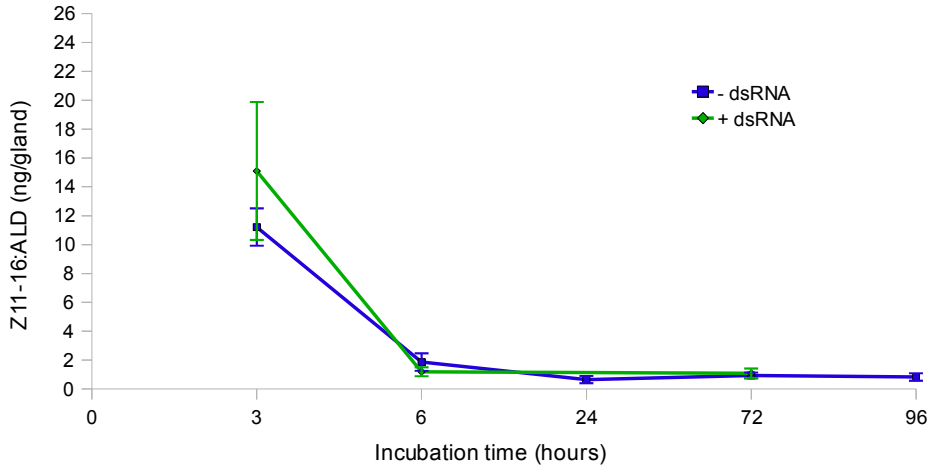

Figure 3.11: Comparison of the time-course of Z11-16:ALD production in PBAN-stimulated sex pheromone glands of *H.v. in vitro* with and without the treatment of dsRNA of FAR1(without lipofectamine). Thin bars represent the standard error (green line: n = 10-15; blue line: n = 8-40).

In summary, Figure 3.12 illustrates the comparison of the relative amount and the realtive percentage of Z11-16:ALD and 16:ALD of glands incubated in control medium and medium supplemented with dsRNA of FAR1 (without lipofectamine). Thus, pheromone glands incubated in medium with dsRNA of FAR1 for 3 hours produced a slightly higher amount of Z11-16:ALD. Nevertheless, high standard deviations were obtained in both treatements. The percent of the major and minor pheromone components in both treatments was almost the same (see Figure 3.12).

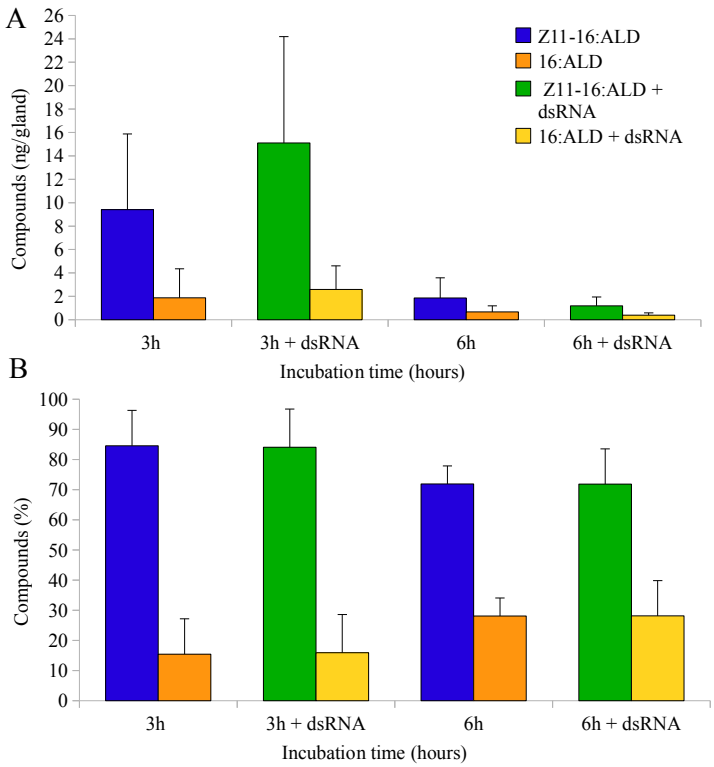

Figure 3.12: Comparison of the *in vitro* Z11-16:ALD and 16:ALD pheromone production at different time points in *H.v.* treated with or without 0.1-0.5 μg dsRNA of FAR1. (A) Amount (ng/gland) of Z11-16:ALD and 16:ALD production after 3h or 6h incubation in Grace's insect medium treated with or without dsRNA. (B) Percent (%) of Z11-16:ALD and 16:ALD production after 3h or 6h incubation in Grace's insect medium treated with or without dsRNA. Thin bars represent the standard derivations (3h: n = 25; 6h: n = 8; 3h + dsRNA: n = 10, 6h + dsRNA: n = 15).

3.2.3 *In vivo* application of RNAi with FAR1

I also tested the effect of RNAi *in vivo* by injection of dsRNA of FAR1 in zero-day old pupae of *H.v.* and injecting the adult females moths with PBAN 90 minutes before gland extraction. In this experiment, the complete pheromone profile could be analyzed, because the glands were dissected directly into hexane, resulting in clean samples so that the pheromone peaks of most components in GC analysis could be integrated. Interestingly, I found that pheromone glands of newly emerged *H.v.* (day 0) also produced pheromone, in the control glands as well as in glands injected with dsRNA, and that these females produced nearly the same amounts as one-day old females (see Figure 3.13). However, I used only a small sample size of zero-day old glands (n = 5-9) compared to the sample size of one-day old glands (n = 24-25), because I had not expected a pheromone production in zero-day old females.

The overall pheromone blend was different between the 4 treatemtents (buffer vs dsRNA at day 0 and day 1; Wilk's lambda: P = 0.0003). This seems to be mostly

due to the fact that the relative amount of the minor component 16:ALD was significantly different between the treatments. One-day old pheromone glands injected with dsRNA or buffer contained significantly more 16:ALD than zero-day old pheromone glands injected with dsRNA, but the amount of 16:ALD of zero-day old pheromone glands injected with buffer was not significantly different in comparison to one-day old glands. The relative amount of 14:ALD, Z9-14:ALD, Z11-16:ALD and Z11-16:OH were not significantly different between the two treatments. However, when looking more closely to each pheromone component, small differences (trends) can be detected in both treatments. A slightly higher amount of Z11-16:ALD was present in freshly emerged females than in one-day old females of both treatments. In glands of 0-day old females injected with buffer, the minor pheromone compound Z11-16:OH was present in slightly higher concentration than in one-day old glands. A reverse result was obtained when females were injected with dsRNA, in which the concentration of Z11-16:OH was slightly higher in one-day old females, than in freshly emerged (day 0) females.

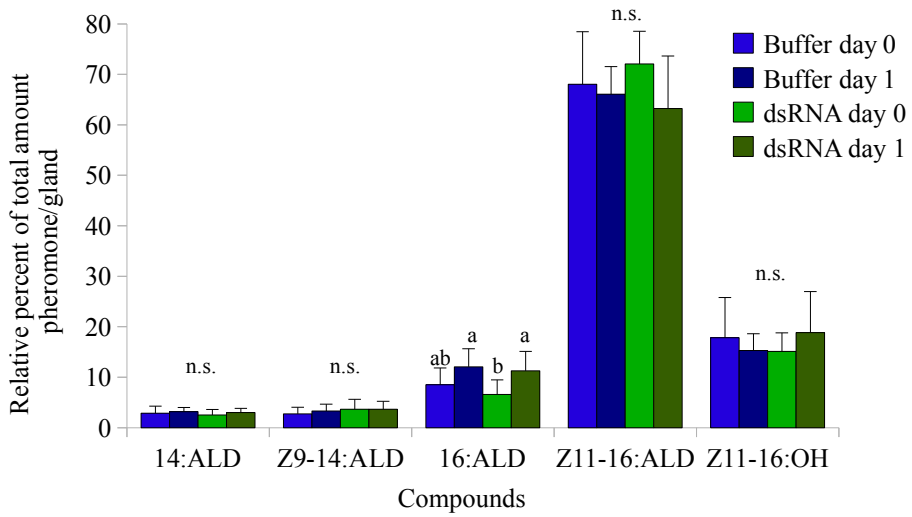

Figure 3.13: *In vivo* Pheromone profile of *H.v.* injected with dsRNA of FAR1 or with buffer as a control. The pheromone production was analyzed direct after female emerging (day 0) or 24-36 hours after female emerging (day 1). Female moths were injected at day 0 of pupation with dsRNA of FAR1 or buffer as a control. Wilk's lambda: P = 0.0003.
N.s. : not significant. Different letters above the bars indicate significant differences. Thin bars represent the standard derivations (buffer day 0 (n = 5); buffer day 1 (n = 24); dsRNA day 0 (n = 9); dsRNA day 1 (n = 25)).

The relative expression level of FAR1 was determined in addition to the pheromone profile of *H.v.* females injected with dsRNA of FAR1 or buffer.
The relative expression level of FAR1 was nearly non-detectable in glands of zero- and one-day old females injected with dsRNA or buffer (Figure 3.14). According to this result, it seems that FAR 1 is not expressed in pheromone glands of zero-day or one-day

old females. A small increase in the expression level of FAR 1 was seen in zero-day old females injected with dsRNA compared to the control.
As compared with Figure 3.6A, the expression of FAR1 in a pool of 1 to 7 day-old pheromone glands without any injection was higher than in glands of freshly emerged or one-day old glands injected with dsRNA of FAR1 or buffer.

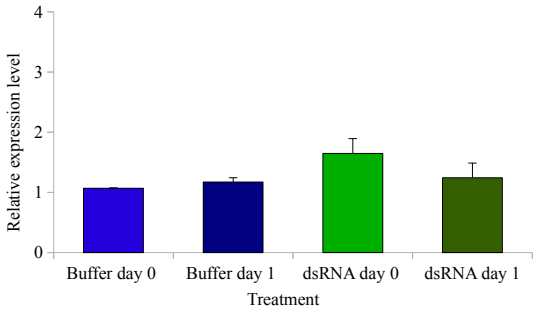

Figure 3.14: FAR1 gene expression (± SEM) in *H.v.* injected with dsRNA of FAR1 or with buffer. The expression level was determined in sex pheromone gland pools of 0-day old (RNA extraction directly after female emergence) and of 1-day old glands (RNA extraction 24 - 36 hours after female emergence).

3.3 Proteome analysis of the sex pheromone gland

Analysis of the proteins present in the sex pheromone gland of *H.v.* when stained with Coomassie blue gave the following results. I was able to separate solubilized proteins by 2D gel electrophoresis. The upper image in Figure 3.15 shows the Coomassie Blue stained map of proteins in the sex pheromone gland injected with PBAN to stimulate pheromone production. When 2D gel electrophoresis was repeated for gland extracts injected with PBS (Lower image in Figure 3.15), a very similar protein pattern emerged. The majority of the resolved protein spots had pI values between pH 3 and pH 11 and the molecular size of the pattern ranged from 250 kDa to less than 10 kDa. Approximate 80 % of the proteome ranged from 100 kDa to 75 kDa. Around 300 ± 50 spots were detected in both gels (Figure 3.15), which were compared for their intensity to identify differentially expressed spots. At first appearance it was not possible to find differences in the spot pattern between glands injected with PBAN or glands injected with PBS. Therefore, I used Delta 2D (Decodon, Bio Technikum Greifswald, Germany) to analyze the expression profiles to determine which spots occur in both and which occur only in one of the two treatments. The wrapped images showed visible differences in expression level of protein spots. In this way, I was able to find spots by choosing the strongest spots and those which are only expressed in one of both gels. As shown in Figure 3.15 I numbered the spots consecutively. In total, I selected and cut 78 spots for MS-MS identification including the most abundant proteins (spots with a letter) and the differentially expressed proteins (spots with a number).

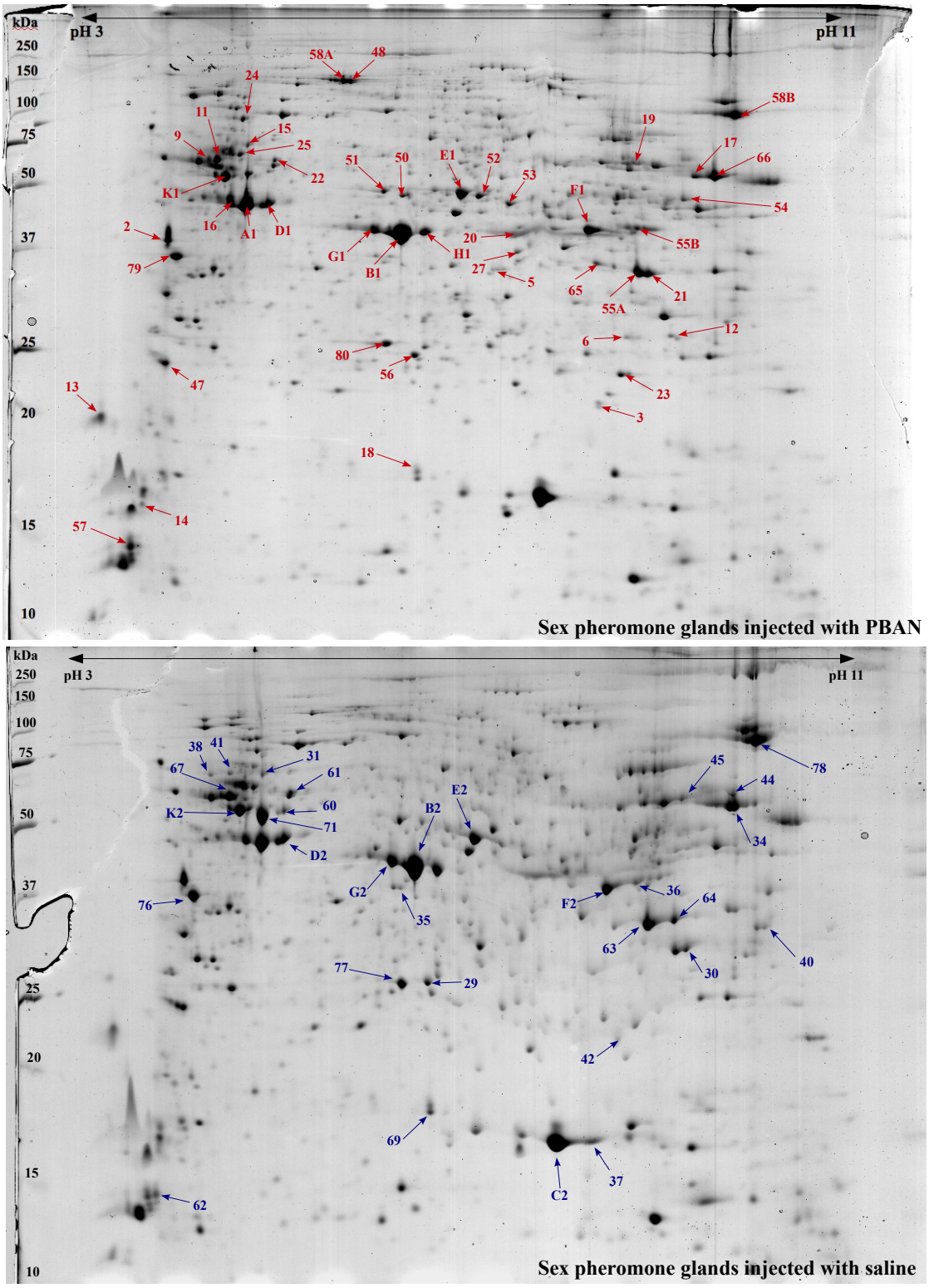

Figure 3.15: Separation of proteins from *H.v.* sex pheromone gland injected with PBAN or with Saline by 2D gel electrophoresis followed by staining with Coomassie Blue. Spot numbers correspond to those denoted in Table 3.1.

3.3.1 Protein identification

I analysed the resulting spectra of MALDI-TOF/MS analysis of 78 isolated spots, using the Protein Lynx Global Server software (PLGS2.2). I was able to identify the protein sequence of 46 out of 78 spots (Table 3.1), most commonly from *H.v.* itself or *H. armigera* which is a closely related lepidopteran species, using the MS-Ento database (http://nougat.ice.mpg.de/msEnto/). When I queried those 46 protein sequences in the NCBI_insecta database (http://blast.ncbi.nlm.nih.gov/Blast.cgi), I identified 46 spots corresponding to the protein sequences (Supporting Information E) with a molecular mass ranging from 150 kDa (paramyosin spot 48) to 18 kDa (actin-depolymerizing factor 1 spot 18). The remaining 32 spots could not be identified.

Identified proteins were assigned to the treatment of the pheromone gland (Table 3.1). Seven of the identified proteins in *H.v.* function in cell structure organization including Topomyosin 1 (spot numbers 2, 76 and 79), Beta-Tubulin (spot numbers 11 and 67), Actin (spot numbers 16, 60, 71,A1, D1 and D2), Actin depolymerizing factor 1 (spot numbers 18 and 69), Alpha-Tubulin (spot numbers 25 and 31) and Paramyosin (spot 48). Among these proteins, Paramyosin was only present in glands injected with PBAN, all other structure proteins were present in both treatments.

Four energy metabolism-associated proteins were identified, namely vacuolar ATP synthase (VATPase subunit A and B, spot numbers 25, 61, K1 and K2), ATP synthase (spot numbers 17, 44, 58B and 66), Voltage dependent anion channel (spot 30) and arginine kinase (spot numbers 50, B1, G2 and H1). The voltage depending anion channel (spot 30), which is an ion channel located on the outer mitochondrial membrane [32], was found to be only expressed in glands without PBAN treatment.

Two types of protein metabolism-associated proteins were detected in this study, chaperonin (spot 15) and a mitochondrial processing peptidase beta subunit (spot 51). Both proteins were only expressed in glands injected with PBAN.

Six enzymes were identified that play an important role in different metabolism pathways including glyceraldehyde-3-phosphate dehydrogenase (spot numbers 21, 55A, 63 and 64), glutathione s-transferase (spot 23), 3-hydroxy-CoA dehydrogenase (spot 27), triosephophate isomerase (spot 29 and 56), fructose-1,6-bisphosphate aldolase (spot numbers 36, 55B, F1 and F2) and enolase (spot numbers E1 and E2). All these proteins were found in glands injected with PBAN and in glands injected with PBS, except for 3-hydroxy-CoA dehydrogenase and glutathione s-transferase which were only found in the PBAN-injected samples. Both enzymes are important for several metabolic pathways.

Table 3.1: Results of the identifications obtained searching the NCBI_insecta protein database using the MS-Ento Database predicted protein sequence

spot	MS-Ento-BLAST identification[a]	Length[b]	NCBI-BLAST accession[c]	NCBI-BLAST description[c]	NCBI-BLAST species[d]	Identity [%][e]	Protein lenght[f]	*E*-Value[g]
***H.virescens* injected with PBAN**								
2	hvipg|HV-PGN_Contig_672_FWD_frame_0	233	NP_732006	Tropomyosin 1	*Drosophila melanogaster*	92%	711	2,00E-106
3	*n.i.*							
5	*n.i.*							
6	*n.i.*							
9	*n.i.*							
11	hvipg|HV-PGN_Contig_5444_FWD_frame_1	182	NP_001036964	Beta-Tubulin	*Bombyx mori*	99%	447	3,00E-104
12	*n.i.*							
13	*n.i.*							
14	*n.i.*							
15	hviV1|Contig19_FWD_frame_0	565	P25420	Chaperonin isoform	*Heliothis virescens*	98%	565	0
16	hvipg|HV-PGN_Contig_1305_FWD_frame_1	193	AAK52066	Actin	*Heliothis virescens*	99%	375	9,00E-112
17	hvipg|HV-PGN_Contig_364_FWD_frame_1	73	NP_001040233	ATP synthase	*Bombyx mori*	94%	553	2,00E-34
18	hviV1|Contig262_FWD_frame_2	148	NP_001093278	Actin-depolymerizing Factor 1	*Bombyx mori*	99%	148	1,00E-80
19	n.i.							
20	n.i.							
21	hvipg|HV-PGN_Contig_6434_FWD_frame_1	232	BAE96011	Glyceraldehyde-3-phosphate dehydrogenase	*Bombyx mori*	95%	332	7,00E-127
22	*n.i.*							
23	hvipg|HV-PGN_Contig_5708_FWD_frame_2	220	ABK40535	Glutathione S-transferase	*Helicoverpa armigera*	88%	220	3,00E-113
24	har454s|HARM_c10816_FWD_frame_1 nseq=2	288	NP_001091829	Vacuolar ATP synthase catalytic subunit A	*Bombyx mori*	93%	617	2,00E-159
25	hvipg|HV-PGN_Contig_1200_FWD_frame_1	215	ACR07789	Alpha tubulin	*Heliothis virescens*	100%	450	1,00E-125
27	har454s|HARM_c2821_FWD_frame_1 nseq=18	315	XP_001601340	similar to 3-Hydroxyacyl CoA dehyrogenase	*Nasonia vitripennis*	68%	317	1,00E-123
47	*n.i.*							
48	hvipg|HV-PGN_Contig_4246_FWD_frame_0	121	NP_001124374	Paramyosin	*Bombyx mori*	91%	878	1,00E-55
50	hvipg|HV-PGN_Contig_1118_FWD_frame_2	91	ABU98622	Arginine kinase	*Helicoverpa armigera*	96%	355	7,00E-48
51	hvipg|HV-PGN_Contig_297_FWD_frame_0	206	XP_001650897	Mitochondrial processing peptidase beta subunit	*Aedes aegypti*	76%	473	7,00E-87
52	*n.i.*							
53	*n.i.*							
54	*n.i.*							
55A	hvipg|HV-PGN_Contig_6434_FWD_frame_1	232	BAE96011	Glyceraldehyde-3-phosphate dehydrogenase	*Bombyx mori*	95%	232	7,00E-127
55B	har454s|HARM_c1903_FWD_frame_1	364	BAD12426	Fructose 1,6-bisphosphate aldolase	*Antheraea yamamai*	93%	364	0
56	hviV1|gi|1036785|gb|U23080.1| HVU23080_FWD_frame_1	215	AAA79847	Triosephosphate isomerase	*Heliothis virescens*	100%	215	4,00E-121
57	*n.i.*							
58A	*n.i.*							
58B	hviV1|Contig3112_FWD_frame_0	555	NP_001040233	ATP Synthase	*Bombyx mori*	94%	553	0
65	*n.i.*							
66	hvipg|HV-PGN_Contig_364_FWD_frame_1	73	NP_001040233	ATP Synthase	*Bombyx mori*	94%	553	2,00E-34
79	hvipg|HV-PGN_Contig_825_FWD_frame_0	159	NP_001040445	Tropomyosin 1	*Bombyx mori*	96%	284	7,00E-78
80	*n.i.*							
A1	hvipg|HV-PGN_Contig_1305_FWD_frame_1	193	AAK52066	Actin	*Heliothis virescens*	99%	375	1,00E-111
B1	hvipg|HV-PGN_Contig_1118_FWD_frame_2	91	ABU98622	Arginine kinase	*Helicoverpa armigera*	96%	355	7,00E-48
D1	hvipg|HV-PGN_Contig_1305_FWD_frame_1	193	AAK52066	Actin	*Heliothis virescens*	99%	375	1,00E-111
E1	hvipg|HV-PGN_Contig_759_FWD_frame_1	147	NP_001091831	Enolase	*Bombyx mori*	95%	433	3,00E-80

F1	hvipg|HV-PGN_Contig_866_FWD_frame_0	177	BAD12426	Fructose 1,6-bisphosphate aldolase	*Antheraea yamamai*	67%	364	1,00E-64
G1	hvipg|HV-PGN_Contig_1118_FWD_frame_2	91	ABU98622	Arginine kinase	*Helicoverpa armigera*	96%	355	7,00E-48
H1	hvipg|HV-PGN_Contig_1118_FWD_frame_2	91	ABU98622	Arginine kinase	*Helicoverpa armigera*	96%	355	7,00E-48
K1	hvipg|HV-PGN_Contig_1395_FWD_frame_0	234	NP_001040450	H+ transporting ATP synthase beta subunit Isoform 1	*Bombyx mori*	93%	516	2,00E-121
***H.virescens* injected with PBS (control)**								
29	hviV1|Contig690_FWD_frame_0	249	AAU84716	Triosephosphate isomerase	*Helicoverpa armigera*	95%	248	7,00E-134
30	har454s|HARM_c47_FWD_frame_2	281	XP_967480	similar to Voltage-dependent Anion-selective Channel Isoform 1	*Tribolium castaneum*	62%	347	1,00E-103
31	hvipg|HV-PGN_Contig_1200_FWD_frame_1	215	ACR07789	Alpha-tubulin	*Heliothis virescens*	100%	450	1,00E-125
34	*n.i.*							
35	*n.i.*							
36	hvil|HV-LN_Contig_7153_FWD_frame_2	149	BAD12426	Fructose 1,6-bisphosphate aldolase	*Antheraea yamamai*	95%	364	5,00E-82
37	*n.i.*							
38	*n.i.*							
40	*n.i.*							
41	*n.i.*							
42	*n.i.*							
44	har454s|HARM_c27888_FWD_frame_0	246	NP_001040233	ATP Synthase	*Bombyx mori*	86%	553	7,00E-112
45	*n.i.*							
60	hvipg|HV-PGN_Contig_1305_FWD_frame_1	193	AAK52066	Actin	*Heliothis virescens*	99%	375	1,00E-111
61	hviV1|Contig17_FWD_frame_0	494	P31410	Vacuolar (V-type) H(+)-ATPase B subunit	*Heliothis virescens*	100%	494	0
62	*n.i.*							
63	hvipg|HV-PGN_Contig_6434_FWD_frame_1	222	ACV44016	Glyceraldehyde-3-phosphate dehydrogenase	*Proterebia afra*	97%	230	5,00E-123
64	hvipg|HV-PGN_Contig_6434_FWD_frame_1	222	ACV44016	Glyceraldehyde-3-phosphate dehydrogenase	*Proterebia afra*	97%	230	5,00E-123
67	hvipg|HV-PGN_Contig_5444_FWD_frame_1	182	NP_001036964	Beta-tubulin	*Bombyx mori*	99%	447	3,00E-104
69	hviV1|Contig262_FWD_frame_2	148	NP_001093278	Actin-depolymerizing factor 1	*Bombyx mori*	99%	148	1,00E-80
71	hvipg|HV-PGN_Contig_1305_FWD_frame_1	193	AAK52066	Actin	*Heliothis virescens*	99%	375	1,00E-111
76	hvipg|HV-PGN_Contig_825_FWD_frame_0	159	NP_001040445	Tropomyosin 1	*Bombyx mori*	96%	284	7,00E-78
77	*n.i.*							
78	*n.i.*							
B2	*n.i.*							
C2	*n.i.*							
D2	hvipg|HV-PGN_Contig_1305_FWD_frame_1	193	AAK52066	Actin	*Heliothis virescens*	99%	375	1,00E-111
E2	hvipg|HV-PGN_Contig_759_FWD_frame_1	147	NP_001091831	Enolase	*Bombyx mori*	95%	433	3,00E-80
F2	hvipg|HV-PGN_Contig_866_FWD_frame_0	177	BAD12426	Fructose 1,6-bisphosphate aldolase	*Antheraea yamamai*	67%	364	1,00E-64
G2	hvipg|HV-PGN_Contig_1118_FWD_frame_2	91	ABU98622	Arginine kinase	*Helicoverpa armigera*	96%	355	7,00E-48
K2	hvipg|HV-PGN_Contig_1395_FWD_frame_0	234	NP_001040450	H+ transporting ATP synthase beta subunit Isoform 1	*Bombyx mori*	93%	516	2,00E-121

[a] = Cluster ID of best hit in MS-Ento by MS BLAST (ni = not identified).[b] = Lenght (number of amino acids) of the identified protein.
[c] = NCBI Accession number and description of the best hit in NCBI_insecta by MS BLAST.[d] = Species of best hit in NCBI_insecta.
[e] = Percentage of Identity of identified protein matching best hit in NCBI_insecta.[f] = Lenght (number of amino acids) of predicted NCBI_insecta protein. [g] = *E*-Value of best hit in blasp search

3.3.2 Detection of 3-Hydroxyacyl-CoA dehydrogenase (EC 1.1.1.35) by qRT-PCR.

Since 3-hydroxyacyl-CoA dehydrogenase (HACD) is an enzyme that catalyzes the chain reactions in the fatty acid ß-oxidation cycle [101] and I found this enzyme only in the PBAN-injected samples, I further analyzed the expression level of HACD by qRT-PCR. Even though I found the protein sequence in the database of *Helicoverpa armigera*, my qRT-PCR results show that HACD was not expressed in glands of *H. armigera* injected with or without PBAN (Figure 3.16A). However, in the sex pheromone glands of *H.v.* injected with PBAN, the relative expression of this enzyme was eight times higher than in control glands injected with PBS. Strangely, when I repeated the experiment with the same cDNA template and a biological replicate, this expression pattern was not reproducible, as Figure 3.16B shows. In the repeated experiment HACD was higher expressed in the body of *H.v.* than in the sex pheromone glands (Figure 3.16B).

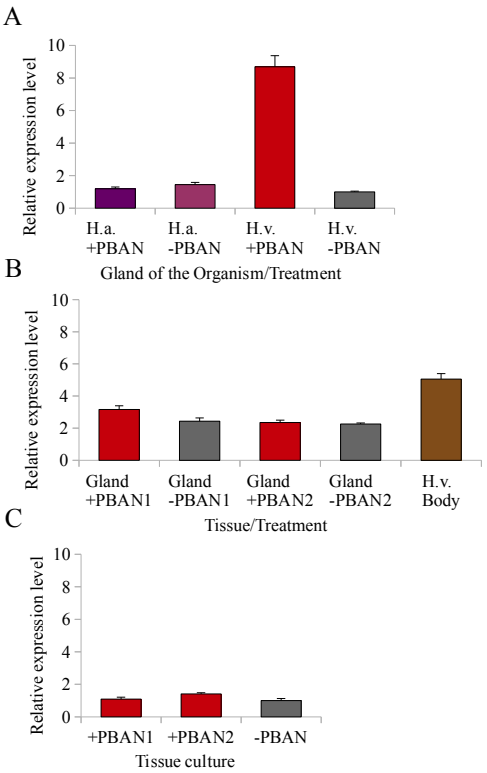

Figure 3.16: (A) Expression level (± SEM) of HACD in the sex pheromone gland of two Lepidopteran species (*H.a.= Helicoverpa armigera*, *H.v.= Heliothis virescens*) with and without PBAN injection. (B) Expression level (± SEM) of HACD in the sex pheromone gland with and without PBAN injection and in the body of *H.v.* in a confirmation experiment. (C) Expression level (± SEM) of HACD in the sex pheromone gland of *H.v.* after the incubation in Grace's insect medium with or without PBAN for 2 1/2 h.

I also determined the expression level of HACD in *in vitro* glands. Figure 3.16C shows a low expression level of HACD of glands incubated in Grace's insect medium for 3 hours, whether the medium contained PBAN or not. Similar expression levels of HACD were obtained when pheromone glands were directly used for RNA extraction (+PBAN1) compared to when glands were extracted in hexane before the RNA extraction (+PBAN2). Additionally, I found no difference in the expression level of HACD in pheromone glands that were incubated with PBAN (+PBAN1 and +PBAN2) or without PBAN (-PBAN) (see Figure 3.16C).

3.3.3 Additional application of 2D-PAGE

In the end of my proteome research, I used Refraction-2D, because this new method is a hundred times more sensitive than the Coomassie blue method. I started the extraction and analysis of proteins from *in vivo* and *in vitro* glands to compare the proteome map of both treatments. Based on a problem of time, I was only able to finish both 2D gel images without further identification or analysis of spots. However, this work will be continued in our department to identify proteome differences of *in vivo* and *in vitro* glands. When visually comparing the 2D gel images of *in vivo* and *in vitro* glands,I found almost the same spot pattern in both treatments. Thus, my identify protein map of *in vivo* glands of *H. virescens* may help to identified proteins from *in vitro* glands.

4 Discussion

The primary aim of this study was to develop an *in vitro* assay to test the effect of RNAi in pheromone glands of *H.v.*. I started these tests by adding dsRNA of FAR1 directly into tissue culture of sex pheromone glands. Secondly, I tested the effect of RNAi *in vivo* by injection of FAR1 in pupae of *H.v.* to compare the possible efficacy of RNAi *in vivo* and *in vitro*. Thirdly, an additional aim of this Diplom study was to analyze the proteome of PBAN-activated and PBAN-non-activated glands *in vivo* and *in vitro*.

4.1 *In vitro* assay to analyze the pheromone production

Recent studies [49, 70, 23, 53, 94, 62] have shown that Grace's insect medium supplemented with 10% FBS, JH (50 μg/ml), 20-E (50 μg/ml) and 10% microbial inhibitors is an optimal medium for maintaining a tissue of Lepidoptera *in vitro*. I also found that this medium is suitable to maintaining sex pheromone glands of *H.v.* alive, but that it is unsuitable to analyze the pheromone profile of *H.v.* glands, because the medium caused a lot of contamination peaks, so that the pheromone peaks of *H.v.* could not be analyzed. Therefore, I analyzed all tissue culture supplements to determine whether a) they were necessary for the maintenance of pheromone gland, and b) whether the addition or deletion would improve the cleanliness of the pheromone extract.

Initially, I used 0.5 pmol of PBAN to stimulate pheromone production in isolated glands to define a tissue medium which improved the cleanliness. Glands incubated in Grace's insect medium supplemented with only 5% microbial inhibitors instead of 10% microbial inhibitors (composition a), improved the cleanliness of the pheromone extract, while the gland remained alive.

FBS (composition b) which is commonly used for cell and tissue culture [94, 62], caused a lot of extra peaks in the pheromone extract, so that I did not use FBS as supplement for the tissue medium of sex pheromone glands of *H.v.*.

20-E (composition c), which is an important endocrine regulator of metamorphosis, reproduction and aging [34], did not influence the cleanliness of the pheromone extract, but inhibited the pheromone production in comparison to control glands which were incubated in medium without 20-E. This result suggest an involvement of 20-E in the regulation of pheromone biosynthesis in female moths. Ramaswamy *et al.* showed that injection of 20-E into virgin females of *H.v.* results in a dose-dependent suppression of the pheromone titer [82]. Thus , the study of Ramaswamy *et al.* [82] and my findings

suggest a pheromone-suppressive activity of 20-E in *H.v.*. In contrast, in Diptera 20-E plays an suppressive role in the regulation of pheromone biosynthesis [7].

JH (composition d), which is also an important endocrine regulator, increased the amount of pheromone when adding this hormone to glands incubated in Grace's insect medium supplemented with 5% microbial inhibitors. This result supports the hypothesis that JH affects pheromone gland competence [71]. Such an effect was also found in cockroaches, which produce sex pheromone through JH regulation [88]. The role of JH in the pheromone production in moths is inconsistent [19]. However, my results indicate that JH also affects the pheromone production of *H. v. in vitro*, as it is reported for *Pseudaletia unipuncta* and *Agrotis ipsilon* [17, 28, 66] . In summary, I found that 20-E, FBS and high concentration of microbial inhibitors are not required for maintaining the gland *in vitro* and supporting the pheromone production in glands of *H.v.*. Therefore, I used Grace's insect medium supplemented with 5% microbial inhibitors and JH (50 μg/ml) in all following assays.

Studies have shown that PBAN stimulates a maximum of pheromone production at 120 minutes of incubation [23, 53]. When I incubated pheromone glands for 120 minutes, I was indeed able to detect pheromone in the gland. Fònagy and coworkers [23] showed that an incubation time of 3 to 4 hours of PBAN has a decreasing effect to the pheromone production. For *H.v.* a concentration of 0.5 pmol and an incubation time of 120 min of PBAN seems to be optimal under the conditions that I used. Other studies [74] have shown that the optimal dose of PBAN was between 3-5 pmol.

When sex pheromone glands were incubated in tissue medium for 3 hours, I found a mean pheromone synthesis of 9 ng Z11-16:ALD (Figure 3.2). The pheromone production of glands incubated for longer than 3 hours decreased to 2 ng Z11-16:ALD (Figure 3.3). Thus, my results show that the developed *in vitro* assay is a capable technique to determine the pheromone production for a short incubation time.

For longer incubation times of pheromone glands *in vitro*, the tissue culture has to be improved. To obtain a more consistent pheromone production over a longer period than 3 days, several factors could be considered to improve the *in vitro* assay. For instance, a time- and dose-dependent study of PBAN in *H.v.* would provide more detailed information about the role of PBAN *in vitro*. Furthermore, it is possible that the pheromone production is inhibited when pheromone glands were incubated in medium lacking an important factor which stimulates pheromone production for a longer incubation time. For example, Ma [53] showed that pheromone glands of *Ostrinia nubilalis* required calcium to produce pheromone *in vitro*. Calcium requirement for *in vitro* studies were also shown for *Helicoverpa armigera* [74], *Helicoverpa zea* [40], *Bombyx mori* [23] and *Spodoptera litura* [23]. Therefore it is likely that *H.v.* pheromone glands required a physiological concentration of calcium as well to produce pheromone *in vitro* for a longer incubation time.

Another factor that could be required is cyclic AMP (cAMP). Findings on PBAN-stimulated biosynthesis of sex pheromone glands *in vitro* of two *Helicoverpa* species indicated that cAMP is involved in mediating the action of PBAN [40, 74]. Rafaeli and coworkers [74] have shown that cAMP stimulates pheromone production in *H. armigera* and that cAMP were stimulated as a direct consequence of PBAN stimulation, suggesting that PBAN acts through cAMP as second messenger. The role of calcium and cAMP in PBAN activity *in vitro* thus seems to be important for Lepidoptera and the addition of calcium and cAMP could improve the pheromone production in my *in vitro* assay for further analysis.

In summary, I was able to establish a tissue culture method to determine pheromone production of *H.v. in vitro*. *In vitro* maintenance of isolated pheromone gland tissue in which sex pheromone production can be measured will most likely facilitate manipulation of genes that are involved in the biosynthesis of sex pheromone.

4.2 *In vitro* and *in vivo* RNAi experiments

RNAi studies were conducted using the developed *in vitro* assay. FAR, which modifies unsaturated fatty acids to form a alcohol or aldehyde as functional group, seems to be an auspicious candidate for RNAi experiments in *H.v.*, because of its central role in pheromone production.

When I analyzed the expression level of FAR1, FAR2, FAR3 and FAR4, I found that FAR1 (gene accession number EZ407233 (Vogel *et al.* [107]); see Figure 3.6) was mostly expressed in the gland of *H.v.*, so that I focused my subsequent RNAi experiments on this FAR. The standard deviation of the qRT-PCR analysis was much higher than in other qRT-PCR analyses, which I found was due to pipetting the cDNA template separately from the master mix. When I repeated this experiment for FAR1 and I used a master mix including the cDNA template (Figure 3.7), I obtained reproducible results with a low standard deviation (Figure 3.7). Thus, the data presented in this study shows that FAR1 is only expressed in sex pheromone glands of *H.v.*. This result supports the hypothesis that FAR1 is the specific FAR which is involved in the pheromone production in the sex pheromone gland of *H.v.* [107]. Based on this fact, RNAi experiments were conducted with dsRNA of FAR1.

4.2.1 *In vitro* RNAi

When pheromone glands were incubated in medium containing dsRNA of FAR1, I found a mean amount of 15 ng Z11-16:ALD (Figure 3.8) compared to 9 ng Z11-16:ALD in glands incubated without dsRNA. Actually, I was able to detect a maximal amount of 32 ng Z11-16:ALD in glands incubated with dsRNA. Thus, I found much higher

amounts of Z11-16:ALD in glands incubated with dsRNA, in comparison to the control glands. This result was thus completely opposite from what I had expected, namely that dsRNA of FAR1 would caused a decrease of pheromone production in the pheromone gland of *H.v.* by knocking down of the corresponding gene transcript. In addition, isolated glands incubated in medium containing dsRNA showed the same percentage of the major and minor component (i.e. Z11-16:ALD and 16:ALD), in comparison to the pheromone profile of control glands (see Figure 3.12). Thus dsRNA did not modify the ratio's of the pheromone components in the glands.

Recently, Ohnishi and coworkers [63] showed that silencing FAR in *Bombyx mori* caused a decrease in pheromone precursors. The discrepancy between our findings and that of Ohnishi and coworkers [63] may be due to differences in ecological and physiological characteristics between *Bombyx mori* and *H.v.*.

One study was published that shows an upregulation in the translation by RNAi [106]. Vasudevan and coworkers [106] showed that microRNAs induce a translation upregulation of target mRNAs on cell cycle arrest and repress translation in proliferating HeLa cells. This upregulation by microRNA is consistent with my data presented in this thesis.

In general, however, microRNA as well as dsRNA induce a degradation of mRNA and thus a repression of the target mRNA. I speculate that the increase of pheromone production in my experiments was the result of an inefficient uptake of dsRNA by the pheromone cells. This hypothesis could be true, because when glands were incubated in addition to dsRNA with lipofectamine, I found a decreased amount of Z11-16:Ald, in comparison to glands incubated only with dsRNA, and control glands (see Figure 3.10). This result suggest that lipofectamine may an efficient transfection reagent for delivering dsRNA into sex pheromone gland cells of *H.v.*. In addition, SID-1 (systemic interference defective), a transmembrane protein, may be involved in the transport of dsRNA into cells by a passive uptake mechanism [112], although the evidence for the involvement of this transmembrane protein in insects is not consistent [103]. It is possible that in my assays *H.v.* lacked this protein or another protein that is necessary for the RNAi mechanism. Thus, such factors could be absent in the developed *in vitro* assay. It may also be possible that dsRNA was not degraded by the RNAi mechanism when it was applied to the pheromone gland cells, which could have increased the total amount of mRNA of FAR1 in gland cells and thus a transcriptonal upregulation of FAR1, which could have resulted in an increasing pheromone production.

4.2.2 *In vivo* RNAi

Most RNAi studies in Lepidoptera have been conducted *in vivo* by injection of dsRNA into pupae [63, 80, 105, 52]. Since not many studies were realized *in vitro* as a comparison to my study, I also attempted to apply dsRNA of FAR1 *in vivo* by injection

into pupae of *H.v.*. I found that injection of dsRNA into zero-day old pupae resulted in a similar pheromone profile of freshly emerged and one-day old females of *H.v.*, compared to the control females injected with buffer (see Figure 3.13). However, zero-day old females injected with dsRNA showed a significantly lower relative amount of 16:ALD and a correspondingly slightly higher amount of Z11-16ALD than one-day old females injected with dsRNA or buffer. This differences between the treatments (0-day dsRNA vs. 1-day dsRNA and 1-day buffer) could be explained by reduced activity of FAR converting unsaturated fatty acids to 16:ALD in zero-day old females injected with dsRNA. This would increase the available relative amount of unsaturated fatty acids to form Z11-16:ALD, the major component that was found in slightly higher relative amounts in the zero-day old females injected with dsRNA than in 1-day old females injected with dsRNA or buffer. No significant differences were found in the relative amount of 14:ALD, Z9-14:ALD, Z11-16:ALD and Z11-16:OH. Furthermore, I did not find any significant differences between the treatments within zero-day and one-day old females (0-day dsRNA vs. 0-day buffer and 1-day dsRNA vs. 1-day buffer). Therefore, dsRNA of FAR1 did not induce an decreasing pheromone production, compared to control glands. My findings could indicate either that FAR1 is not involved in the pheromone biosynthesis of *H.v.* or that the incubation time or the amount of dsRNA in *H.v.* was not optimal to induce induce gene silencing. It could also be possible that dsRNA is degraded already in the pupae, or that the amount of dsRNA was not high enough to induce a significantly decrease in the pheromone production.

As mentioned above, it is also possible that dsRNA of FAR1 is not degraded by the mechanism of RNAi, so that the relative expression level of FAR1 is actually increased with the injections or the same as the control. However, the relative expression level of FAR1 was nearly the sane in glands of zero-day old and one-day old females injected with dsRNA or buffer (see Figure 3.14). I found only a small increase in the expression level of FAR1 in freshly emerged females injected with dsRNA, compared to the other three treatments. In contrast, I found very high expression levels of FAR1 in four pool of 1 to 7-day old glands without any injection (see Figure 3.7). Therefore, it could be possible that FAR1 is generally not expressed in zero-day old and one-day old females. Subsequent studies should probably not compare the expression level of FAR1 in females injected with dsRNA or buffer in very young adult females. On the other hand, there is another explanation for the qRT-PCR results. It is possible, that control females were injected with slight amounts of dsRNA of FAR1 because of an unclean mode of practice (i.e I used the same needle), which may have caused the nearly non-detectable level of FAR1 in both treatments compared to non-injected females as in Figure 3.14.

Surprisingly, I was able to detect pheromone in freshly emerged females, which is not usual, because pheromone is not expected to be found in freshly emerged females. All earlier studies I am aware of were performed on adult females (at least 1-day old females)[54, 55, 77]. In summary, I was not able to find significant differences in the

pheromone and the expression level of FAR1 in females treated with dsRNA, compared to control glands.

4.2.3 An outlook on RNAi in *Heliothis virescens*

Because of the negative result of my *in vitro* and *in vivo* RNAi experiments in *H.v.*, several factors should be improved to get RNAi in *H.v.* to work.

First, it is necessary to determine the expression levels of FAR1 in an age-dependent study to detect the incipient transcription of this gene in *H.v.*, so that it is possible to compare the effect of dsRNA to control glands that express FAR1.

Secondly, it is necessary that qRT-PCR analysis is also conducted with *in vitro* experiments to compare both, *in vitro* and *in vivo*, methods in a more precise way. When I tested whether the same pool of pheromone glands could be first extracted in hexane for GC analysis and then in Trizol to extract RNA, I found that the same pool of glands can indeed be used first for GC-analysis and afterwards for RNA extraction. Thus, it may be possible to determine the pheromone profile and the expression level of a specific gene in the same pool of glands.

In addition, it might be useful to apply unrelated dsRNA (e.g. FAR of a different organism) to isolated glands. If there is a specific effect of FAR1 then the unrelated dsRNA should not show an effect on the pheromone production, no decrease but also not an increase. Furthermore, different methods of RNAi technology could be used to improve the effect of RNAi in *H.v.*. For instance, dsRNA could be applied by feeding experiments with larvae. Turner and coworkers [103] showed that feeding of dsRNA to larvae can trigger knockout of a gene in adult life stages. It might be intresting to see whether oral delivery of dsRNA in *H.v.* larvae is able to influence the pheromone production in adult females. Further, varieties of RNAi, like siRNA or stealth RNAi, could be applied to *H.v.* by feeding, injection or addition to tissue culture to improve the effect of RNAi in *H.v.*. For further RNAi experiments in *H.v.*, it might be interesting to see whether other enzymes, like delta-D11-desatures, which are also involved in the biosynthesis of pheromone, are able to decrease the pheromone production by gene silencing.

4.3 Protein analysis

This is the first report about the effect of PBAN to the proteome of sex pheromone glands of *H. virescens*. First I will discuss the proteins that I found to be present in PBAN-activated and non-PBAN activated (control) glands, then I will discuss the proteins that I only found in control glands, and finally I will discuss the proteins that I only found in PBAN-activated glands which thus may play a role in sex pheromone

biosynthesis.

4.3.1 Common characteristics of PBAN-activated and non-PBAN-activated sex pheromone glands

I found four proteins that function in cell structure. For instance, alpha-tubulin and beta-tubulin (spot 11, 67, 25 and 31) are are essential for cell division, locomotion and maintenance of the cytoskeleton [25]. Actin (spot 16, 60, 71, A1, D1 and D2) is important for many cellular processes, like endocytosis, exocytosis, cytokinesis, maintaining motility and signal transduction [57] and thus it is highly conserved in the evolution: the protein sequence differ only 3 to 7 % between mammals and insects [58]. Additionally, actin depolymerizing factor 1 (spot 18 and 69) is reported to function as actin-binding protein that regulate the level of actin polymerization [110]. The fact that I found those four cell structure proteins in PBAN-activated and non-PBAN-activated glands indicates a general role of those proteins in the pheromone gland.

Furthermore, I found two energy metabolism-associated proteins, ATP synthase (spot 25, 61, K1, K2, 17, 44, 58B and 66) and arginine kinase (spot 50, B1, G2 and H1). ATP synthases are highly conserved proton pumps that function as ATP-dependent proton pumps in mitochondria, occurring in the majority of eukaryotes [60]. Furthermore, it is a housekeeping protein, that activates the energy needed for active protein synthesis [113]. Arginine kinase catalyzes arginine to form phosphoarginine [61], a vital energy reserve as well which plays a key role in the interconnection of energy production and utilization in invertebrates. Since I found these proteins in both PBAN and non-PBAN activated glands, it seems that these proteins are PBAN independent and generally expressed in glands as well.

I identified four enzymes of metabolism-related proteins, namely fructose-1,6-bisphosphate aldolases (spot 36, 55B, F1 and F2), enolase (E1 and E2), glyceraldehyde-3-phosphate dehydrogenase (spot 21, 55A, 63 and 64) and triosephosphate isomerase (spot 29 and 56), which were found in PBAN-activated and non-activated glands. Fructose-1,6-bisphosphate aldolases is known to act in the glycolysis as catalyst of the cleavage of fructose-1,6-bisphophate into a ketose and an aldose [16]. Enolase is involved in the transformation of 2-phosphoglycerate to phospoenolpyrovate [1]. Glyceraldehyde-3-phosphate dehydrogenase is involved in endocytosis and membrane fusion, translational control, vesicular secretory transport, nuclear tRNA transport, DNA replication and DNA repair [92] and triosephosphate isomerase is involved in the carbohydrate metabolism and appears only in the cytosol [45]. Since I identified a number of proteins related to the energy metabolism, the sex pheromone gland seems to be generally an important tissue which is involved in the energy

metabolism independent from a PBAN activation.

4.3.2 Characteristics of non-PBAN-activated sex pheromone glands

One protein that I found only in the control glands and not in PBAN-activated glands was a voltage depending anion channel (spot 30), which function as transporter of ions, nucleotides and metabolites between the cytosol and mitochondria [35]. Thus, this channel is not present in PBAN-activated glands. It could be possible that the function of this channel is not necessary in the present of PBAN, if e.g. PBAN activates other ion channels that are more efficient than this voltage-dependent anion channel. For instance, the calcium channel in pheromone glands of *H. zea* was suggested to be a non-voltage-activated calcium channel or ligand-activated calcium channel [40, 13]. Extracellular calcium is required for the initial binding and activation of the PBAN receptor and thus for the activation of the biosynthetic pathway [40, 13]. Jurenka and coworkers suggested that the calcium channels of pheromone gland cells in *H. zea* are receptor-activated by PBAN [40, 13]. Thus these calcium channels could be more active than voltage depending anion channels in the present of PBAN in *H.v.*. However more research about non-voltage-activated calcium channels is necessary [40].

4.3.3 Characteristics of PBAN-activated sex pheromone glands

The first two proteins that were present in PBAN-activated glands and absent in non-activated glands were tropomyosin 1 (spot 2, 76 and 79) and paramyosin. Both molecules have been reported as proteins of the filaments of many invertebrate muscles [27, 84]. Thus, I speculate that this proteins function as assistance in the transport of important factors for the pheromone biosynthesis in the gland, which may explain why the protein amount is increased by PBAN activation in glands.

Another two proteins that were only present in PBAN-activated glands were 2 proteins including chaperonin (spot 15) and a mitochondrial processing peptidase beta subunit (spot 51), both of which are involved in the protein synthesis. Chaperonin functions as mediator of protein folding in all organisms [47], and mitochondrial processing peptidase beta subunit functions as transporter of mitochondrial proteins [9].

Surprisingly, I only found two specific proteins in the PBAN-activated glands that are most likely involved in the pheromone biosynthesis and energy metabolism: glutathione s-transferase (spot 23), which has an important role in protecting cell structures from oxidative damage and stress [26], and 3-hydroxyacyl-CoA dehydrogenase, which catalyzes the conversion of L-3-hydroxyacyl-CoA to 3-ketoacyl-Co in the mitochondrial fatty acid oxidation. The presence of glutathione s-transferase in the PBAN-activated glands might be the result of higher stress which could occur when glands are stimulated by PBAN to produce higher amounts of pheromone.

3-Hydroxyacyl-CoA dehydrogenase is a strong candidate protein that may actually be involved in the pheromone production.

4.3.4 Identification of proteins by the MS-Ento database

The 46 protein spots that are identified correspond to 17 unique proteins; thus, several proteins gave rise to more than one protein spot. Thirteen proteins corresponded to already characterized *H.v.* sex pheromone gland proteins, two correspond to proteins from general *H.v.* proteins, and further two proteins were found only in the library of *H. armigera*. Therefore, I identified four proteins that had not been described to occur in the sex pheromone gland of *H. virescens* so far. The protein sequence of an actin depolymerizing factor 1 and chaperonin were only found in the Heliobase of *H.v.* and the sequence of a voltage depending anion channel and 3-hydroxyacyl-CoA dehydrogenase were found only in the library of *Helicoverpa armigera*. Thus, it is the first report that actin depolymerizing factor 1 and chaperonin exist in the pheromone gland of *H.v.* and even that a voltage depending anion channel and 3-hydroxyacyl-CoA dehydrogenase exist in the pheromone gland of *H.v.*.

I found no studies on proteome research in sex pheromone glands of other organisms to which I can compare my findings. In order to compare my findings to other published data, I chose protein studies on the fat body and the silk gland of *Bombyx mori*. The fat body is known to function in energy storage, protein synthesis and fat metabolism, which is also known for sex pheromone glands. Thus, I expected that the sex pheromone gland and the fat body share common characteristics in their proteome. Kajiwara and coworkers [42] detected several enzymes in the fat body of *Bombyx mori*, namely glycolysis and sugar metabolism-related proteins, energy-metabolism-associated proteins, protein synthesis related proteins, kinases and structure proteins. Of the specific proteins that I found in the sex pheromone gland, Kajiwara and coworkers [42] also found tubulin, tropomyosin, actin, ATP synthase, chaperonin and enolase in the fat body. Zhang and coworkers [113] detected proteins in the silk gland of *Bomby mori*, which function in apoptosis, nucleic acid metabolism, signal transduction, secretion, transport and storage proteins. Of the sex pheromone gland proteins that I found, Zhang and coworkers [113] also found tubulin, actin and ATP synthase in the silk gland. Therefore, less similarities were found in comparison to the silk gland than to the fat body of *Bomby mori* [113].

4.3.5 Characterization of 3-hydroxy-CoA dehydrogenase (HACD)

The biosynthesis of sex pheromone compounds involves *de novo* synthesis of hexadecanoates and octadecanoates from acetyl-CoA and malonyl-CoA [4]. HACD (EC 1.1.1.35) acts in several elongation steps from acetyl-CoA to hexadecanoate, as shown

in Figure 4.1 [37]. Therefore, HACD is likely to play an important role in the pheromone biosynthesis of sex pheromone glands. The enzyme activity of HACD is actually triggered by the presence of PBAN and thus HACD support the pheromone biosynthesis in *H.v.* (see Figure 4.2). Based on these facts and that HACD is present in PBAN-activated glands and absent in non-activated glands, I focused my attention on this enzyme.

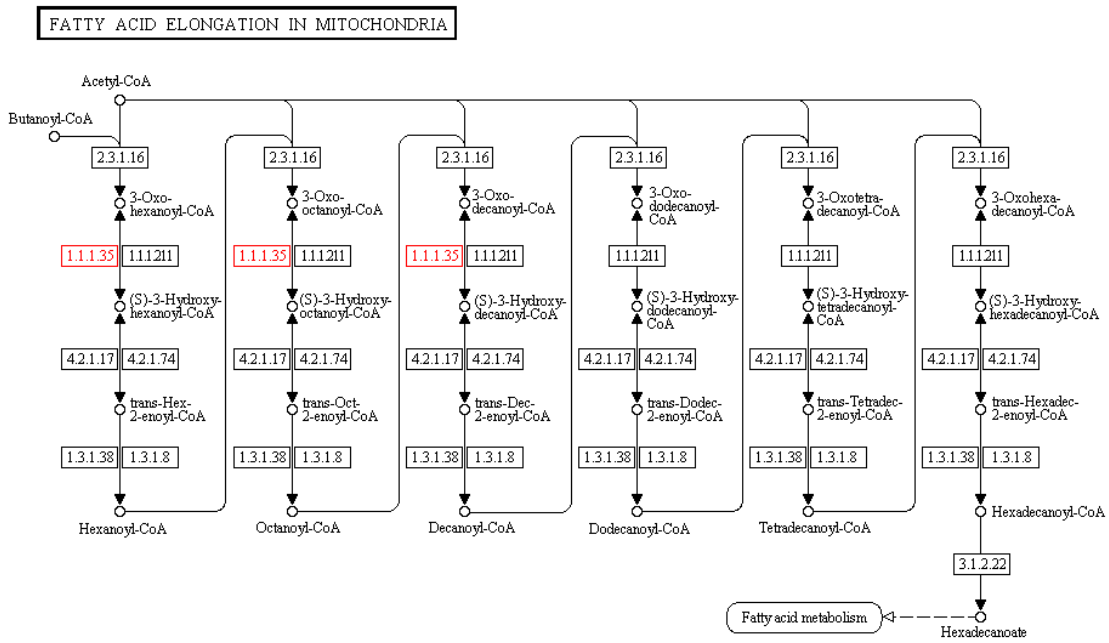

Figure 4.1: Fatty acid elongation in the mitochondria. Adapted from [51]

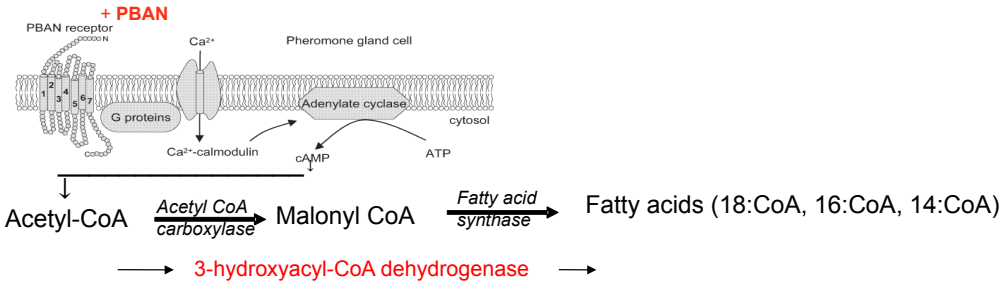

Figure 4.2: Proposed pheromone biosynthesis pathway in *H.v.* including the function of HACD adapted from [38] and [107].

As I found HACD only in the proteome of PBAN-activated glands, I attempted to detect an up-regulation of HACD also in the transcript level by qRT-PCR using cDNA of both *H. armigera* and *H.v.* (see Figure 3.16). Strangely, even though I had found the sequence of HACD in the cDNA of *H. armigera*, I was not able to detect a expression of HACD in PBAN-activated or non-activated glands of *H. armigera*. A possible explanation for this result is that HACD seems to be only present in the body and not

in the pheromone gland of *H. armigera*. In *H.v.*, I found a ten times higher expression level of HACD in PBAN-activated glands in comparison to non-activated glands, which was thus consistently with the findings of the proteome analysis. However, I was not able to reproduce this result in a technical replicate (the same cDNA template) or in a biological replicate.

The discrepancy between the initial result and the biological replicate is partly comprehensible. For instance, high variation of mRNA levels of HACD could be one explanation for the non-reproducibility. The level of mRNA could be influenced by the daytime of RNA extraction of female glands, because the level of HACD may change within a day. It could be also possible that the expression of HACD in the pheromone gland is dependent not only on PBAN, but also on fitness components of individuals (i.e. stress, diseases, female fecundity), because physiological properties may influence the enzyme activity. Studies have been shown that enzyme activity changes in response to environmental or dietary variances [14, 30]. This could also be one explanation for indifferent expression levels between PBAN-activated and non PBAN-activated pheromone glands. Therefore, these factors may have caused a different expression level of HACD between the initially result and the biological replicate. To resolve this problem it is necessary to determine the expression level of HACD in different pools of pheromone glands of females with the same age to detected the age-dependent amount of enzyme in PBAN-activated glands. Furthermore, RNA could be extract from pheromone glands at different daytimes to except HACD variation within a day.

However, to find an explanation for the different expression level in the same cDNA template is difficult. One explanation might be that the cDNA samples in the technical replicate in the second experiment was not pure anymore, because of impurities or inhibitors, i.e., salts and unsoluble proteins, which accrued within the experimental procedure and, therefore, may have inhibited the amplification of HACD. Also, preparation of samples, reagent variation, array to array variation, labeling and other steps of qRT-PCR experiments can contribute to technical variations. Another issue is that the presence of the mRNA of HACD does not completely match the enzyme activity of HACD in female moths and therefore it is complicated to find an upregulation in the expression level. I studied the expression level of HACD mRNA, but not the activity of this enzyme. This could be one explanation for indifferent expression levels of HACD between PBAN- and non-PBAN-activated glands.

When I determined the expression level of HACD in *in vitro* PBAN-activated or non-activated glands (see Figure 3.16), I was not able to detect any expression of HACD, either in PBAN-activated or in non-activated glands. This result suggests that HACD is present only in very low levels (below detection) in *in vitro* glands or not present at all, which is possible if HACD is synthesized in the body and transported to the gland.

Another possibility is that an important factor to synthesize HACD in the gland was not available in the tissue medium.

Finally, I was able to successfully extract RNA with Trizol from glands that were first extracted in hexane to analyze the pheromone profile. Thus, sex pheromones can individually analyzed by GC to investigate the pheromone profile and then pooled for RNA extraction to determine the expression level of specific genes.

4.3.6 An outlook on protein analysis of *Heliothis virescens*

To date, protein studies on sex pheromone glands in lepidoptera are largely unexploited. I have carried out some initial efforts to study the protein profile of the *H.v.* pheromone gland. My initial results suggest that proteome research can provide valuable information that will allow us to determine the pheromone biosynthesis at the protein level in the future. Further work will be required to understand the pheromone biosynthesis process and how the proteome level shifts by the presence of PBAN. The establishment and use of the *in vitro* assay for protein analyses could be a key for the discovery of proteins which might be involved in the pheromone biosynthesis. Moreover, it would be worthwhile to determine the impact of chemicals, hormones and enzymes on the pheromone gland *in vitro* at the protein level. In addition, novel 2D technologies may be used to provide more detailed information. The Refraction 2D technology was already being applied in my study to assess proteins. This method is hundred times more sensitive than the Coomassie blue method and thus offers high potential to detect proteins with a very low expression in the gland. Thus, Refraction 2D maps of pheromone glands are excellent tools to identify modification of pheromone signaling pathways in the future.

In conclusion, this study shows that HACD is present in the proteome of PBAN-activated glands and its presence could be important in pheromone biosynthesis of female *H.v.*. The results of the proteome research described in this study represent a basis for further studies on the effect of PBAN on the proteome of the sex pheromone gland of *H.v.*. Protein analysis remains necessary because of possible post-transcriptional changes which can not detected by e.g. microarray analysis, because the transcription of genes (mRNA levels) may not correspond to the translation, i.e. the proteins that are actually formed.

5 Acknowledgements

I would first like to thank my thesis advisor Astrid T. Groot for her encouragement and support throughout my study. The door to Astrid office was always open whenever I had questions about my research or writing. Without her this thesis would not have been possible. I would also like to thank David G. Heckel for his constant support. I am extremely grateful to Christin Borgwardt for her technical assistance. Furthermore, I would like to thank Heiko Vogel for giving me the opportunity to work with his cDNA library of *Heliothis virescens* and his general support. For crucial help with 2D analyses, I would like to thank Juliette Courtiade. I would like to acknowledge Sybille Lorenz for analyzing my samples by GC-MS. I am grateful to Antje Loele and Alexander Muck for performing mass spectrometry analyses. Lastly, I would like to thank my colleagues of the Entomology group for sharing experiences and knowledge during the time of my study. I am extremely grateful to all group members for the nice atmosphere and for making my time enjoyable. This thesis was supported by the Max-Planck-Gesellschaft.

6 References

[1] AARONSON, R., GRAVEN, K. K., TUCCI, M., MCDONALD, R. J., AND FARBER, H. W. Non-neuronal enolase is an endothelial hypoxic stress protein. *The Journal of Biological Chemistry 270*, 27752-27757 (1995).

[2] ADAMS, T. S., DILLWITH, J. W., AND BLOMQUIST, G. J. The role of 20-hydroxyecdysone in housefly sex pheromone biosynthesis. *Journal of Insect Physiology 30* (1984), 287–294.

[3] ALJAMALI, M. N., BIOR, A. D., SAUER, J. R., AND ESSENBERG, R. C. RNA interference in ticks: a study using histamine binding protein dsRNA in the femal tick *Amblyomma americanum*. *Insect Molecular Biology 12*, 3 (2003), 299–305.

[4] BARYCKI, J. J., O'BRIEN, L. K., BRATT, J. M., ZHANG, R., SANISHVILI, R., STRAUSS, A. W., AND BANASZAK, L. J. Biochemical characterization and crystal structure determination of human heart short chain L-3-hydroxyacyl-CoA dehydrogenase provide insights into catalytic mechanism. *Journal of Biochemistry 38* (1999), 5786–5798.

[5] BETTENCOURT, R., TERENIUS, O., AND FAYE, I. Hemolin gene silencing by dsRNA injected into *Cecropia* pupae is lethal to next generation embryos. *Insect Molecular Biology 3*, 11 (2002), 267–271.

[6] BJOSTAD, L. B., WOLF, W. A., AND ROELOFS, W. L. Pheromone bioynthesis in lepidopterans: Desaturation and chain shortening. In *Pheromone Biochemistry* (1987), G. J. Blomquist and G. D. Prestwich, Eds., Academic Press, Orlando, Folida, pp. 77–120.

[7] BLOMQUIST, G. J., DILLWITH, J. W., AND ADAMS, T. S. Biosynthesis and endocrine regulation of sex pheromone production in diptera. In *Pheromone Biochemistry* (1987), G. J. Blomquist and G. D. Prestwich, Eds., New York: Academic Press, pp. 217–250.

[8] BLUM, M. S. Biosynthesis of arthropod exocrine compounds. *Annals of the Entomological Society of America 32* (1987), 381–413.

[9] BRAUN, H. P., AND SCHMITZ, U. K. The mitochondrial processing peptidase. *The international Journal of Biochemistry and Cell Biology 29*, 8-9 (1997), 1043–1045.

[10] BUSZAK, M., FREEMAN, W. R., CARLSON, J. R., BENDER, M., COOLEY, L., AND SEGRAVES, W. A. Ecdysone response genes govern egg chamber development during mid-oogenesis in *Drosophila*. *Development 126* (1999), 4581–4589.

[11] CAPLEN, N. J., FLEENOR, J., AND MORGAN, R. A. dsRNA-mediated gene silencing in cultured *Drosophila* cells: a tissue culture model for analysis of RNA interference. *Gene 252*, 1-2 (2000), 95–105.

[12] CHOI, M. Y., HAN, K. S., BOO, K. S., AND JURENKA, R. A. Pheromone biosynthetic pathways in the moth *Helicoverpa zea* and *Helicoverpa assulta*. *Insect Biochemistry and Molecular Biology 32* (2002), 1353–1359.

[13] CHOI, M. Y., AND JURENKA, R. A. PBAN stimulation of pheromone biosynthesis by inducing calcium influx in pheromone glands of *Helicoverpa zea*. *Journal of Insect Physiology 50* (2004), 555–560.

[14] CLARK, A. Causes and consequences of variation in energy storage in *Drosophila melanogaster*. *Genetics 123*, 131-144 (1989).

[15] CLEMENS, J. C., WORBY, C. A., SIMONSON-LEFF, N., MUDA, M., MAEHAMA, T., HEMMINGS, B. A., AND DIXON, J. E. Use of double-stranded RNA interference in *Drodophila* cell lines to dissect signal transduction pathways. *Proceedings of the National Academy of Sciences ot the United States of America 97*, 12 (2000), 6499–6503.

[16] COOPER, S. J., LEONARD, G. A., MCSWEENEY, S. M., THOMPSON, A. W., NAISMITH, J. H., QAMAR, S., PLATER, A., BERRY, A., AND HUNTER, W. N. The crystal structure of a class II fructose-1,6-bisphosphate aldolase shows a novel binuclear metal-binding active site embedded in a familiar fold. *Structure 4* (1996), 1303–1315.

[17] CUSSON, M., TOBE, S. S., AND MCNEIL, J. N. Juvenile hormones: Their role in the regulation of the pheromonal communication system of the armyworm moth, *Pseudaletia unipuncta*. *Archives of Insect Biochemistry and Physiology 25* (1994), 329–345.

[18] DE MORAES, R. R., NATION, J. L., AND MARUNIAK, J. E. Organ culture of salivary glands of male *Anastrpha suspensa* (Diptera: Tephritidae). *The Folrida Entomologist 78* (1995), 467–473.

[19] FAN, Y., RAFAELI, A., GILEADI, C., AND APPLEBAUM, S. W. Juvenile hormone induction of pheromone gland PBAN-responsiveness in *Helicoverpa armigera* females. *Insect Biochemistry and Molecular Biology 29* (1999), 635–641.

[20] FIRE, A. RNA triggered gene silencing. *TIG 15* (1999), 358–363.

[21] FIRE, A., XU, S., MONTOGOMERY, M. K., KOSTAS, S. A., DRIVER, S. E., AND MELLO, C. C. Potent and specific genetic interference by double stranded RNA in *Caenorhabditis elegans*. *Nature 391*, 6669 (1998), 806–811.

[22] FITT, G. P. The ecology of *Heliothis* species in relation to agroecosystems. *Annual Review of Entomology 34* (1989), 17–53.

[23] FÒNAGY, A., MATSUMOTO, S., KYOICHI, U., ORIKASA, C., AND MITSUI, T. Action of pheromone biosynthesis activating neuropeptide on pheromone glands of *Bombyx mori* and *Spodoptera litura*. *Journal of Pesticide Science 17* (1992), 47–54.

[24] FÒNAGY, A., MATSUMOTO, S., KYOICHI, U., ORIKASA, C., AND MITSUI, T. Role of calcium ion and cyclic nucleotides in pheromone production in *Bombyx mori*. *Journal of Pesticide Science 17* (1992), 115–121.

[25] FOSKET, D. E., AND MOREJOHN, L. C. Structural and functional organization of tubulin. *Annual Review of Plant Physiology and Plant Molecular Biology 43* (1992), 201–240.

[26] FOURNIER, D., BRIDE, J. M., POIRIE, M., BERGE, J. B., AND PLAPP JR., F. W. Insect glutathione s-transferase. *The Journal of Biological Chemistry 267*, 3 (1992), 1840–1845.

[27] G., B., ASHTON, F. T., AND PEPE, F. A. The invertebrate myosin filament: subfilament arrangement of the solid filaments of insect flight muscles. *Biophysical Journal 61*, 6 (1992), 1495–1512.

[28] GADENNE, C. Effects of fenoxycarb, juvenile hormone mimetic, on female sexual behaviour of the black cutworm, *Agrotis ipsilon* (Lepidoptera: Noctuidae). *Journal of Insect Physiology 39* (1993), 25–29.

[29] GE HEALTHCARE. *2-D Electrophoresis Principles and Methods Handbook*. Elanders Östervåla, 2007.

[30] GEER, B. W., AND LAURIE-AHLBERG, C. C. Genetic variation in the dietary sucrose modulation of enzyme activities in *Drosophila melanogaster*. *Genetic Research 43* (1984), 307–321.

[31] GOTO, A., BLANDIN, S., ROYET, J., REICHHART, J. M., AND LEVASHINA, E. A. Silencing of toll pathway components by direct injection of double-stranded RNA into *Drosophila* adult flies. *Nucleic Acids Research 31*, 22 (2003), 6619–6623.

[32] GRANVILLE, D. J., AND GOTTLIEB, R. A. The mitochondrial voltage-dependent anion channel (VDAC) as a therapeutic target for initiating cell death. *Current medicinal Chemistry 16*, 10 (2003), 1527–1533.

[33] GROOT, A. T., FAN, Y., BROWNIE, C., JURENKA, R. A., GOULD, F., AND SCHAL, C. Effect of PBAN on pheromone production by mated *Heliothis virescens* and *Heliothis subflexa* females. *Journal of Chemical Ecology 31*, 1 (2005).

[34] HIRUMA, K., HARDIE, J., AND RIDDIFORD, L. M. Hormonal regulation of epidermal metamorphosis *in vitro*: control of expression of a larval-specific cuticle gene. *Developmental Biology 144* (1991), 369–378.

[35] HOOGENBOOM, B. W., SUDA, K., ENGEL, A., AND FOTIADIS, D. The supramolecular assemblies of voltage-dependent anion channels in the native membrane. *Journal of Molecular Biology 370* (2007), 246–255.

[36] JEFFERSON, R. N., SHOREY, H. H., AND RUBIN, R. E. Sex pheromones of noctuid moths. XVI. the morphology of the female sex pheromone glands of eight species. *Annals of the Entomological Society of America 61*, 4 (1968), 861–865.

[37] JURENKA, R. Biochemistry of female moth sex pheromones. In *Pheromone Biochemistry and Molecular Biology.* (2003), G. Blomquist and R. Vogt, Eds., New York: Academic Press, pp. 53–80.

[38] JURENKA, R. Insect pheromone biosynthesis. *Topics in current Chemistry 239* (2004), 97–132.

[39] JURENKA, R. A. Signal transduction in the stimulation of sex pheromone biosynthesis in moths. *Archives of Insect Biochemistry and Physiology 33* (1996), 245–258.

[40] JURENKA, R. A., JACQUIN, E., AND ROELOFS, W. L. Stimulation of pheromone biosynthesis in the moth *Helicoverpa zea*: Action of a brain hormone on pheromone glands involves Ca^{2+} and cAMP as second messengers. *Proceedings of the National Academy of Sciences ot the United States of America 88* (1991), 8621–8625.

[41] JURENKA, R. A., AND ROELOFS, W. L. Biosynthesis and endocrine regulation of fatty acid derived sex pheromones in moths. In *Insect lipids: chemistry, biochemistry, and biology* (1993), D. W. Stanley-Samuelson and D. R. Nelson, Eds., University of Nebraska Press.

[42] KAIJAWARA, H., IMAMAKI, A., NAKAMURA, M., MITA, K., AND ISHIZAKA, M. Proteomic analysis of silkworm fat boby. *Journal of Insect Biotechnology and Sericology 75* (2006), 47–56.

[43] KARIM, S., RAMAKRISHNAN, V. G., TRUCKER, J. S., ESSENBERG, R. C., AND SAUER, J. R. *Amblyomma americanum* salivary glands: double-stranded RNA-mediated gene silencing of synaptobrevin homologie and inhibition of PGE_2 stimulated protein secretion. *Insect Biochemistry and Molecular Biology 34* (2004), 407–413.

[44] KARLSON, P., AND LÜSCHER, M. "Pheromones": A new term for a class of biologically active substances. *Nature 183* (1959), 55–56.

[45] KEELING, P. J., AND DOOLITTLE, W. F. Evidence that eukaryotic triosephosphate isomerase is of alpha-proteobacterial origin. *Proceedings of the National Academy of Sciences ot the United States of America 94*, 4 (1997), 1270–1275.

[46] KIM, Y. J., NACHMAN, R. J., AIMANOVA, K., GILL, S., AND ADAMS, M. E. The pheromone biosynthesis activating neuropeptide (PBAN) receptor of *Heliothis virescens*: Identification, functional expression, and structure-activity relationships of ligand analogs. *Peptides 29* (2008), 268–275.

[47] KLANNER, C., NEUPERT, W., AND LANGER, T. The chaperonin-releated protein Tcm62p ensures mitochondrial gene expression under heat stress. *Federation of European Biochemical Societies 470*, 3 (2000), 365–369.

[48] KLUN, J. A., BIERL-LEONHARDT, B. A., PLIMMER, J. R., SPARKS, A. N., PRIMIANI, M., CHAPMAN, O. L., LEPONE, G., AND LEE, G. H. Sex pheromone chemistry of the female tobacco budworm moth, *Heliothis virescens*. *Journal of Chemical Ecology 6* (1980), 177–184.

[49] KOTWICA, J., BEBAS, P., GVAKHARIA, B. O., AND GIEBULTOWICZ, J. M. RNA interference of the period gene affects the rhythm of sperm release in moths. *Journal of biological rhythms 24*, 1 (2009), 25–34.

[50] KRISHNAMOORTHY, M., JURAT-FUENTES, J. L., MCNALL, R. J., ANDACHT, T., AND ADANG, M. J. Identification of novel Cry1Ac binding proteins in midghut membranes from *Heliothis virescens* using proteomic analyses. *Insect Biochemistry and Molecular Biology 37* (2007), 189–201.

[51] LABORATORIES, K. EC1.1.1.35 3-hydroxyacyl-CoA dehydrogenase. http://www.brenda-enzymes.org/php/result_flat.php4?ecno=1.1.1.35, December 2009.

[52] LEVIN, D. M., BREUER, L. N., ZHUANG, S., ANDERSON, S. A., NARDI, J. B., AND KANOST, M. R. A hemocyte-specific integrin required for hemocytic encapsulation in the tobacco hornworm, *Mandua sexta*. *Insect Biochemistry and Molecular Biology 35* (2005), 369–380.

[53] MA, P. W. K., AND ROELOFS, W. L. Calcium involvement in the stimulation of sex pheromone production by PBAN in the European Corn Borer, *Ostrinia nubilalis* (Lepidoptera: Pyralidae). *Insect Biochemistry and Molecular Biology 25*, 4 (1995), 467–473.

[54] MAZOR, M., AND DUNKELBAUM, E. Circadian rhythms of sexual behavior and pheromone titers of two closely related moth species *Autographa gamma* and *Cornutiplusia circumflexa*. *Journal of Chemical Ecology 31*, 9 (2005), 2153–2168.

[55] MBATA, G. N., AND RAMASWAMY, S. B. Rhythmicity of sex pheromone content in female *Heliothis virescens*: Impact of mating. *Physiological Entomology 15*, 423-432 (1990).

[56] MOTO, K., YOSHIGA, T., YAMAMOTO, M., TAKAHASHI, S., OKANO, S., ANDO, T., NAKATA, T., AND MATSUMOTO, S. Pheromone gland-specific fatty acyl reductase of the silkmoth, *Bomby mori*. *Proceedings of the National Academy of Sciences ot the United States of America 100*, 16 (2003), 9156–9161.

[57] MOUNIER, N., AND ARRIGO, A. P. Actin cytoskeleton and small heat shock proteins: How do they interact? *Cell Stress Chaperones 7*, 2 (2002), 167–176.

[58] MOUNIER, N., GOUY, M., MOUCHIROUD, D., AND PRUDHOMME, J. C. Insect muscle actins differ distinctly from invertebrate and vertebrate cytoplamic actins. *Journal of Molecular Evolution 34* (1992), 406–415.

[59] NAKANO, H., AMEMIYA, S., SHIOKAWA, K., AND TAIRA, M. RNA interference for the organizer-specific gene *xlim-1* in Xenopus embryos. *Biochemical and Biophysical Research Communications 274*, 2 (2000), 434–439.

[60] NELSON, N., AND HARVEY, W. R. Vacuolar and plasma membrane proton-adenosinetriphosphatases. *Physiological Reviews 79*, 2 (1999), 361–385.

[61] NEWSHOLME, E. A., BEIS, I., LEECH, A. R., AND ZAMMIT, V. A. The role of creatine kinase and arginine kinase in muscle. *Journal of Biochemistry 3*, 172 (1978), 533–537.

[62] NIJHOUT, H. F., AND GRUNERT, L. W. Bombyxin is a growth factor for wing imaginal disks in Lepidoptera. *Proceedings of the National Academy of Sciences ot the United States of America 99*, 24 (2002), 15446–15450.

[63] OHNISHI, A., HULL, J. J., AND MATSUMOTO, S. Targeted disruption of genes in the *Bombyx mori* sex pheromone biosynthetic pathway. *Proceedings of the National Academy of Sciences ot the United States of America 103*, 12 (2006), 4398–4403.

[64] PATEL, A., FONDRIK, M. K., KAFTANOGLU, O., EMORE, C., HUNT, G., FREDERICK, K., AND AMDAM, G. V. The making of a queen: Tor pathway is a key player in diphenic caste development. *PLoS ONE 2*, 6 (2007), e509.

[65] PAUCHET, Y., MUCK, A., SVATOŠ, A., HECKEL, D. G., AND PREISS, S. Mapping the larval midgut lumen proteome of *Helicoverpa amigera*, a generalist herbivorous insect. *Journal of Proteome Research 7* (2008), 1629–1639.

[66] PICIMBON, J. F., BECARD, J. M., STRENG, L., CLEMENT, J. L., AND GADENNE, C. Juvenile hormone stimulates pheromonotropic brain factor release in the female black cutworm *Agrotis ipsilon*. *Journal of Insect Physiology 41* (1995), 377–382.

[67] POPE, M. M., GASTON, L. K., AND BAKER, T. C. Composition, quantification, and periodicity of sex pheromone gland volatiles from individual *Heliothis virescens* females. *Journal of Chemical Ecology 8*, 7 (1982), 1043–1055.

[68] PRICE, D. R. G., AND GATEHOUSE, J. A. RNAi-mediated crop protection against insects. *Trends in Biotechnology 26*, 7 (2008), 393–400.

[69] QUAN, G. X., KANDA, T., AND TAMURA, T. Induction of the *white egg 3* mutant phenotype by injection of the double-stranded RNA of the silkworm *white* gene. *Insect Molecular Biology 11*, 3 (2002), 217–222.

[70] RAFAELI, A. Pheromonotropic stimulation of moth pheromone gland cultures *in vitro*. *Archives of Insect Biochemistry and Physiology 25* (1994), 287–299.

[71] RAFAELI, A. Mechanisms involved in the control of pheromone produciton in female moths: Recent developments. *Entomologia Experimentalis et Applicata 115* (2005), 7–15.

[72] RAFAELI, A., AND GILEADI, C. Modulation of the PBAN-stimulated pheromonotropic activity in *Helicoverpa armigera*. *Insect Molecular Biology 25*, 7 (1995), 827–834.

[73] RAFAELI, A., AND SOROKER, V. Cyclic AMP mediation of the hormonal stimulation of ^{14}C-acetate incorporation by *Heliothis armigera* pheromone glands *in vitro*. *Molecular and Cellular Endocrinology 65* (1989), 43–48.

[74] RAFAELI, A., SOROKER, V., KAMENSKY, B., AND RAINA, A. K. Action of pheromone biosynthesis activating neuropeptide on *in vitro* pheromone glands of *Heliothis amigera* females. *Journal of Insect Physiology 36*, 9 (1990), 641–646.

[75] RAFAELI, A., SOROKER, V., KLUN, J. A., AND RAINA, A. K. Stimulation of *de novo* pheromone biosynthesis by *in vitro* pheromone glands of *Heliothis* spp. In *Insect Neurochemistry and Neurophysiology* (1990), A. B. Borkovec and E. P. Masler, Eds., The Humana Press Inc., pp. 309–312.

[76] RAINA, A. K., JAFFE, H., KEMPE, T. G., KEIM, P., BLACHER, R. W., FALES, H. M., RILEY, C. T., KLUN, J. A., RIDGWAY, R. L., AND HAYES, D. K. Identification of a neuropeptide hormone that regulates sex pheromone production in female moths. *Science 244* (1989), 796–798.

[77] RAINA, A. K., KLUN, J. A., AND STADELBACHER, E. A. Diel periodicity and effect of age and mating on female sex pheromone titer *Heliothis zea* (Lepidoptera: Noctuidae). *Annals of the Entomological Society of America 79*, 1 (1986), 128–131.

[78] RAINA, A. K., AND MENN, J. J. Endocrine regulation of pheromone production in lepidopters. In *Pheromone Biochemistry* (1987), G. D. Prestwich and G. J. Blomquist, Eds., Academic Press, Orlando, Folida, pp. 159–174.

[79] RAINA, A. K., WERGIN, W. P., MURPHY, C. A., AND ERBE, E. F. Structural organization of the sex pheromone gland in *Helicoverpa zea* in relation to pheromone production and release. *Arthropod Structure and Development 29* (2000), 343–353.

[80] RAJAGOPAL, R., SIVAKUMAR, S., AGRAWAL, N., MALHORTA, P., AND BHATNAGAR, R. J. Silencing of midgut aminopeptidase N of *Spodoptera litura* by double-stranded RNA establishes its role as *Bacillus thuringiensis* toxin receptor. *The Journal of biological chemistry 277*, 40 (2002), 46849–46851.

[81] RAMASWAMY, S. B., AND COHEN, N. E. Comparative activity of juvenile hormones I, II, III in promoting egg maturation in the moth *Heliothis virescens* (Noctuidae). *Zoological Science 8* (1991), 747–750.

[82] RAMASWAMY, S. B., AND COHEN, N. E. Ecdysone: An inhibitor of receptivity in the moth, *Heliothis virescens*? *Naturwissenschaften 79* (1992), 29–31.

[83] RAMASWAMY, S. B., RANDLE, S. A., AND MA, W. K. Field evaluation of the sex pheromone components of *Heliothis virescens* (Lepidoptera: Noctuidae) in cone traps. *Environmental Entomology 14* (1985), 293–296.

[84] REESE, G., AYUSO, R., AND LEHRER, S. B. Tropomyosin: An invertebrate panallergen. *International Archievs of Allergy and Immunology 119*, 4 (1999), 247–258.

[85] ROELOFS, W. L. Chemistry of sex attraction. *Proceedings of the National Academy of Sciences ot the United States of America 92* (1995), 44–49.

[86] ROELOFS, W. L., HILL, A. S., CARDÈ, R. T., AND BAKER, T. C. Two sex pheromone components of the tobacco budworm moth, *Heliothis virescens*. *Life science 14* (1974), 1555–1562.

[87] SATYANARAYANA, K., BHASKARAN, G., DAHM, K. H., AND MEOLA, R. Regulation of vitellogenin synthesis by juvenile hormone in the corn earworm, *Helicoverpa armigera*. *Invertebrate Reproduction and Development 21* (1992), 169–178.

[88] SCHAL, C., HOLBROOK, G. L., BACHMANN, J. A. S., AND SEVALA, V. L. Reproductive biology of the german cockroach, *Blattella germanica*: Juvenile hormone as a pleiotropic master regulator. *Archives of Insect Biochemistry and Physiology 35* (1997), 405–426.

[89] SEYBOLD, S. J., AND VANDERWEL, D. Biosynthesis and endocrine regulation of pheromone production in the coleoptera. In *Pheromone Biochemistry and Molecular Biology* (2003), G. J. Blomquist and R. Vogt, Eds., Elsevier Academic Press, London, UK, pp. 137–200.

[90] SIMONET, G., POELS, J., CLAEYS, I., VAN LOY, T., FRANSSENS, V., DE LOOF, T., AND VANDENBROECK, J. Neuroendocrinological and molecular aspects of insect reproduction. *Journal of Neuroendocrinology 16* (2004), 649–659.

[91] SIMPSON, R. J. *Proteins and Proteomics: A Laboratory Manual*. COLD SPRING HARBOR LABORATORY PRESS, 2003.

[92] SIROVER, M. A. New nuclear functions of glycolytic protein, glyceraldehyde-3-phosphate dehydrogenase, in mammalian cells. *Journal of Cellular Biochemistry 95* (2005), 45–52.

[93] SOROKER, V., AND RAFAELI, A. *In vitro* hormonal stimulation of [^{14}C]acetate incorporation by *Heliothis armigera* pheromone glands. *Insect Biochemistry 19*, 1 (1989), 1–5.

[94] SRINIVASAN, A., COFFELT, J., AND OBERLANDER, H. *In vitro* maintenance of the sex pheromone gland of the female indian meal moth *Plodia interpunctella* (Hübner). *Journal of Chemical Ecology 5*, 5 (1979), 653–662.

[95] TAMAKI, Y. Sex pheromones. In *Comprehensive Insect Physiology, Biochemistry and Pharmacology* (1985), G. A. Kerkut and L. I. Gilbert, Eds., vol. 9, Pergamon, Oxford, pp. 145–191.

[96] TANG, J. D., CHARLTON, R. E., JURENKA, R. A., WOLF, W. A., PHELAN, P. L., SRENG, L., AND ROELOFS, W. L. Regulation of pheromone biosynthesis by a brain hormone in two moth species. *Proceedings of the National Academy of Sciences ot the United States of America 86* (1989), 1806–1810.

[97] TANG, J. D., WOLF, W. A., ROELOFS, W. L., AND KNIPPLE, D. C. Development of functionally competent cabbage looper moth sex pheromone glands. *Insect Biochemistry 21* (1991), 573–581.

[98] TEAL, P. E. A., TUMLINSON, J. H., AND OBERLANDER, H. Neural regulation of sex pheromone biosynthesis in heliothis moth. *Proceedings of the National Academy of Sciences ot the United States of America 86* (1989), 2488–2492.

[99] TILLMAN, J. A., SEYBOLD, S. J., JURENKA, R. A., AND BLOMQUIST, G. J. Insect pheromones - an overview of biosynthesis and endocrine regulation. *Insect Biochemistry and Molecular Biology 29* (1999), 481–514.

[100] TOMOYASU, Y., MILLER, S. C., TOMITA, S., SCHOPPMEIER, M., GROSSMAN, D., AND BUCHER, G. Exploring systemic RNA interference in insects: a genome-wide survey for RNAi genes in *Tribolium*. *Genome Biology 9*, 1 (2008).

[101] TSCHIYA, D., SHIMIZU, N., ISHIKAWA, M., SUZUKI, Y., AND MORIKAWA, K. Ligand-induced domain rearrangement of fatty acid ß-oxidation multienzyme complex. *Structure 14* (2006), 237–246.

[102] TUMLINSON, J. H., HENDRICKS, D. E., MITCHELL, E. R., DOOLITTLE, R. E., AND BRENNAN, M. M. Isolation, identification and synthesis of the sex pheromone of the tobacco budworm. *Journal of Chemical Ecology 1*, 2 (1975), 203–214.

[103] TURNER, C. T., DAVY, M. W., MACDIARMID, R. M., PLUMMER, K. M., BIRCH, N. P., AND NEWCOMB, R. D. RNA interference in the light brown apple moth, *Epiphyas postvittana* (walker) induced by double-stranded RNA feeding. *Insect Molecular Biology 15*, 3 (2006), 383–391.

[104] TUSCHI, T., ZAMORE, P. D., LEHMANN, R., BARTEL, D. P., AND SHARP, P. A. Targed mRNA degradation by double-stranded RNA *in vitro*. *Genes and Development 13* (1999), 3191–3197.

[105] UHLIROVA, M., FOY, B. D., BEATY, B. J., OLSON, K. E., RIDDIFORD, L. M., AND JINDRA, M. Use of sindbis virus-mediated RNA interderence to demonstrated a conserved role of broad-complex in insect metamorphosis. *Proceedings of the National Academy of Sciences ot the United States of America 100*, 26 (2003), 15607–15612.

[106] VASUDEVAN, S., AND NAD J. A. STEITZ, Y. T. Switching from repression to activation: MicroRNAs can up-regulate translation. *Science 318*, 5858 (2007), 1931–1934.

[107] VOGEL, H., HEIDEL, A. J., HECKEL, D. G., AND GROOT, A. T. Transcriptome analysis of the sex pheromone gland of the noctuid moth *H. virescens*. *BMC Genomics 11*, 29 (2010).

[108] WARGELLUS, A., AND ANDA. FJOSE, S. E. Double-stranded RNA induces specific developmental defects in zebrafish embryos. *Biochemical and Biophysical Research Communications 263*, 1 (1999), 156–161.

[109] WEDELL, N. Female receptivity in butterflies and moths. *Journal of Experimental Biology 208* (2005), 3433–3440.

[110] WEEDS, A. Actin-binding proteins-regulators of cell architecture and motility. *Nature 296* (1982).

[111] WIANNY, F., AND ZERNICKA-GOETZ, M. Specific interference with gene function by double-stranded RNA in early mouse development. *Nature Cell Biology 2* (2000), 70–75.

[112] WINSTON, W. M., MOLODOWITCH, C., AND HUNTER, C. P. Systemic RNAi in *C. elegans* requires the putative transmembrane protein SID-1. *Science 295* (2002), 2456–2459.

[113] ZHANG, P., ASO, Y., YAMAMOTO, K., BANNO, Y., WANG, Y., TSUCHIDA, K., KAWAGUCHI, Y., AND FUJII, H. Proteome analysis of silk gland proteins from the silkworm, *Bombyx mori*. *Proteomics 6*, 2586-2599 (2006).

7 Appendices

Appendix A : Composition of the pinto bean diet (2L)

Substance	quantity
Pinto Beans[c]	125 g
Wheat germ[a]	100g
Soy protein[a]	50 g
Casein[a]	50 g
Torula yeast[a]	62.5 g
Ascorbic acid[a]	6 g
Sorbic acid[b]	3 g
Methyl paraben[a]	5 g
Vanderzant Vitaminmix[b]	10g
Tetracycline[b]	0.25 g
Agar-Agar[a]	35 g

[a]= Bio-Serv; Frenchtown, NJ

[b]= Sigma-Aldrich Chemikals, Steinheim, Germany

[c]= MEX-AL EL SOMBRERO Import Export GmbH, Aachen, Germany

Appendix B : Chemicals and Kits

Chemicals and Kits	Manufacturer
Acetic acid	Carl Roth, Karlsruhe, Germany
Acetone	Carl Roth, Karlsruhe, Germany
Acryl amide	BioRAD, München, Germany
Agarose	Biozym, Hessisch Oldendorf, Germany
Ampholytes	Amersham Biosciences, Freiburg, Germany
Antibiotic-Antimycotic	Invitrogen, Karlsruhe, Germany
Bradford reagent	BioRAD,München, Germany
Bovine serum albumin	BioRAD, München, Germany
Butanol	Carl Roth, Karlsruhe, Germany
CHAPS	Amersham Biosciences, Freiburg, Germany
DNAse	Ambion, Darmstadt, Germany
DNAse buffer	Ambion, Darmstadt, Germany
dNTPs	Metabion, Martinsried, Germany
DTT (1,4- Dithiothreitol)	Carl Roth, Karlsruhe, Germany
Ethanol	Merck, Darmstadt,Germany
Ethylendiamine-tetraacetic acid (EDTA)	Carl Roth, Karlsruhe, Germany
FBS	Invitrogen, Karlsruhe, Germany
GeneRuler™ DNA Ladder Mix (10kbp)	Fermentas, St.Leon-Rot, Germany
Glycerol	Carl Roth, Karlsruhe, Germany
Grace medium	Invitrogen, Karlsruhe, Germany
Hexane	Carl Roth, Karlsruhe, Germany
Hydrochloric acid	Carl Roth, Karlsruhe, Germany
IAA (Indole-3-acetic acid)	Amersham Biosciences, Freiburg, Germany
Immobiline DryStrip	Amersham Biosciences, Freiburg, Germany
Juvenile hormone III	Sigma-Aldrich Chemikals, Steinheim, Germany
MEGAscript RNAi Kit	Ambion, Darmstadt, Germany
Mineral oil	BioRAD, München, Germany
Octane	Sigma-Aldrich Chemikals, Steinheim, Germany
PageBlue staining solution	Fermentas, St.Leon-Rot, Germany

Page Ruler™ Prestained Protein Ladder Plus	Fermentas, St.Leon-Rot, Germany
PBS (10x)	BioRAD, München, Germany
Precision Plus Protein™ Standard Plugs	BioRAD, München, Germany
Taq-Polymerase	Metabion, Martinsried, Germany
Taq-Buffer	Metabion, Martinsried, Germany
TCA	Sigma-Aldrich Chemikals, Steinheim, Germany
TEMED	Invitrogen, Karlsruhe, Germany
TGS-running-buffer	BioRAD, München, Germany
Thiourea	Amersham Biosciences, Freiburg, Germany
Tris(hydroxymethyl)aminomethane	Carl Roth, Karlsruhe, Germany
TRIzol® Reagent	Invitrogen, Karlsruhe, Germany
Trypan blue (0.4% solution)	Sigma-Aldrich Chemikals, Steinheim, Germany
SDS	Amersham Biosciences, Freiburg, Germany
RNA storage solution	Ambion, Darmstadt, Germany
RNase free water	Ambion, Darmstadt, Germany
RNeasy®MiniElute™ Cleanup Kit	Qiagen, Hilden, Germany
Refraction-2D Labeling Kit	NH DyeAGNOSTICS UG, Halle, Germany
Urea	Amersham Biosciences, Freiburg, Germany
Verso™SYBR® Green 2-Step QRT-PCR Kit	Abgene, Hamburg, Germany
1-Bromo-3-chloropropanol	Sigma-Aldrich Chemikals, Steinheim, Germany
2 D-Quant-Kit	Amersham Biosciences, Freiburg, Germany
2-Propanol	Carl Roth, Karlsruhe, Germany
20-Hydroxyecdysteron	Sigma-Aldrich Chemikals, Steinheim, Germany

Appendix C : Solution and Buffer

Solution and Buffer	Concentration
Homogenization buffer	
CHAPS	0.4 g
Protease Inhibitor	200 μl
PBS	add 10 ml
SDS equilibration buffer	
1,5 M Tris-HCL, pH 8,8	10 ml
Urea	72.07 g
Glycerol	60 ml
SDS	4 g
H_2O	add 200 ml
Lysis buffer	
7 M Urea	4.2 g
2 M Thiourea	1.52 g
4% CHAPS	0.4 g
60 mM DTT	92.4 mg
1% Ampholytes	100 μl
H_2O	add 10 ml
Tris/EDTA buffer	
10 mM Tris-HCl, pH7	0.607 g
1mM EDTA	0.1861 g
H_2O	add 500 ml

Appendix D : Technical equipments and Instruments

Instruments	Manufacturer
Centrifuge	Eppendorf AG, Hamburg, Germany
Criterion™ Cell	BioRAD, München, Germany
Ettan DALT 6 Gel Caster	Amersham Biosciences, Freiburg, Germany
Ettan DALT 6 Large Vertical Electrophoresis System	Amersham Biosciences, Freiburg Germany
Mini Centrifuge	Eppendorf AG, Hamburg, Germany
Plate Reader (Tecan Infinite® 200)	Tecan Group, Männedorf, Switzerland
Protean IEF Cell	BioRAD, München, Germany
Shaker (Heidolph Duomax 1300)	Heidolph Instruments GmbH & Co. KG Schwabach, Germany
Spectrophometer UV-1650 PC	SHIMADZU, Champs-sur-Gaulle, France
Thermomixer	Eppendorf AG, Hamburg, Germany
Vortexer	Scientific Industries Inc., New York, USA

Appendix E : Sequence of MS-Ento BLAST

spot	MS-Ento-BLAST identification[a]	NCBI-BLAST accession[c]	NCBI-BLAST description[c]	NCBI-BLAST species[d]	Identity [%][e]	MS-Ento BLASTSequence[b]	C- or N-Terminus[f]
2	hvipg|HV-PGN_Contig_672_FWD_frame_0	NP_732006	Tropomyosin 1	*Drosophila melanogaster*	92%	SIFSSDTMMKFSIIKNELQNIKNTALKRAESEVAALNR RIQLLEEDLERSEERLATATAKLSEASQAADESERARK VLENRSSADEERMDALENQXKEARFLAEEAXKKYDE VARKLAMVEADLERAEERAESGESKIVELEEELRVVG NNLKSLEVSEEKANQREEEYKNQIKTLITRLKEAEAR AEFAERSVQKLQKEVDRLEDELVAEKEKYKDIGDDLD TAFVELILKE*MSRSV*FVNVRVRSPRGCYHLPPKKKK KK	C
3	*n.i.*						
5	*n.i.*						
6	*n.i.*						
9	*n.i.*						
11	hvipg|HV-PGN_Contig_5444_FWD_frame_1	NP_001036964	Beta-Tubulin	*Bombyx mori*	99%	FMPGFAPLTSRGSQQYRALTVPELTQQMFDAKNMMA ACDPRHGRYLTVAAIFRGRMSMKEVDEQMLNIQNKN SSYFVEWIPNNVKTAVCDIPPRGLKMAATFIGNSTAIQ ELFKRIPEQFTAMFRRKAFLHWYTGEGMDEMEFTEA ESNMNDLVSEYQQYQEATADEDAEFDEEQEQEIEDN* ALTPNNPLPLPLTPPPAPYPSVRRVARDVF*FALVFP	C
12	*n.i.*						
13	*n.i.*						
14	*n.i.*						
15	hviV1|Contig19_FWD_frame_0	P25420	Chaperonin isoform	*Heliothis virescens*	98%	RSPHITRNSFKYLKATNINSCRFYAKEVRFGPDVRSLM LQGVDILADAVAVTMGPKGRNVILEQSLGPPKITKDG VTVAKGIDLKDKFQNIGARLVQNVANKTNEEAGDGT TTATVLARAIAKEGFENISRGANPIEIRKGVMLAVESV KRQLKEMSKPVNTSEEIEQVATISANGDESIGKLIAAA MNRVGKNGVITVKDGKTLEDELEIIEGMKFDRGYVSP YFINSNKGPKVEYNDALVLYSEKKIYYASQVVPALEL ANSQKKPLVIIAEDYDGEPLSVLVVNKLKIGLPVVAVK APGFGEYRTNALLDMAAATGGVVFEDDTNLVRLEDC QAESFGQVGEVIITKDSTLLLKGKGDPNEIKQRIDQIK EELETATSNYDRERLIDRLGRLQSGVAVLIGGCSEVE VNEKKDRVNDALNATRAAVEEGIVPGGGAALLRCIPA LDLLKPANKDQEIGVSIIKKALRTPCTIASNAGFDGAV VVSKVEDMGPEYGYDALNNEYVNMIEKGIIDPTKVV RRALTDASGVASLLTTAEAVICDMPKQKDPPPEYAPIG GGDY*NGLFVHIYFKFNKIYFSRCPIILIFNLNHLQAFN KSIC	C
16	hvipg|HV-PGN_Contig_1305_FWD_frame_1	AAK52066	Actin	*Heliothis virescens*	99%	LAVSLP*SQHPPRPKPNTNAKMCDDDVAALVVDNGS GMCKAGFAGDDAPRAVFPSIVGRPRHQGVMVGMGQ KDSYVGDEAQSKRGILTLKYPIEHGIITNWDDMEKIW HHTFYNELRVAPEEHPVLLTEAPLNPKANREKMTQIM FETFNSPAMYVAIQAVLSLYASGRTXGIVLDSGDGVSH TVPIYEGYALPHAILRLDLAGRDLTDYLMKI	N

17	hvipg|HV-PGN_Contig_364_FWD_frame_1	NP_001040233	ATP synthase	*Bombyx mori*	94%	EEQVAIIYCGVRGHLDKLDPSKITAFEKEFTQHIKTSH QSLLATIAKDGQITPESDASLKKIVSDFLATFTQAAAR* TFSFYELWLWQEIVSRI*ETTSDPLVAQSHVKHHCMLT AGSWKHSYQLLFRFGMLPLAA***LSIVWTVLNVDTI MECIYLERQEWLYINKYS*N*K	C
18	hviV1|Contig262_FWD_frame_2	NP_001093278	Actin-depolymerizing Factor 1	*Bombyx mori*	99%	RSSIELLV*FSESCQLAAATYFSNNI*SLGISQINYKINIK L*YKVTQYTSESVNWALF*KDAILILPVSLTHALIGCR KKGLANIPNSVVPVAVVVVSVKLVVEFLRV*HQKMAS GVTVSDACKTTYEEIKKDKKHRYVVFYIRDEKQIDVE TVGERNAEYDQFLEDLQKGGTGECRYGLFDFEYTHQ CQGTSEASKKQKLFLMSWCPDTAKVKKKMLYSSSFD ALKKSLVGVQKYIQATDLSEASQEAVEEKLRATDRQ* VSIYRHDRRVAHRDRPTETTSAATDWPRALGYQRTYC TKPPLCGLSQYCQWFAVRPTVSHGFFLYIVSILKLLQSI PLRSGLAQVGSELMYS*L*THGRLRDSL*L*QKESLCL *YN*RVN*AQTKFKYSVRVFFNCKTG*RTRSAFILFRL* YKECTILISFEIHLAKGCKLELRLDTWRALDKYFVTDL SRNTLDIRGK	C
19	n.i.						
20	n.i.						
21	hvipg|HV-PGN_Contig_6434_FWD_frame_1	BAE96011	Glyceraldehyde-3-phosphate dehydrogenase	*Bombyx mori*	95%	TTEKASAHLEGGAKKVIISAPSADAPMFVVGVNLEAY DPSYKVISNASCTTNCLAPLAKVIHDNFEIIEGLMTTV HATTATQKTVDGPSGKLWRDGRGAQQNIIPASTGAAK AVGKVIPALNGKLTGMAFRVPVPNVSVVDLTVRLGKP ASYDAIKQKVKEAAQGPLKGILDYTEEQVVSSDFIGD SHSSIFDAAAGISLNDNFVKLISWYDNEFGYSNRVIDLI KYIQTKD*MFACCVERNVVM	/
22	*n.i.*						
23	hvipg|HV-PGN_Contig_5708_FWD_frame_2	ABK40535	Glutathione S-transferase	*Helicoverpa armigera*	88%	YYFVC*LQTQ*QTRMSIDLYYTPGSSPCRVVLLVAAAL DLHLNLNILNLRNGEHLTPDFLKLNPQHTVPTIVDGDF SLWESRAISKYLVNKYGGENNDLYPTDPKARAIVDQR LDFDLGTLYPRFGNYFYPQVFGGAKADEALLKKVEE ALQFLNTFLEGQKYAAGDKLTLADLSIVATVSTIDAAG ISLKEYPNIEKWFDLVKTTAPGYQEANEAGVKMFKD MVAQLKAKTEL*V*QKRCYYLLDK	C and N
24	har454s|HARM_c10816_FWD_frame_1 nseq=2	NP_001091829	Vacuolar ATP synthase catalytic subunit A	*Bombyx mori*	93%	SRSVFSIFLVPKN***FTMARALTGGGLRTIADEEIEERF GFVFAVSGPVVTAEKMSGSAMYELVRVGYNELVGEII RLEGDMATXQVYEETSGVTVGDPVLRTGKPLSVELG PGILGSIFDGIQRPLKDINELTQSIYIPKGVNVPSLARDV SWEFVPMNVKTGSHITGGDLYGLVHENTLVKHRMLIP PKAKGTVTYIAPAGNYKVTDVVLETEFDGEKEKYTM LQVWPVRQPRPVTEKLPANHPLLTGQRVLDSLFPCVQ GGTTAIPGAFGCGKTVISQALSKYSNSDVIVYVGCGE RGNEMSEVLRD	N
25	hvipg|HV-PGN_Contig_1200_FWD_frame_1	ACR07789	Alpha tubulin	*Heliothis virescens*	100%	ITFVWQAS*PVALNDD*YLN*FIFYIKFNKTQFKMRECI SVHVGQAGVQIGNACWELYCLEHGIQPDGQMPTDKT VGGGDDSFNTFFSETGAGKHVPRAVFVDLEPTVVDE VRTGTYRQLFHPEQLITGKEDAANNYARGHYTIGKEI VDLVLDRIRKLADQCTGLQGFLIFHSFGGGTGSGFTSL LMERLSVDYGKKSKLEFAIYPAPQVSTAVVEPYNSILT THTTLEHSDCAFMVDNEAIYDICRR	N

27	har454s|HARM_c2821_FWD_frame_1 nseq=18	XP_001601340	similar to 3-Hydroxyacyl-coA dehyrogenase	*Nasonia vitripennis*	68%	NAMASVKTEKVGIVGSGLIGRSWAMLFASVGYQVTIF DIIPQQVTDALADIKVQLKTLEXDGLLRGKLDADAQF KCIKGTSDLASLAKGAIFIQECVPESLELKKKVFADLD KVVDDKTILSSSTSTTLPSKFSENLKHKAQVIVSHPVN PPYYVPLVEIVPAPWTKKEVCEKTKAIMLEIGQEPVVL TREIDGFVLNRIQYAILDEVWRLVDAKVVNVEDIDKVI SEGLGMRYAFLGSLETAHLNAEGMKSYIERYGDTIHS VSQTMGEIPRMTTSPSAATICEQLNRMVPLDKLQERR AWRDACLTRLAVLKNEMNTLKHKYNLN*LS**LKKIL S*YLNKMLMRSIQISTTRMSDRLLYNNI*EYLPTKIFC* CYTLCNLYCKRVYILHMNILHVI	C
29	hviV1|Contig690_FWD_frame_0	AAU84716	Triosephosphate isomerase	*Helicoverpa armigera*	95%	K*RSLRLI*NHSKMGRKFVVGGNWKMNGDKKQVTDI VETLKKGPLDPNVEVVIGVPAIYLAYVQSIVPGTISVA AQNCWKVAKGAFTGEISPAMIKDIGANWVILGHSERR TIFGEKDELVAEKVAHALENGLKVIACIGETLEEREAG KTEEVVFRQTKALLPAIGNNWANVVLAYEPVWAIGT GKTASPQQAQDVHASLRNWLSSNASPDVAASERIQY GGSVTAANAKELAACPDIDGFLVRWQPSLKPKLVDIV NATQ*TSIHNVSLPIDLCVSERFSNLFYNVVVSLFMNV R*NYGNRIMDS*IRITFVCLLLPTLLRFIIFTCQAVPIE	C and N
30	har454s|HARM_c47_FWD_frame_2	XP_967480	similar to Voltage-dependent Anion-selective Channel Isoform 1	*Tribolium castaneum*	62%	RFLSN*XVLWCGSVGGLVLGKLPGIQCKIVLICE*IQPA GMAPPYYADLGKKANDVFSKGYHFGVFKFDLKTKSE TGVEFASGITSNQEXGXXFGSLXSKYAVKDYGLTFTE KWNTDNTLATDITIQDKIAAGLKVTLEGTFAPQTGTK TGKLKTSFANDTVAVNTNLDLDLAGPIVDVAAVLSFQ GWLAGVHGQFDSQKTKFSKNNFSLGYESKDFNLHTN VDNGKDFGGSIYQKVSEKIDCGISMKWTAGSADTLFG VGAKFALDADASLHAKVNNKSLIGLGYQQKLRPGVT LTISAAIDGQNFNAGGHKVGVALELEP*VHRGASAFSP VDNT*CHTDCYY*QKRKRN*KKSIY*TVSSSVLCIVYS SVQNATIKLSYIR*LRLCCICELRRQSIL*FLFQDGGRFF PQMFRVLKVLCISTRRMSIPVLLNKEPT*RHYVRCLVN KHLWCID*MVIKLNSLLESS	C
31	hvipg|HV-PGN_Contig_1200_FWD_frame_1	ACR07789	Alpha-tubulin	*Heliothis virescens*	100%	ITFVWQAS*PVALNDD*YLN*FIFYIKFNKTQFKMRECI SVHVGQAGVQIGNACWELYCLEHGIQPDGQMPTDKT VGGGDDSFNTFFSETGAGKHVPRAVFVDLEPTVVDE VRTGTYRQLFHPEQLITGKEDAANNYARGHYTIGKEI VDLVLDRIRKLADQCTGLQGFLIFHSFGGGTGSGFTSL LMERLSVDYGKKSKLEFAIYPAPQVSTAVVEPYNSILT THTTLEHSDCAFMVDNEAIYDICRR	N
34	*n.i.*						
35	*n.i.*						
36	hvil|HV-LN_Contig_7153_FWD_frame_2	BAD12426	Fructose 1,6-bisphosphate aldolase	*Antheraea yamamai*	95%	PPDKLK*KTTMSTYFQYPTPELQEELRKIAQAIVAPDK GILAADESTGTMGKRLQDIGVENTEENRRKYRQLLFS SDPAVSENISGVILFHETLYQKADDGTPLVTLLEKRGII PGIKVDKGVVPLFGSEDECTTQGLDDLAQRCAQYKK DGCHFAKWR	N
37	*n.i.*						
38	*n.i.*						
40	*n.i.*						

41	*n.i.*						
42	*n.i.*						
44	har454s|HARM_c27888_FWD_frame_0	NP_001040233	ATP Synthase	*Bombyx mori*	86%	WCPGGRLPSSAICDGSPGSAVGRWCPSSAISRWRPGG RLPSSAICDGSPGSAIGYGLPSSAISGWCPSSAISGWCP GGRLPSSAICDGSPGSAIGYGLPSSAISGWCPGGAISR WRPGGRLPSSAICDGSPGSAIGYGLPSSAISGWCPSSAI SGWCPGGRLPSSAICDGSPGSAIGYGLPSSAISGWCPG XAIXRWXPGGXLXSSXXXXGSPGSXXGXGXPXSXIS GWCPSSAISGWCPGGRXPSSAICDGSPGSAIGYGLPSS AIVDVPVGEQLLGRVVDALGNAIDGKGPVDTKSRTRV GIKAPGIIPRVSVREPMQTGIKAVDSLVPIGRGQREXIIG DRQTGKTALAIDTIINQQRFNKGDDEKKKLYCIYVAIG QKRSTVAQIVKRLTDAGAINYTIIVSATASDAAPLQYL APYSGXAMGEFFRDNGKHXLIIYDDLSKQAVAYRQM SLLLRRPPGREAYPGDVFYLHSRLLERAAKMSDKMG GGSLTALPVIETQAGDVSAXXXXXXVISITDGQIFLET ELFYKGIRPAINVGLSVSRVGSAAQTKAMKQVAGSM KLELAQYREVAAFAQFGSDLDAATQQLLNRGMRLTE LLKQGQYVPMAIEEQVAIIYCGVRGHLDKLDPSKITAF EXEFTQHIKTSHQGLLATIAKDGQITXESDXSLKKXVS DFLATFTQAASR*TSSFYELWL*QEIVSRI*ETTSDPLVA QSRVKHHCMLTAGSWKHSYQLLSRLGMLPLAA***LS FVWTVLNVDTIMECIYLVRQEWLYIIKYS*KLX	C
45	*n.i.*						
47	*n.i.*						
48	hvipg|HV-PGN_Contig_4246_FWD_frame_0	NP_001124374	Paramyosin	*Bombyx mori*	91%	NYEQALRAKRTVEQSYEEAVTRINELTVINVNLSSSKA KIE*ELAAVAADYDEIAKELRIADERYQRVQTELKHTV EHLHEEQERIVKIEAVKKSLEIEVKNISVRLEEVEANAI VGGKRLRHPPSASRDGRSALRLALTLPCLRTTPAKRRP LVPTDVF	/
50	hvipg|HV-PGN_Contig_1118_FWD_frame_2	ABU98622	Arginine kinase	*Helicoverpa armigera*	96%	LIDDHFLFKEGGRFLQAANACRFWPSGRGIYHNENKT FLVWCNEEDHLRLISMQMGGDLKQVYKRLVTAVXDI EKRIPFSHDDRLGFLTFC	/
51	hvipg|HV-PGN_Contig_297_FWD_frame_0	XP_001650897	Mitochondrial processing peptidase beta subunit	*Aedes aegypti*	76%	VTFSLQPFLTSWNYCPFIT*ICEQKFIILKIRITAKMLKL ATTLRLVSKQGNQVRCLATAAGYKEALVNVPPTKLSV LDNGIRVASEDSGAATATVGLWIDAGSRYENSKNNGV AHFLEHMAFKGTSKRSQTDLELLVENMGAHLNAYTS REQTVFYAKCLANDVPAAVEILADIIQNSSLAEPEIERE RGVILREMQDVESNLQEVVFDHLHATAFQGTPLGQTI LGPTKNIKKISK	N
52	*n.i.*						
53	*n.i.*						
54	*n.i.*						
55A	hvipg|HV-PGN_Contig_6434_FWD_frame_1	BAE96011	Glyceraldehyde-3-phosphate dehydrogenase	*Bombyx mori*	95%	TTEKASAHLEGGAKKVIISAPSADAPMFVVGVNLEAY DPSYKVISNASCTTNCLAPLAKVIHDNFEIIEGLMTTV HATTATQKTVDGPSGKLWRDGRGAQQNIIPASTGAAK AVGKVIPALNGKLTGMAFRVPVPNVSVVDLTVRLGKP ASYDAIKQKVKEAAQGPLKGILDYTEEQVVSSDFIGD SHSSIFDAAAGISLNDNFVKLISWYDNEFGYSNRVIDLI KYIQTKD*MFACCVERNVVM	C

55B	har454s|HARM_c1903_FWD_frame_1	BAD12426	Fructose 1,6-bisphosphate aldolase	*Antheraea yamamai*	93%	YQRSSSGVXVFHRIN*NKKTTMSTYFQYPTPELQEEL RKIAXAIVAPGKGILAADESTGTMGKRLQDIGVENTE ENRRKYRQLLFSSDPVVSENISGVILFHETLYQKADDG TPLVALLEKRGIIPGIKVDKGVVPLFGSEDECTTQGLD DLAQRCAQYKKDGCHFAKWRCVLKIGRFTPSYQAIM ENANVLARYASICQSQRIVPIVEPEVLPDGDHDLDRAQ KVTEVVLAAVYKALSDHHVYLEGTLLKPNMVTPGQ GCKKTYTPMDXGRATVTALLRTVXAAVPGVTFLSGG QSEEEASVNLNAINTVDLKRPWALTFSYGRALQASVL RAWAGKPENVLAGQQELIKRAKANGLACVGKYEAG SIPSLAADKSNFVKSHAY*KVLSLSKKKLYFVDNLTTL PCYGRVKLNLLLALKLIQDF*SHNMMKLFFIKSRIAIF TFHKV*KLFNF*SNHKFYLEL*SIKWHLFFYSLSFIIIYL C*VVFNQEKIY*Y*NLDQSMTDFSSCIICKGSNFITLNS YPESGKCTEQNITILSLNGYSFTNNTTFSRRNHDNTFKI *NKMAAKLVFYL*KKCKRHVRKLGVFCCPGNWVEE VR*AVAPCKTLVAVLLRYSAASE*TGSRPQHSWEKASQ MIITRKKTE*PPFFRYNSKRVIVCMYYPIVCLNSV*YQ HYLLCVYNIVRNK***LS*	C and N
56	hviV1|gi|1036785|gb|U23080.1| HVU23080_FWD_frame_1 Full Sequence	AAA79847	Triosephosphate isomerase	*Heliothis virescens*	100%	gatgaatggtgacaagaagcaagtcacagatattgttgagacactgaaaaagggcc cattagatcccaatgttgaggtacaatgcaaattctttgaagagtatgtgtattgtgtcat tctctttgctagtagtttaatacttttacgtgtgcaggttgttattggtgttccagcaatcta cctagcatatgttcagtctattgtccctggcacaatcagtgttgccgcacaaaactgttg gaaagttgctaaaggcgctttcactggtaagtatatcaccagaaaatacgtcaaacac aattgttacattatgcatgttctataacattttgtttttttcttcaggtgaaatctccccagcca tgattaaagatattggagccaattgggttatcctgggtcattccgaaaggagaacaatt ttcggagagaaagatgatctggttgcagagaaagtaagttaacacacaaccataaaa ttttacaaaataaccatttattattagactaagtatgtataatttattgtttgtaggtagcaca tgcacttgagaatggactgaaggtcattgcctgtatcggtgagactctagaagagag ggaggcaggcaaaactgaggaggtagtcttcaggcagaccaaggctcttctgccc gctatcggcaacaactgggccaatgttgtacttgcttatgagccagtatgggccatcg gtaccggcaagactgcatcacctcaacaggtgaaactgattatttcttttaaaaataac cgatcgcccaacagatttataatttacaccatacaacctgtccatgataaaatttattgct aaaccagtgatttcatacacaagacaagcagttgtaaatatatatgatatcagcacaat tctcctgctcaattaatgttcctaactcctatctagctatcaatacagtctgtcggcagaa gatatagataaaaattcgagatatattggaaactaaaatagatttctgaatgaaggacc tattttaacagttttctttgatatgtttaaggctcaagatgtccacgcttccctgcgcaact ggttg	C and N
57	*n.i.*						
58A	*n.i.*						

58B	hviV1|Contig3112_FWD_frame_0	NP_001040233	ATP Synthase	*Bombyx mori*	94%	PQRVASGELRLARASIYSSAIVIRI**NMSLISARIAGSV ARRLPNAASQVSKVAGVAAPAVSVASRNFHATPTQKA AEISTILEERILGSAPKADLEETGRVLSIGDGIARVYGL KNIQAEEMVEFSSGLKGMALNLEPDNVGVVVFGNDR HIKEGDIVKRTGAIVDVPVGEQLLGRVVDALGNAIDG KGPVDTKSRMRVGIKAPGIIPRVSVREPMQTGIKAVDS LVPIGRGQRELIIGDRQTGKTALAIDTIINQQRFNKGDD EKKKLYCIYVAIGQKRSTVAQIVKRLTDAGAINYTIIVS ATASDAAPLQYLAPYSGCAMGEFFRDNGKHALIIYDD LSKQAVAYRQMSLLLRRPPGREAYPGDVFYLHSRLLE RAAKMSDKMGGGSLTALPVIETQAGDVSAYIPTNVISI TDGQIFLETELFYKGIRPAINVGLSVSRVGSAAQTKAM KQVAGSMKLDLAQYREVAAFAQVGSHLDAATHHLLN RGMRLTELLKQGQYVPMAIEEQVAIIYCGVRGHLDKL DPSKITAFEKEFTQHIKTSHQSLLATIAKDGQITPESDA SLKKIVSDFLATFTQAAAR*TFSFYELWL*QEIVSRI*E TTSDPFVAQSHVKHHCMLTAGSWKHSYQLLFRLGML PLAA***LSFVWTVLNVDTIMECIYLERQEWLYINKYS *N*K	C and N
60	hvipg|HV-PGN_Contig_1305_FWD_frame_1	AAK52066	Actin	*Heliothis virescens*	99%	LAVSLP*SQHPPRPKPNTNAKMCDDDVAALVVDNGS GMCKAGFAGDDAPRAVFPSIVGRPRHQGVMVGMGQ KDSYVGDEAQSKRGILTLKYPIEHGIITNWDDMEKIW HHTFYNELRVAPEEHPVLLTEAPLNPKANREKMTQIM FETFNSPAMYVAIQAVLSLYASGRTXGIVLDSGDGVSH TVPIYEGYALPHAILRLDLAGRDLTDYLMKI	N
61	hviV1|Contig17_FWD_frame_0	P31410	Vacuolar (V-type) H(+)-ATPase B subunit	*Heliothis virescens*	100%	TSIRQFSGEEAAQFAVLLSGLPKSEN*KMAKTLTASQA AKEHVLAVSRDFISQPRLIYKTVSGVNGPLVILDDVKF PKFSEIVQLRLADGTLRSGQVLEVSGTKAVVQVFEGT SGIDAKNTLCEFTGDILRTPVSEDMLGRVFNGSGKPID KGPPILAEDFLDIQGQPINPWSRIYPEEMIQTGISAIDV MNSIARGQKIPIFSAAGLPHNEIAAQICRQAGLVKIPGK SVLDDHEDNFAIVFAAMGVNMETARFFKQDFEENGS MENVCLFLNLANDPTIERIITPRLALTAAEFLAYQCEK HVLVILTDMSSYAEALREVSAAREEVPGRRGFPGYMY TDLATIYERAGRVEGRNGSITQIPILTMPNDDITHPIPDL TGYITEGQIYVDRQLHNRQIYPPVNVLPSLSRLMKSAI GEGMTRKDHSDVSNQLYACYAIGKDVQAMKAVVGE EALTPDDLLYLEFLTKFEKNFISQGNYENRTVFESLDIG WQLLRIFPKEMLKRIPASILAEFYPRDSRH*TIMSGHGP HTLVR*N*YCLIVSC**LI*CVSHTCIMIR*KIR**ELK**I TTYIYYDHAKNYIKAFQS*ITTCVYIFTLYPYTERLNY YRCHLFCLVLVLRTQYKGY*KIKQLFLCAQIVDMCSN YM*LSKSVVNQDIITIYCVV*HVHLQSNRYLCK*TNSP VTKRYIPN*VFQFTPKLHSVFS**K*IRILL	N
62	*n.i.*						

63	hvipg|HV-PGN_Contig_6434_FWD_frame_1	ACV44016	Glyceraldehyde-3-phosphate dehydrogenase	*Proterebia afra*	97%	TTEKASAHLEGGAKKVIISAPSADAPMFVVGVNLEAY DPSYKVISNASCTTNCLAPLAKVIHDNFEIIEGLMTTV HATTATQKTVDGPSGKLWRDGRGAQQNIIPASTGAAK AVGKVIPALNGKLTGMAFRVPVPNVSVVDLTVRLGKP ASYDAIKQKVKEAAQGPLKGILDYTEEQVVSSDFIGD SHSSIFDAAAGISLNDNFVKLISWYDNEFGYSNRVIDLI KYIQTKD*MFACCVERNVVM	C
64	hvipg|HV-PGN_Contig_6434_FWD_frame_1	ACV44016	Glyceraldehyde-3-phosphate dehydrogenase	*Proterebia afra*	97%	TTEKASAHLEGGAKKVIISAPSADAPMFVVGVNLEAY DPSYKVISNASCTTNCLAPLAKVIHDNFEIIEGLMTTV HATTATQKTVDGPSGKLWRDGRGAQQNIIPASTGAAK AVGKVIPALNGKLTGMAFRVPVPNVSVVDLTVRLGKP ASYDAIKQKVKEAAQGPLKGILDYTEEQVVSSDFIGD SHSSIFDAAAGISLNDNFVKLISWYDNEFGYSNRVIDLI KYIQTKD*MFACCVERNVVM	C
65	*n.i.*						
66	hvipg|HV-PGN_Contig_364_FWD_frame_1	NP_001040233	ATP Synthase	*Bombyx mori*	94%	EEQVAIIYCGVRGHLDKLDPSKITAFEKEFTQHIKTSH QSLLATIAKDGQITPESDASLKKIVSDFLATFTQAAAR* TFSFYELWLWQEIVSRI*ETTSDPLVAQSHVKHHCMLT AGSWKHSYQLLFRFGMLPLAA***LSIVWTVLNVDTI MECIYLERQEWLYINKYS*N*K	C
67	hvipg|HV-PGN_Contig_5444_FWD_frame_1	NP_001036964	Beta-tubulin	*Bombyx mori*	99%	FMPGFAPLTSRGSQQYRALTVPELTQQMFDAKNMMA ACDPRHGRYLTVAAIFRGRMSMKEVDEQMLNIQNKN SSYFVEWIPNNVKTAVCDIPPRGLKMAATFIGNSTAIQ ELFKRIPEQFTAMFRRKAFLHWYTGEGMDEMEFTEA ESNMNDLVSEYQQYQEATADEDAEFDEEQEQEIEDN* ALTPNNPLPLPLTPPPAPYPSVRRVARDVF*FALVFP	C
69	hviV1|Contig262_FWD_frame_2	NP_001093278	Actin-depolymerizing factor 1	*Bombyx mori*	99%	RSSIELLV*FSESCQLAAATYFSNNI*SLGISQINYKINIK L*YKVTQYTSESVNWALF*KDAILILPVSLTHALIGCR KKGLANIPNSVVPVAVVVVSVKLVVEFLRV*HQKMAS GVTVSDACKTTYEEIKKDKKHRYVVFYIRDEKQIDVE TVGERNAEYDQFLEDLQKGGTGECRYGLFDFEYTHQ CQGTSEASKKQKLFLMSWCPDTAKVKKKMLYSSSFD ALKKSLVGVQKYIQATDLSEASQEAVEEKLRATDRQ* VSIYRHDRRVAHRDRPTETTSAATDWPRALGYQRTYC TKPPLCGLSQYCQWFAVRPTVSHGFFLYIVSILKLLQSI PLRSGLAQVGSELMYS*L*THGRLRDSL*L*QKESLCL *YN*RVN*AQTKFKYSVRVFFNCKTG*RTRSAFILFRL* YKECTILISFEIHLAKGCKLELRLDTWRALDKYFVTDL SRNTLDIRGK	C and N
71	hvipg|HV-PGN_Contig_1305_FWD_frame_1	AAK52066	Actin	*Heliothis virescens*	99%	LAVSLP*SQHPPRPKPNTNAKMCDDDVAALVVDNGS GMCKAGFAGDDAPRAVFPSIVGRPRHQGVMVGMGQ KDSYVGDEAQSKRGILTLKYPIEHGIITNWDDMEKIW HHTFYNELRVAPEEHPVLLTEAPLNPKANREKMTQIM FETFNSPAMYVAIQAVLSLYASGRTXGIVLDSGDGVSH TVPIYEGYALPHAILRLDLAGRDLTDYLMKI	N

76	hvipg|HV-PGN_Contig_825_FWD_frame_0	NP_001040445	Tropomyosin 1	*Bombyx mori*	96%	SACRSAV*TARS*GRNWRIFSTGP*RHKATTMDAIKKK MQAMKLEKDNAMDKADTCEQQARDANLRAEKVNE EVRELQKKLAQVEXDLILNKNKXEQANKDLXEKEKT LTATEAEVASLNRKVQQIEEDLEKSEERSGTAQQKLLE AQQSADENNRMCKVLENRAQQDEERMDQLTNQLKE ARLLAEDAD	N
77	*n.i.*						
78	*n.i.*						
79	hvipg|HV-PGN_Contig_825_FWD_frame_0	NP_001040445	Tropomyosin 1	*Bombyx mori*	96%	SACRSAV*TARS*GRNWRIFSTGP*RHKATTMDAIKKK MQAMKLEKDNAMDKADTCEQQARDANLRAEKVNE EVRELQKKLAQVEXDLILNKNKXEQANKDLXEKEKT LTATEAEVASLNRKVQQIEEDLEKSEERSGTAQQKLLE AQQSADENNRMCKVLENRAQQDEERMDQLTNQLKE ARLLAEDAD	N
80	*n.i.*						
A1	hvipg|HV-PGN_Contig_1305_FWD_frame_1	AAK52066	Actin	*Heliothis virescens*	99%	LAVSLP*SQHPPRPKPNTNAKMCDDDVAALVVDNGS GMCKAGFAGDDAPRAVFPSIVGRPRHQGVMVGMGQ KDSYVGDEAQSKRGILTLKYPIEHGIITNWDDMEKIW HHTFYNELRVAPEEHPVLLTEAPLNPKANREKMTQIM FETFNSPAMYVAIQAVLSLYASGRTXGIVLDSGDGVSH TVPIYEGYALPHAILRLDLAGRDLTDYLMKI	N
B1	hvipg|HV-PGN_Contig_1118_FWD_frame_2	ABU98622	Arginine kinase	*Helicoverpa armigera*	96%	LIDDHFLFKEGGRFLQAANACRFWPSGRGIYHNENKT FLVWCNEEDHLRLISMQMGGDLKQVYKRLVTAVXDI EKRIPFSHDDRLGFLTFC	/
B2	*n.i.*						
C2	*n.i.*						
D1	hvipg|HV-PGN_Contig_1305_FWD_frame_1	AAK52066	Actin	*Heliothis virescens*	99%	LAVSLP*SQHPPRPKPNTNAKMCDDDVAALVVDNGS GMCKAGFAGDDAPRAVFPSIVGRPRHQGVMVGMGQ KDSYVGDEAQSKRGILTLKYPIEHGIITNWDDMEKIW HHTFYNELRVAPEEHPVLLTEAPLNPKANREKMTQIM FETFNSPAMYVAIQAVLSLYASGRTXGIVLDSGDGVSH TVPIYEGYALPHAILRLDLAGRDLTDYLMKI	N
D2	hvipg|HV-PGN_Contig_1305_FWD_frame_1	AAK52066	Actin	*Heliothis virescens*	99%	LAVSLP*SQHPPRPKPNTNAKMCDDDVAALVVDNGS GMCKAGFAGDDAPRAVFPSIVGRPRHQGVMVGMGQ KDSYVGDEAQSKRGILTLKYPIEHGIITNWDDMEKIW HHTFYNELRVAPEEHPVLLTEAPLNPKANREKMTQIM FETFNSPAMYVAIQAVLSLYASGRTXGIVLDSGDGVSH TVPIYEGYALPHAILRLDLAGRDLTDYLMKI	N
E1	hvipg|HV-PGN_Contig_759_FWD_frame_1	NP_001091831	Enolase	*Bombyx mori*	95%	DFPMVSIEDPFDQDDWAAWASLTSRTPIQIVGDDLTVT NPKRIATAVEKKACNCLLLKVNQIGSVTESIDAHLLAK KNGWGTMVSHRSGETEDTFIADLVVGLSTGQIKTGAP CRSERLAKYNQILRIEEELGSAAKYAGKNFRRPV*TY KDVIKRACSSTIVRCD*NEYALKMLYSILPSVEYIDT*C NKLRYYFSTYCQKIVIYL*EITGCSDCISVE	C
E2	hvipg|HV-PGN_Contig_759_FWD_frame_1	NP_001091831	Enolase	*Bombyx mori*	95%	DFPMVSIEDPFDQDDWAAWASLTSRTPIQIVGDDLTVT NPKRIATAVEKKACNCLLLKVNQIGSVTESIDAHLLAK KNGWGTMVSHRSGETEDTFIADLVVGLSTGQIKTGAP CRSERLAKYNQILRIEEELGSAAKYAGKNFRRPV*TY KDVIKRACSSTIVRCD*NEYALKMLYSILPSVEYIDT*C NKLRYYFSTYCQKIVIYL*EITGCSDCISVE	C

F1	hvipg|HV-PGN_Contig_866_FWD_frame_0	BAD12426	Fructose 1,6-bisphosphate aldolase	*Antheraea yamamai*	67%	SPT*VLLEDRMPTYFSYPXPALQKELKDTAEAIVAPGK GILAVDETNEGIGKLLAAVGLQNTENNRRRYRQLLFT TDNLSEHVSATILFHETVYQKTDDGTPFIELLKKNIIPG IKVDMDTVPLFLSQDEVTTQGLDNLATRCAEYKKQG CRFAKWRCPIKIGEHIPSVQAINDTAHVLARYASI	N
F2	hvipg|HV-PGN_Contig_866_FWD_frame_0	BAD12426	Fructose 1,6-bisphosphate aldolase	*Antheraea yamamai*	67%	SPT*VLLEDRMPTYFSYPXPALQKELKDTAEAIVAPGK GILAVDETNEGIGKLLAAVGLQNTENNRRRYRQLLFT TDNLSEHVSATILFHETVYQKTDDGTPFIELLKKNIIPG IKVDMDTVPLFLSQDEVTTQGLDNLATRCAEYKKQG CRFAKWRCPIKIGEHIPSVQAINDTAHVLARYASI	C
G1	hvipg|HV-PGN_Contig_1118_FWD_frame_2	ABU98622	Arginine kinase	*Helicoverpa armigera*	96%	LIDDHFLFKEGGRFLQAANACRFWPSGRGIYHNENKT FLVWCNEEDHLRLISMQMGGDLKQVYKRLVTAVXDI EKRIPFSHDDRLGFLTFC	/
G2	hvipg|HV-PGN_Contig_1118_FWD_frame_2	ABU98622	Arginine kinase	*Helicoverpa armigera*	96%	LIDDHFLFKEGGRFLQAANACRFWPSGRGIYHNENKT FLVWCNEEDHLRLISMQMGGDLKQVYKRLVTAVXDI EKRIPFSHDDRLGFLTFC	/
H1	hvipg|HV-PGN_Contig_1118_FWD_frame_2	ABU98622	Arginine kinase	*Helicoverpa armigera*	96%	LIDDHFLFKEGGRFLQAANACRFWPSGRGIYHNENKT FLVWCNEEDHLRLISMQMGGDLKQVYKRLVTAVXDI EKRIPFSHDDRLGFLTFC	/
K1	hvipg|HV-PGN_Contig_1395_FWD_frame_0	NP_001040450	H+ transporting ATP synthase beta subunit Isoform 1	*Bombyx mori*	93%	IVFLRLHNLRAADSTPKCIKLSKMLGAVSRVGSGLLA AKSVAEKTLTECGKIATVSAINKRDYAAKAAAGKGQG KVVAVIGAVVDVQFEDNLPPILNALEVQNRQPRLVLEV AQHLGENTVRTIAMDGTEGLVRGQPVQDCGSPIRIPV GAETLGRIINVIGEPIDERGPIPTDKTAAIHAEAPEFVD MSVQQEILVTGIKVVDLLAPYAEGGKIGLFGGAGVGK TVLIMELINNVAKAHGGYSVFAGVGERTREGN	N
K2	hvipg|HV-PGN_Contig_1395_FWD_frame_0	NP_001040450	H+ transporting ATP synthase beta subunit Isoform 1	*Bombyx mori*	93%	IVFLRLHNLRAADSTPKCIKLSKMLGAVSRVGSGLLA AKSVAEKTLTECGKIATVSAINKRDYAAKAAAGKGQG KVVAVIGAVVDVQFEDNLPPILNALEVQNRQPRLVLEV AQHLGENTVRTIAMDGTEGLVRGQPVQDCGSPIRIPV GAETLGRIINVIGEPIDERGPIPTDKTAAIHAEAPEFVD MSVQQEILVTGIKVVDLLAPYAEGGKIGLFGGAGVGK TVLIMELINNVAKAHGGYSVFAGVGERTREGN	N

[a] = Cluster ID of best hit in MS-Ento by MS BLAST (ni = not identified). [b] = Sequence of MS-Ento BLAST searches
[c] = NCBI Accession number and description of the best hit in NCBI_insecta by MS BLAST. [d] = Species of best hit in NCBI_insecta.
[e] = Percentage of Identity of identified protein matching best hit in NCBI_insecta. [f] = If the C-or N-Terminus of the predicted protein of NCBI is known NCBI_insecta protein. [g] = *E*-Value of best hit in blasp search

8 Declaration of Authorship

I certify that this thesis and the work presented in it are the result of my knowledge and the result of my own invastigations and has not been submitted, either in part or whole, for a degree at this or any other University. Where I have consulted the published work of others, this is always attributed.

Date

Andrea Barthel